HORIZON 2020
The EU Framework Programme for Research and Innovation

Urban Cross-cutting Applications Preparation

Deliverable D3.1

DATE
31 December 2020

ISSUE
1.0

GRANT AGREEMENT
no 870337

DISSEMINATION LEVEL
PU

PROJECT WEB-SITE
http://cure-copernicus.eu/

LEAD AUTHOR
Dirk Lauwaet (VITO)

CO-AUTHORS
Nektarios Chrysoulakis, Zina Mitraka, Giannis Lantzanakis (FORTH), Benjamin Leutner, Mattia Marconcini (DLR), Christian Feigenwinter (UNIBAS), Katerina Jupova, Jan Kolomaznik, Miroslav Kopecky, Tomas Soukup (GISAT), Hans Hooyberghs (VITO), Alessandra Gandini, Laura Gutierrez, Efren Feliu (TECNALIA), Birgitte Holt Andersen, Louise Kjær-Hansen (CWare)

CONTENTS

LIST OF TABLES

LIST OF FIGURES

1 INTRODUCTION

1.1 Purpose of this document

This document is the first deliverable of Work Package (WP) 3 of the CURE (Copernicus for Urban Resilience in Europe) Project, Deliverable D3.1 'Urban Cross-cutting Applications Preparation Project Management Plan'. The goal of this deliverable is to describe in more detail the CURE Cross-Cutting Applications and to summarize the preparatory activities for the individual applications development, following the first description in Deliverable D1.3. The purpose of each CURE application, the data and methodology used, as well as the output features and characteristics are presented. Preliminary results of some applications for the front-runner cities are demonstrated where possible (Table 1) and feedback is provided on the stakeholder needs, as identified in D1.1.

The CURE applications are developed for at least one front-runner cities and will be then applied to one or more follower cities. Table 1 lists the applications per front-runner city, as decided after consultation with the users (detailed in D1.1). The application areas are slightly different from the original plan, as indicated in Table 1.

Figure 1 shows the dependency of the CURE applications to the Copernicus Core Services. More details on this dependency are described in Deliverable D2.1.

In the next Chapters, the applications are presented one by one, in the same order as Table 1.

Table 1. *CURE Applications Development for the front-runner cities.*

AP	CURE Cross-Cutting Applications	Berlin	Copenhagen	Sofia	Heraklion
01	Local Scale Surface Temperature Dynamics (FORTH)	●	●	●	●
02	Surface Urban Heat Island Assessment (DLR)	●	●	●	●
03	Urban Heat Emissions Monitoring (UNIBAS)				●
04	Urban CO_2 Emissions Monitoring (UNIBAS)				●
05	Urban Flood Risk (GISAT)		●		●
06	Urban Subsidence, Movements and Deformation Risk (GISAT)			●	●
07	Urban Air Quality (VITO)			●	
08	Urban Thermal Comfort (VITO)		●	●	
09	Urban Heat Storage Monitoring (FORTH)				●
10	Nature Based Solutions (TECNALIA)		●	●	
11	Health Impacts (CWARE)		●	●	

● Application to be implemented for this city; ● originally planned, but changed.

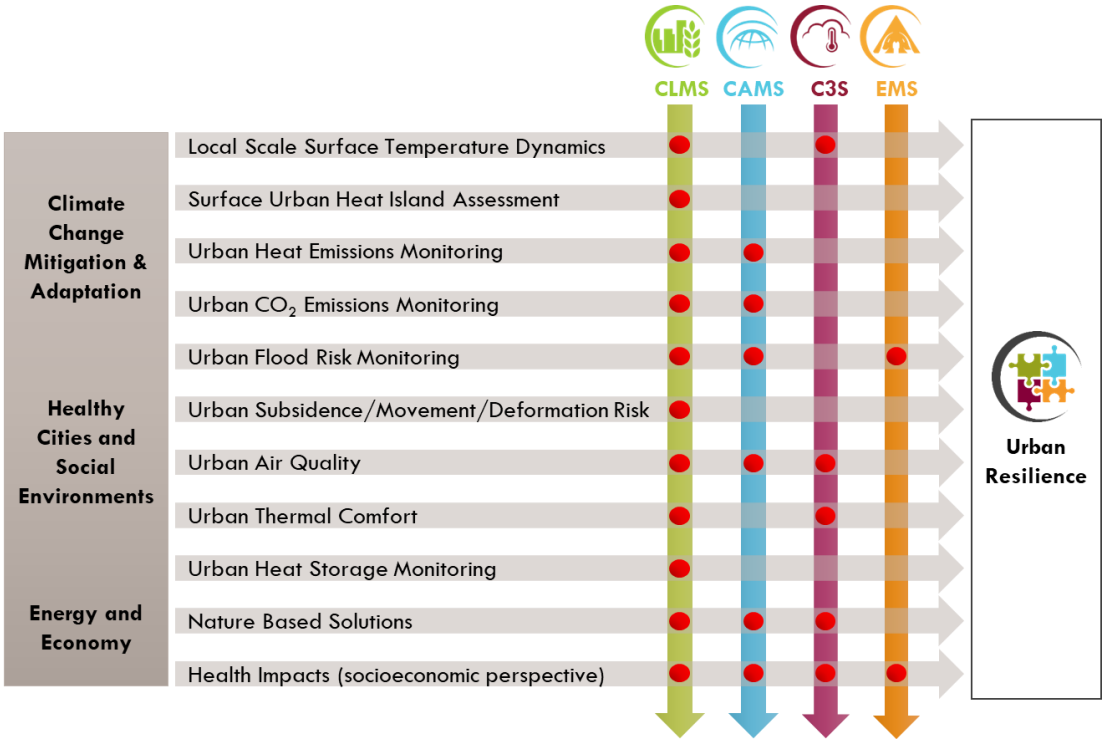

Figure 1. CURE cross-cutting applications among the Copernicus Core Services.

1.2 Definitions and acronyms

Acronyms

CURE	Copernicus for Urban Resilience in Europe
WP	Work Package
UHI	Urban Heat Island
UHII	UHI indicators
SUHII	Surface Heat Island Intensity Indicator
IMD HRL	imperviousness density
ARM	Aerodynamic Resistance Method
EC	Eddy Covariance
DOM	Digital Object Model
MOST	Monin-Obukhov similarity theory
UMEP	Urban Multi-scale Environmental Predictor
QA/QC	quality assessment and quality control
AOI	Area of Interest
WSFE	World Surface Footprint Evolution
DTM	Detailed terrain model
DSM	Digital Surface Model
EO	Earth Observation
NRT	Near Real Time
InSAR	Synthetic Aperture Radar Interferometry
PSI	Persistent Scatterer Interferometry
IFDM	Immission Frequency Distribution Model
CAMS	Copernicus Atmospheric Service
CLMS	Copernicus Land Monitoring Service
C3S	Copernicus Climate Change Service
EMS	Copernicus Emergency Service
NBS	Nature-based solutions
EVA	Economic Valuation of Air pollution

2 AP01 LOCAL SCALE SURFACE TEMPERATURE DYNAMICS

2.1 Purpose of the Application

Temperature is one of the most important variables in climate monitoring and the Land Surface Temperature (LST) is an important parameter for understanding and therefore modifying the urban climate (Oke et al., 2017). LST helps describing the processes of the urban energy and water balance, meaning the exchange of energy and water between the land surface and the atmosphere (Chrysoulakis et al., 2018). Therefore, accurately quantifying LST for cities at a local scale helps to understand and evaluate the land surface – atmosphere exchange processes at a neighbourhood level and therefore provides valuable information source for city planning.

The LST in cities is a dynamically changing parameter, with diurnal and seasonal variations presenting distinct characteristics, attributed to the highly variable urban surface properties and the unique three-dimensional nature of the urban surface (Oke et al., 2017). Therefore, in order to make conclusions about a city's LST behaviour, having detailed information on the spatial pattern of the LST distribution is not sufficient, but monitoring its evolution through time is an emerging need (Mitraka et al., 2015).

Therefore, the CURE Local Scale Surface Temperature Dynamics Application (AP01) is developing time series of maps of urban surface temperature of 100 m x 100 m spatial resolution (local scale). This refers to the skin temperature that is the temperature of the surface elements (°C) at the time of the satellite acquisition and should not be confused with the air temperature near the ground. The products of AP01 will be maps (at the above resolution) of the city's surface temperature (°C) and will allow the quantitative analysis of the temperature 4 times per day, depending on cloud coverage.

The LST dynamics of a city may provide valuable information for urban planners and when combined with other physical properties of the surface it allows insights on phenomena like the Surface Urban Heat Island (CURE AP02 described in Section 3), and monitoring the Urban Heat Emissions (CURE AP03 described in Section 4) and Urban Heat Storage (CURE AP09 described in Section 10).

2.2 Data & Methodology

2.2.1 Data

AP01 will be implemented for all four front-runners cities: Berlin, Copenhagen, Heraklion and Sofia and all the follower cities: Bristol, Ostrava, Basel, Munich, San Sebastian and Vitoria-Gasteiz.

Table 2 lists the data that are used for the AP01. AP01 is using data from two of the Copernicus Services (CLMS and C3S), data from two Copernicus Satellites, Sentinel-2 and Sentinel-3, and

very high resolution optical third-party data from the Copernicus Contributing missions Data Warehouse (Copernicus, 2020).

Table 2. Summary of data used for AP01.

Data Source	Description of the Product
CLMS	Imperviousness
CLMS	Urban Atlas
CLMS	Urban Atlas: Building Heights
CLMS	High Resolution Vegetation Phenology and Productivity (Under Development)
C3S	UERRA regional reanalysis for Europe on single levels from 1961 to 2019
C3S	ERA5 hourly data on single levels from 1979 to present
Copernicus Satellite	Sentinel-2, Level-2A Bottom Of Atmosphere (BOA) reflectance images
Copernicus Satellite	Sentinel-3, SLSTR Level-1B thermal imagery
Third-party	Baseline Land Cover from VHR (from the DWH)
Third-party	Material emissivity information from spectral libraries (Kotthaus et al., 2014)

2.2.2 Methodology

The CURE methodology for deriving the local scale urban surface temperature dynamics is outlined in Figure 2. Data from various sources, including the CLMS, are used to achieve the surface characterization and this information is then used to estimate the urban surface emissivity and to downscale the thermal imagery in order to retrieve LST, given atmospheric information from C3S. The methodology described in Mitraka et al. (2015) is used to downscale the Sentinel-3 thermal infrared (TIR) imagery, which are of 1 km spatial resolution, in order to retrieve the final LST products at local scale (100 m). The methodology for downscaling the thermal bands, requires higher spatial resolution surface cover information.

The VHR land cover map is then used to derive a local scale (100 m) surface cover fractions map, which contains information on the abundance of each land cover class in the local scale pixel. The surface cover fractions baseline map is then updated to capture changes in time. Emissivity maps are estimated using the surface cover maps and ancillary information from spectral libraries. The LST time series is estimated from the downscaled TIR information (using the surface cover), the emissivity and water vapour products.

A surface cover map of very high spatial resolution (2 m) is initially created, from the VHR data available from the DWH (Copernicus, 2020) to serve as baseline, assuming 5 classes (i.e. buildings, paved surfaces, bare soil, vegetation, water surfaces). It is essential to have this information in VHR, to ensure the quality of the resulting products. Surface cover fractions of

100 m spatial resolution are then estimated from the VHR surface cover map, to be used as baseline. The update in time of the baseline map is performed using Sentinel-2 imagery and (when available) CLMS Vegetation Phenology and Productivity data, to capture the changes of the 5 classes.

The vegetation, bare soil and water surfaces classes update is performed using vegetation and water indices approach. The buildings and paved surfaces classes are updated using VHR imagery, CLMS Urban Atlas and CLMS imperviousness data when available and Sentinel-2 optical imagery in the meantime.

The resulting surface cover maps are used to downscale the thermal measurements and to estimate the surface emissivity in local scale using ancillary information from third-party spectral libraries (Mitraka et al., 2012). Different spectral libraries are considered, in order to obtain emissivity information for the different classes. The emissivity information along with the local scale thermal products are then used along with water vapour information from C3S, for the derivation of LST maps using a split-window algorithm (Mitraka et al., 2015).

The LST products of AP01 will be validated against in situ measured LST for Heraklion and Basel where these data are available and compared against the other local scale LST high level products (i.e. Landsat and/or ASTER LST products).

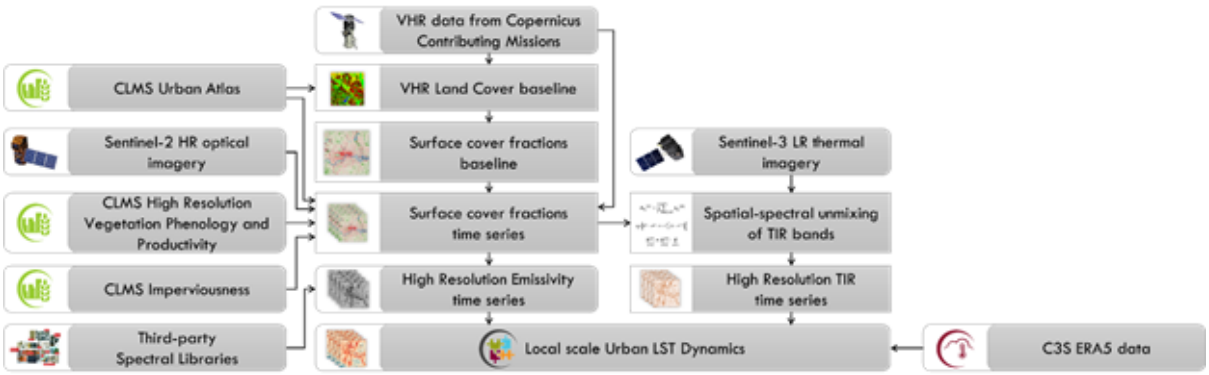

Figure 2. Methodology for the estimation of Urban Land surface Temperature (LST) dynamics at local scale.

2.3 Output features & characteristics

The CURE Local Scale Surface Temperature Dynamics Application (AP01) is developing time series (4 times per day, depending on the cloud cover) of urban surface temperature maps of 100 m x 100 m spatial resolution (local scale). This refers to the skin temperature that is the temperature of the surface elements (°C) at the time of the satellite acquisition.

The output maps will be made available as one GeoTiff (image files with geographic information) per Sentinel-3 acquisition.

Within CURE, local scale urban temperature maps will be delivered for 2018 and 2019. The area coverage for the front-runner cities is shown in Figure 3 below. Figure 4 shows an example of output urban surface temperature map for the case of Berlin corresponding to 24 July 2019, 21:26 local time, along with the intermediate products created to achieve local scale surface temperature corresponding to Sentinel-3 acquisition.

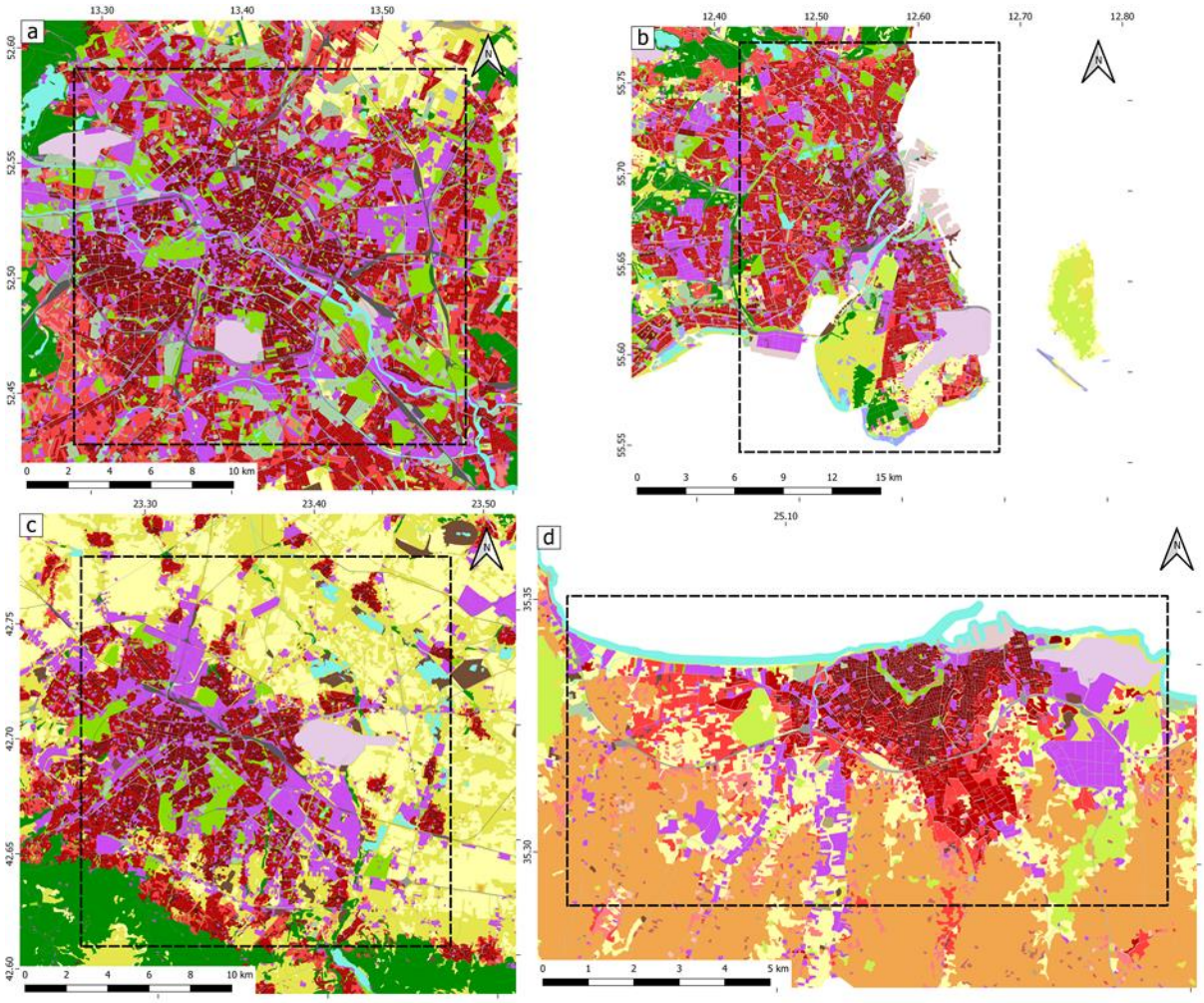

Figure 3. *The areal coverage of the AP01 products for the four CURE front-runner cities, i.e. (a) Berlin, (b) Copenhagen, (c) Sofia and (d) Heraklion.*

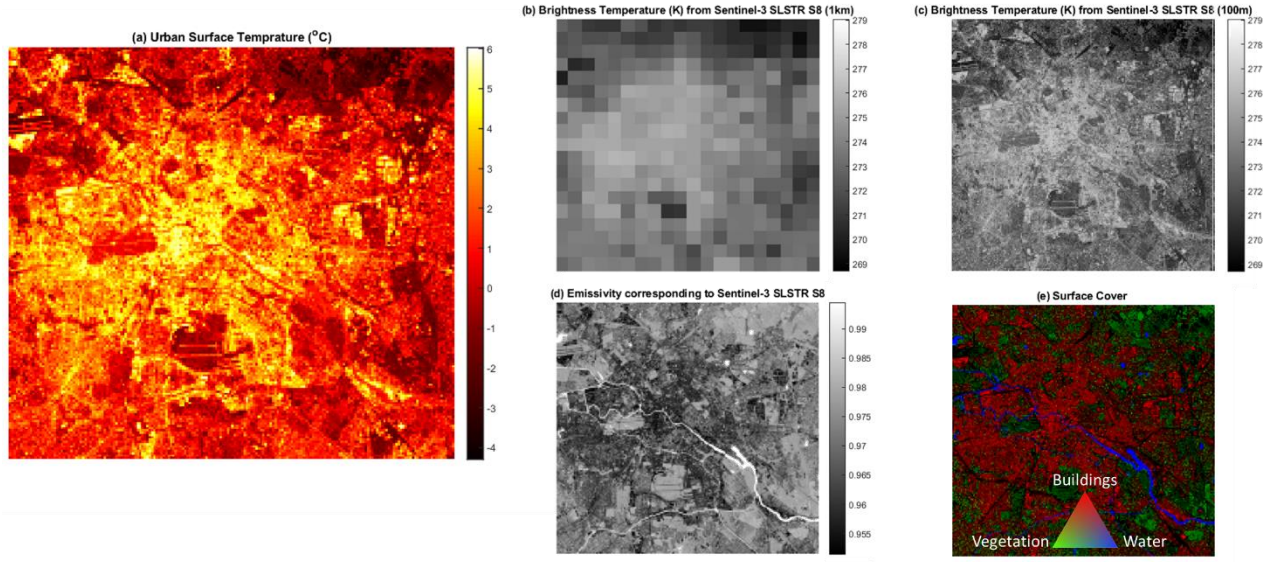

Figure 4. *(a) Local scale urban surface temperature for Berlin corresponding to 24 July 2019, 21:26 local time, as derived by AP01. The intermediate products are also shown: i.e. (b) Brightness Temperature (K) from Sentinel-3 SLSTR S8 (1km), (c) Brightness Temperature (K) from Sentinel-3 SLSTR S8 (100 m), (d) Emissivity corresponding to Sentinel-3 SLSTR S8 and (e) surface cover fractions.*

2.4 Stakeholder needs addressed by the application

Comments on the response of AP01 in regards to the stakeholder requirements as described in Khan et al. (2020) are listed below. Only the requirements relevant to AP01 are used, using the same notation as Khan et al. (2020).

Requirement G.1: AP01 will use and provide access to past data (2018 – 2019), but it can be extendable for most recent data.

Requirement G.3: Time series data would be available from AP01.

Requirement G.4: In terms of spatial resolution, AP01 is using dowscaling techniques to achieve 100 m spatial resolution (from 1 km of the original data). Achieving higher spatial resolutions, i.e. 10 m, would require satellite thermal acquisition of higher spatial resolution, currently not available. In terms of frequency, from Copernicus data only, it is possible to provide products corresponding to satellite acquisitions, i.e. 4 times per day maximum. Hourly products would further require modeling.

Requirement G.5: It is not common to have local (in-situ) data for surface temperature in cities. If available, AP01 could use these data for method validation, rather than calibration (as in the case of Heraklion and Basel).

Requirement G.6: The AP01 output will be compared against other land surface temperature products of the same scale, i.e. Landsat (Parastatidis et al., 2017) and ASTER (NASA/METI/AIST/Japan Spacesystems, and U.S./Japan ASTER Science Team, 2001)

Requirement G.7: AP01 is developing transitional products, such as percentage of green areas and land cover change, but these are not made available as CURE products.

Requirement G.8: AP01 data products will used by other CURE apps and will be coupled with other data (i.e. for Surface Urban Heat Island Assessment, AP02).

Requirement G.11: Similarly to G.7, AP01 is developing transitional products, such as percentage of green areas and land cover change, but these are not made available as CURE products.

Requirement G.18: AP01 is using data from Open Street Maps to complement the VHR land cover maps. It is using building footprint data, whenever these are available, to adjust/correct the VHR land cover map derived from VHR satellite imagery.

Requirement G.19: As described in G.4, AP01 is using dowscaling techniques to achieve 100 m spatial resolution (from 1 km of the original data). Upcoming satellite missions, like the Copernicus High Spatio-Temporal Resolution Land Surface Temperature Mission (ESA, 2019), may allow products of higher spatial resolution, with downscaling techniques up to a few tens of meters. It is highly unlike that spatial resolutions up to a few meters will be achieved in the near future from satellite missions. Drones may provide this kind of information, very limited in terms of frequency. Surface temperature products of few kms and tens of kms spatial resolution are already available from CLMS.

Requirement G.21: As described in G.4, AP01 is providing temperature maps, maximum 4 times per day, i.e. Daily Frequency. For higher frequency (hourly) modelling techniques should be employed, which are out of the scope of CURE. Weekly, monthly, quarterly and annual temperature maps could be derived too.

Requirement G.22: AP01 does provide day and night data.

Requirement G.28: AP01 cannot provide hourly data. See also Requirement G.4 and G.21 above.

Requirement G.29: AP01 provides 24/7 geo-referenced data.

Requirement G.30: All CURE data will be accompanied by metadata. Details are provided in Deliverable D7.4 (Poursanidis et al., 2020).

Requirement G.33: AP01 does provide time series of data.

Requirement G.34: AP01 will be implemented for part of the Moravian Silesian region (Ostrava).

Requirement B.1: AP01 will be implemented for Berlin.

Requirement B.2: AP01 cannot be operated in 10 m spatial resolution, as explained in G.4 and G.19 above.

Requirement B.3: AP01 will provide daily data.

Requirement B.4: AP01 will be implemented for the area covered by available VHR data. It will cover large part of the city of Berlin. The area is shown in Figure 4.

Requirement C.5: AP01 will produce data capable of providing insights for urban heat assessment.

Requirement H.2: AP02 will provide data at local scale.

Requirement H.3: AP03 will provide data for 2018-2019 for Heraklion and there is the possibility to extend this to present data.

3 AP02 SURFACE URBAN HEAT ISLAND ASSESSMENT

3.1 Purpose of the Application

Human well-being in urban environments is, among others, strongly driven by local climatic conditions, in particular temperature, and, as such, is expected to be impacted heavily by recent and forecasted temperature variability and increase due to climate change. In general, urban areas are warmer than their rural surroundings, which is commonly referred to as the Urban Heat Island (UHI) effect. However, cities differ strongly in how pronounced this effect is, due to complex interactions of local and regional climatic conditions with the urban fabric, such as roads and buildings but also vegetation and their respective spatial arrangement. A reliable characterisation of the urban heat island effect can, on the one hand, contribute to the evaluation of potential heat risks of Europe's cities and on the other hand, guide the planning of resilient urban development in face of global climate change.

The quantification of the urban heat island effect can be accomplished by UHI indicators (UHII), one of which – the surface heat island intensity indicator (SUHII) – will be provided by this application. Specifically, AP02 provides a framework to objectively quantify the SUHII through regression analysis of land-surface temperature and the density of the urban fabric and can be derived for any target city. AP02 makes use of space-borne measurements of land-surface temperature developed in AP01 with existing CLMS High Resolution Layers on urban imperviousness. Based on a delineated urban extent and its surroundings, AP02 will then provide an estimate of the SUHII and potentially also its temporal dynamics.

Thus, calculating the SUHII will then allow to rank cities by their thermal characteristics and their resulting vulnerability to urban heat stress, which may allow to focus efforts on cities most affected and steer urban developments.

3.2 Data & Methodology

Theoretically, the SUHII is defined as the difference in temperature between urban and surrounding rural regions. Traditionally, the quantification of UHII is conducted at two fixed in-situ stations, one in urban and the other in rural regions. Similarly, the remote sensing-based variant, the SUHII, has been derived using selected pixels that are located in the urban and rural regions, respectively. However, it is immediately clear, that single locations or pixels can only reflect part of the SUHI characteristics, especially in cities with multiple UHI centres, and do not necessarily generalize to an entire city. Moreover, the different definitions of "urban" and "rural" regions make the inter-comparison study of SUHII among different cities particularly challenging. To overcome these limitations, the methodology recently presented by Li et al. (2018) is used in CURE. In particular, the intended approach will allow calculating SUHII and its temporal dynamics by exploiting the relationship between land surface temperature (LST) and the percentage impervious surface (PIS), which – according to the

literature – proved consistent for cities in biomes dominated by forests and grasslands as in Europe.

3.2.1 Input Data

There are a number of urban imperviousness products provided through the Copernicus program. In particular, AP02 will make use of the CLMS High Resolution Layers of imperviousness density (IMD HRL), which have been published for the years 2006, 2009, 2012, 2015 and 2018. These will serve as the primary data source for the PIS layer. These status layers are available in 20m spatial resolution for the years 2006 to 2015 and 10m spatial resolution for the year 2018.

Figure 5 displays the 2018 IMD HRL for the CURE front-runner cities after pre-processing with the convolution step described in the Methodology section.

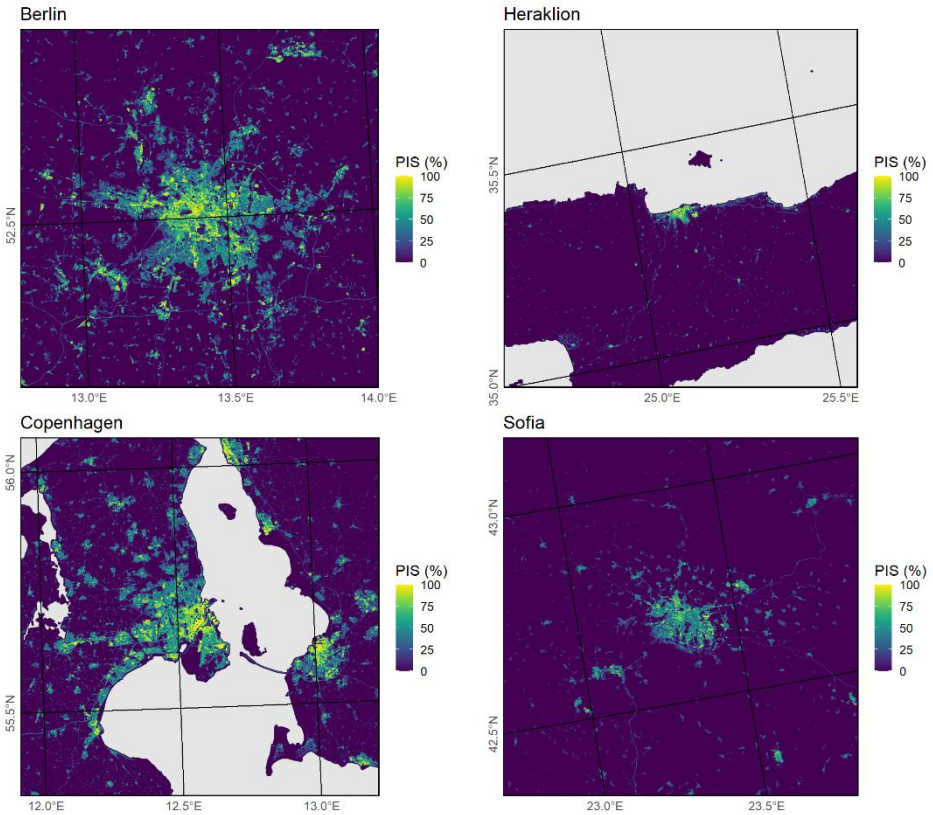

Figure 5. *PIS layer derived from CLMS IMD HRL 2018 for the CURE front-runner cities after convolution with PSF kernel.*

Furthermore, it is anticipated to base the framework in addition also on an improved imperviousness product developed in the processing framework of the World Settlement Footprint (Marconcini et al. 2020), which is based on Copernicus Sentinel-2 data for the year 2019 (which can be extended backwards to 2015) and on Landsat-5/7/8 for the period 1985-2015.

For the LST layer, AP02 relies on land surface temperature data developed and processed in AP01, thus making use of both CLMS and CAMS data sources. For initial development and pre-Sentinel era analyses, AP02 makes use of Landsat 5, Landsat 7 and Landsat 8 derived LST data (Parastatidis et al. 2017).

Figure 6 displays LST composites derived from Landsat 8 TIRS data over the summer months of 2017-2018 for all CURE front-runner as described in the Methodology section.

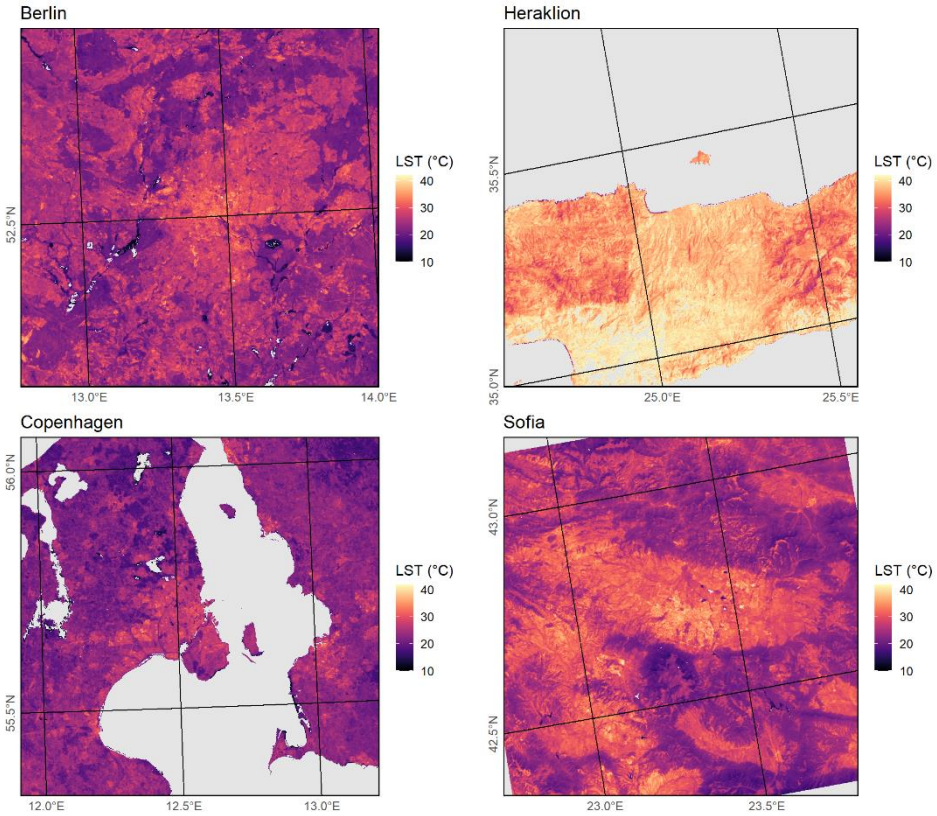

Figure 6. *LST multi-temporal composite layer derived from Landsat 8 TIRS data for the CURE front-runner cities.*

3.2.2 Methodology

Following the state-of-the-art summary given in D1.3, the selected methodology for SUHII derivation is based on performing a regression of the measured LST against the imperviousness degree following the method of Li et al. (2018). The SUHII is then defined as the slope of a linear regression line. While this method avoids having to define “urban” and “rural” pixels explicitly, defining the cutoff distance or condition of which rural surroundings around a city to consider, is still an unsolved challenge and is part of the development analyses within AP02.

Figure 7 summarizes the processing steps needed to implement the AP02 processor. The LST data from AP01 described in the previous section will be provided on a per-scene basis. LST from individual acquisitions is subject to gaps due to cloud-cover, as well as natural variability of temperatures due to weather. Therefore, in order to obtain a robust characterization of the LST properties, the individual acquisitions are composited by calculating the median over a

given timeframe, to be determined by a dedicated sensitivity analysis. In our preliminary experiments with the Landsat-based LST, to take into consideration the months May to October for two consecutive years proved to be a promising choice. However, this is mostly driven by the 16-day Landsat acquisition frequency in contrast to the daily information expected to be derived based on Sentinel-3 imagery by AP01.

Next, the imperviousness layer from the CLMS IMD HRLs is processed to match the LST data. Since the spatial resolution of the thermal Landsat bands is 100m plus adjacency effects due to the sensor's point spread function (PSF), the high-resolution PIS data is convolved with a Gaussian kernel of width σ = 50m to correspond to the LST measurement.

Subsequently, pixel values are sampled from both the IMD and LST composite using a regular sampling grid and discarding no-data, as well as water pixels. Using these samples, we fit a robust linear model, in order to avoid undue influence of extreme values, as:

$$LST = \beta_0 + \beta_1 \cdot PIS,$$

where finally β_1 defines the SUHII.

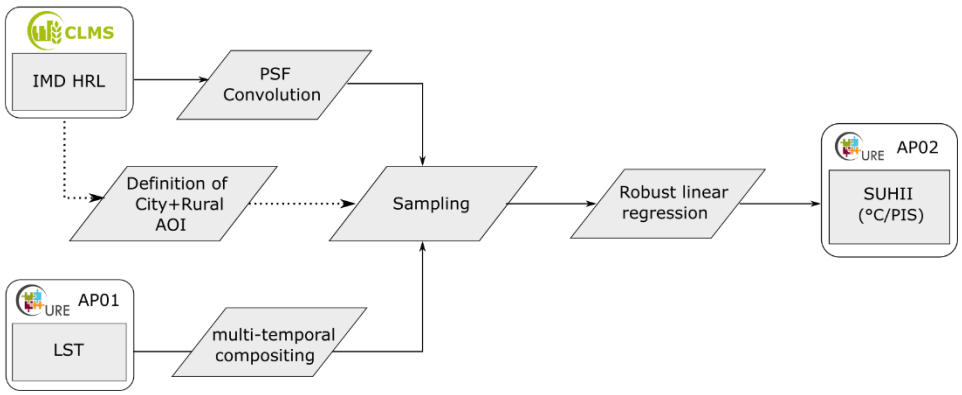

Figure 7. *Simplified flowchart of the AP02 SUHII processor.*

Initial results have been produced for all four CURE front-runner cities with the CLMS IMD HRL 2018 and Landsat 8 LST data, which were calibrated using an emissivity based on Landsat NDVI as well as atmospheric water vapour content derived from the NCEP/NCAR Reanalysis Project as described in Parastatidis (2017).

Figure 8 displays the resulting SUHII index values with their corresponding confidence intervals over variably sized buffers around the city centres. This clearly highlights the sensitivity of the SUHII to the definition of the urban extent, yet also provides an opportunity to define the cut-off in a data-driven manner, for example as the point of initial saturation. As lined out earlier, this is still very much a matter of investigation. An alternative, data-drive approach towards testing AOI delineation based on clustering and thresholding the PIS layer is currently being tested.

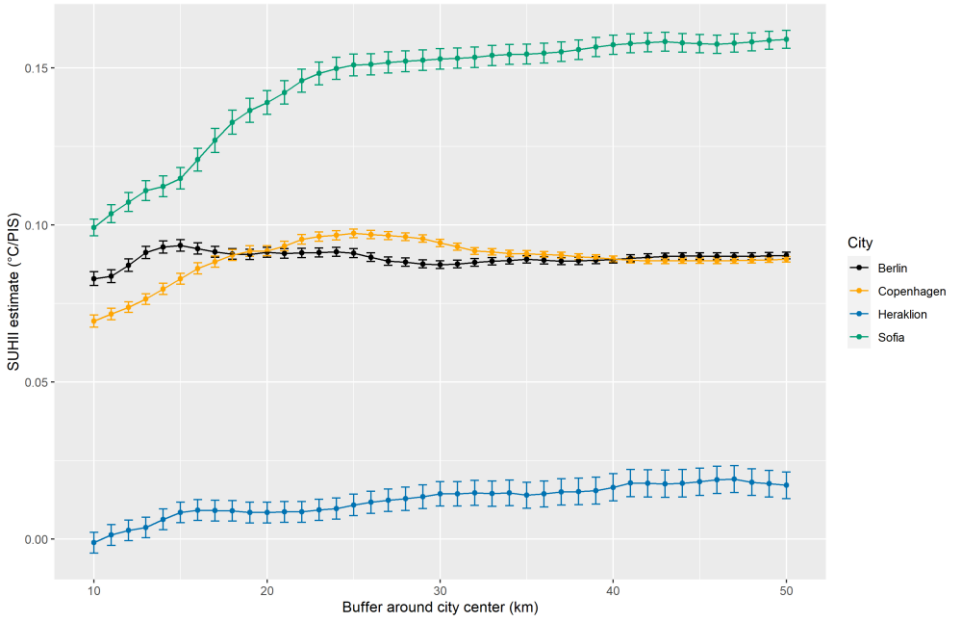

Figure 8. *Estimates of SUHII vary depending on the definition of the city and encompassing rural extent. It is yet to be determined how to delineate the city body.*

3.3 Output features & characteristics

An atomic output of AP02 will be a single number summarizing the SUHII for a given city. This output will be provided as a summary table or, depending on user requirements, as a JSON or CSV response. Moreover, a statistical figure will be provided to display the underlying LST and PIS data as well as the fitted robust linear model and measures of model fit, as shown in Figure 9, along with a spatial representation of the input data as depicted in Figure 5 and Figure 6.

SUHII estimates will be made available for each year of available imperviousness input layers. That is, for years 2006, 2009, 2012, 2015 and 2018, when based on the CLMS IMD HRLs.

For the CURE front-runner cites the SUHII estimates can be pre-calculated. In addition, if technically feasible, users should be enabled to provide custom regions of interest, for which the SUHII is calculated on-the-fly.

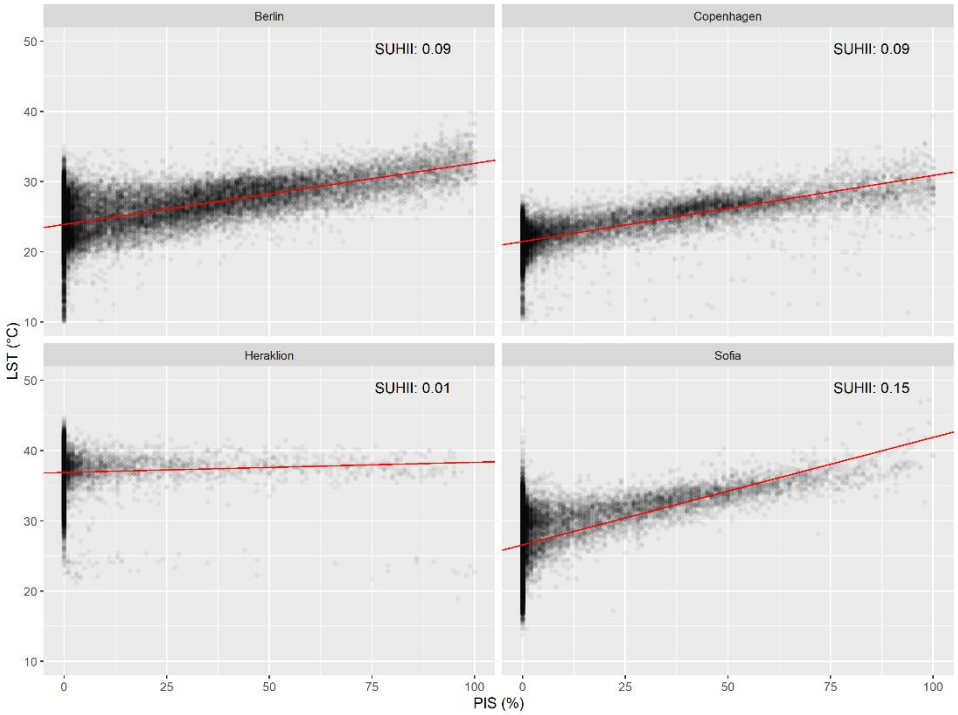

Figure 9. *Underlying data and robust linear model fit (red line) for the CURE frontrunner cities calculated for a radius of 30km around the city center.*

3.4 Stakeholder needs addressed by the application

AP02 addresses the stakeholder needs of both local city planners, but also larger scale policy makers. It can assist urban planners to optimize their adaption strategies with regard to heat stress, and sustainable development optimization. An intended use-case scenario for the roll-out of such an app could be the relative ranking of SUHII vulnerability of different cities, for example on a national level. This demonstrator app will provide the functionality for the CURE front-runner cities. The stakeholder needs identified in D1.1 and addressed by AP02 are lined out in detail in Table 3.

Table 3. *Requirements as defined in D.1.1 with relevance to AP02 (left column) and how these requirements are met by AP02 (right column).*

G.1: CURE should use and provide access to the most recent data for different applications	AP02 will exploit Landsat and Sentinel-3 data as well as, amongst others, the most recent CLMS IMD HRLs.
G.2: CURE should provide single point of access for various datasets of different applications through one map.	Does not apply to AP02, since it is not a spatially explicit product.

G.3: CURE should provide the possibility to extract timeseries at specified coordinates through APIs	Time-series of SUHII values per city will be provided.
G.4: CURE should provide high resolution data and high frequency data e.g., hourly dynamics of heat emission	The employment of Sentinel-3-based LST information shall potentially enable most likely down to weekly updated.
G.5: CURE should be able to use and provide data combination of satellite-based, EU databases and local data	AP02 combines, via the output of AP01, the satellite-based thermal information with CLMS data.
G.6: CURE should compare and/or validate CURE application outputs with other existing data sources such as local climate zones from wudapt database	It is intended to compare the results based on CLMS IMD HRLs and an improved PIS product derived following the framework of the World Settlement Footprint.
G.7: CURE should provide data outputs including […] imperviousness […]	Imperviousness data relied upon in AP02 are already published via the CLMS.
G.13: CURE should provide interoperability i.e. ability to interface with existing or future information systems in cities	Through the ability to output json or csv data, the outputs of AP02, are ready to be easily and effectively integrated into cities' information systems.
G.13: access requirements	Given the non-spatially explicit nature, AP02 outputs will be provided as downloads.
B.1: Berlin's main interest is in climate and energy related applications including	SUHII estimation over Berlin will be performed for multiple years
B.4: The scope of the application should be the whole city as it falls within the scope of the urban climate.	The whole city of Berlin is considered. In addition, delineation of the thermally relevant footprint will include some part of the non-urban matrix, hence delineating the spatial scope of urban climate.
C.3 CURE applications should assess the environmental […] impact of tree plantation in Copenhagen.	While AP02 cannot perform explicit forecasting of the SUHII, it provides a retrospective analysis of SUHII development since 2006, which would be sensitive to potential changes in urban green inventory.

C.5' Urban heat, heat island assessment, noise and correlation with health can provide useful insights for planning and decision making. CURE applications could investigate the above correlation through satellite and local data.	Health modelling is out of scope for this app, yet the SUHII assessment could serve as input predictor for such models in the future.
H.1: Heraklion is interested in the following CURE applications: Surface Urban Heat Island […]	This is supported via AP01 and AP02.
H.2: The scale of CURE applications, especially, heat related applications should be local.	The primary output of AP02 is not spatially explicit.
H.3: Heraklion wants to use the most recent data i.e. from 2019 onwards, in the CURE applications.	While the PIS layer is rather static and updated on a bi-annual basis, analyses of SUHII effects may be conducted on more recent thermal data.
S.1: Sofia is interested in the following CURE applications: Local Scale Surface Temperature Dynamics, Surface Urban Heat Island Assessment […]	Is addressed via AP01 and AP02
S.3: The geographical coverage should be for the whole territory of the municipality	The whole city of Sofia is considered. In addition, delineation of the thermally relevant footprint will include some part of the non-urban matrix, hence delineating the spatial scope of urban climate.
S.6: CURE applications […] machine readable text format and shape files with attributive information.	AP02 will output machine readable formats json or csv. If needed it may provide the delineated urban area as vector data with SUHII attributes.
S.7: In terms of data access, CURE should provide file download access mechanism for Sofia.	AP02 will provide download access in the form of json or csv format.
S.8: Sofia is primarily interested in the most recent data. CURE applications should use	While the PIS layer is rather static and updated on a bi-annual basis, analyses of SUHII effects may be conducted on more recent thermal data. Retrospective analyses

historical data to perform retrospective analysis	will be conducted beginning with 2006, given PIS and LST data availability.
S.11: A number of UHI and modelling studies have been performed in the past and these studies should be used for developing and cross-comparing with the specific CURE application	The already published studies provide valuable reference information and will be used for comparison.

4 AP03 URBAN HEAT EMISSIONS MONITORING

4.1 Purpose of the Application

Urban heat emission refers to the turbulent sensible heat flux, i.e. the heat exchange between the urban surface and the atmosphere. The sensible heat flux defines the amount of energy that is available for heating the urban atmosphere and it is thus closely related to air temperature. This amount of energy is strongly modified by the properties of the surface (land cover/ land use, 3D geometry) and the input of heat by human activities (traffic, buildings, industry). The localization of hot spots of high heat emissions will help urban planners to optimize their adaption strategies also regarding heat stress, urban green space and building development.

4.2 Data & Methodology

CURE AP03 is based on the Aerodynamic Resistance Method (ARM) for the estimation of sensible heat flux Q_H at local scale (Voogt and Grimmond, 2000). The ARM was successfully applied in the former URBANFLUXES project (Chrysoulakis et al., 2018) for the calculation of citywide sensible and latent heat flux in a spatial resolution of 100 m x 100 m. In CURE, the ARM implementation described in Feigenwinter et al. (2018) is further developed and adapted to suit the requirements of CURE end users, i.e. city planners and stakeholders. The model results are evaluated with in-situ turbulent sensible heat fluxes measured by the Eddy Covariance (EC) method at urban flux towers (Feigenwinter et al., 2012).

4.2.1 Input data

In a first step, AP03 will rely mainly on local (non-Copernicus) data to produce a first implementation of the application. In a second step, the local input data is replaced by Copernicus data, where possible.

- Digital Object Model (DOM): A high resolution (1 m x 1 m) model of buildings and trees is the essential base for calculation of roughness parameters and aerodynamic resistances (see Section 4.2.2).
- Land Surface Temperature (LST): For the LST layer, AP03 relies on land surface temperature data developed and processed in AP01
- Meteorological data: Air temperature, humidity, wind velocity, wind direction, radiation from in-situ measurements
- Turbulent fluxes for evaluation: in-situ measurements from urban flux towers equipped with Eddy Covariance systems

Table 4 provides an overview of the datasets used in AP03.

Table 4. *Input data for AP03 (local and Copernicus).*

Data	Local	Copernicus service
DOM	Available in high resolution for front-runner city Heraklion and follower-city Basel (buildings and trees)	CLMS building heights CLMS street tree layer
LST	LST derived from upwelling longwave radiation measurements for evaluation of AP01 LST product	AP01 LST product
Meteorological data	In-situ measurement network	C3S ERA5 Reanalysis data
Turbulent sensible heat flux Q_H	In-situ EC flux tower	

4.2.2 Methodology

The estimation of sensible heat flux with remote sensing data is based on the bulk transfer approach (Yang et al., 2019), where the surface temperature is derived from satellite data. An implementation of the bulk transfer method is ARM (Voogt and Grimmond, 2000), which is used in several microscale urban climate models.

ARM uses the Monin-Obukhov similarity theory (MOST) (e.g. Foken, 2006) as the theoretical basis to estimate momentum and scalar fluxes in the atmospheric surface layer. MOST is commonly used in meteorological numerical modeling systems. In the MOST framework, roughness lengths for momentum and heat (z_{0m} and z_{0h}, respectively) are the key parameters identifying the aerodynamic features of underlying surfaces (Kanda et al., 2007).

The ARM is a common approach for modelling surface fluxes. Q_H is basically calculated as

$$Q_H = c_p \rho \frac{T_0 - T_A}{r_H} \qquad (4.1)$$

where c_p is the heat capacity of the air (J kg^{-1} K^{-1}), ρ is the air density (kg m^{-3}), T_0 is the surface temperature (K), T_{air} is the air temperature (K) and r_H is the bulk aerodynamic resistance for heat (s m^{-1}) of the complete 3D urban surface (Crawford et al., 2018). T_0 is replaced with the satellite-derived LST product from AP01. Using the radiative surface temperature instead of T_0 requires the completion of r_H with a radiometric excess resistance (Voogt and Grimmond, 2000).

In detail, the aerodynamic resistance for heat r_H will be calculated with

$$r_H = \frac{1}{u_* k}\left[ln\left(\frac{z-z_d}{z_{0m}}\right) - \psi_h\left(\frac{z-z_d}{L}\right) + \ln\left(\frac{z_{0m}}{z_{0h}}\right)\right] \qquad (4.2)$$

$$u_* = Uk\left[ln\left(\frac{z-z_d}{z_{0m}}\right) - \psi_m\left(\frac{z-z_d}{L}\right) - \psi_m\left(\frac{z_{0m}}{L}\right)\right]^{-1} \qquad (4.3)$$

where $u*$ is the friction velocity, k is the von Karman constant (0.4), z refers to a reference height (usually the height of wind measurements), z_d is the zero-plane displacement height, L is the Monin-Obukhov length, z_{0m} and z_{0h} are the roughness lengths and $\psi_{m,h}$ are the stability functions for momentum and heat, respectively. Equation (4.3) can be used to estimate $u*$ from wind velocity U, if no direct measurements of the friction velocity is available. z_{0h} values are usually reported as the dimensionless number $k\beta^{-1}$, defined as

$$k\beta^{-1} = ln\left(\frac{z_{0m}}{z_{0h}}\right) \qquad (4.4)$$

$k\beta^{-1}$ is a key parameter in the ARM. In literature, reported values for $k\beta^{-1}$ show a large variability, even for similar types of surfaces. Lowest values of around 2 correspond to homogeneous vegetative surfaces (Brutsaert 1982), but also to flat semi-arid areas (Koshiek et al. 1993). Higher values are reported for heterogeneous surfaces and urban land use classes, e.g. with values around 20-27 for a light industrial site as reported by Voogt and Grimmond (2000). Kato and Yamaguchi (2007) list values for $k\beta^{-1}$ of 7 (industrial, urban, forest), 4.6 (grassland) and 3.9 (lawn, bare soil). Several studies used Eddy Covariance (EC) and/or scintillometry measurements to determine $k\beta^{-1}$ in the footprint of their measured fluxes. z_{0h} may also be calculated from the roughness Reynold's number (e.g. Kanda et al., 2007)

$$z_{0h} = z_{0m}[7.4\ exp(-\alpha Re_*^{0.25})] \qquad (4.5)$$

where α = 1.29 and $Re*=z_{0m}u*/\nu$ is the roughness Reynolds number with a kinematic molecular viscosity ν of 1.461 × 10^{-5} ms^{-1}. This z_{0h} value is used in Equation (4.4) for the calculation of aerodynamic resistance r_H.

The Urban Multi-scale Environmental Predictor (UMEP, Lindberg et al., 2018) provides the framework for calculation of the spatial distribution of roughness parameters and derived aerodynamical resistances needed for the calculation of Q_H in Equation (4.1) with the input data listed in Table 4. The zero-plane displacement height z_d is calculated after Kanda et al. (2013), using additional morphological parameters like the plan area index λ_p and the frontal area index λ_f.

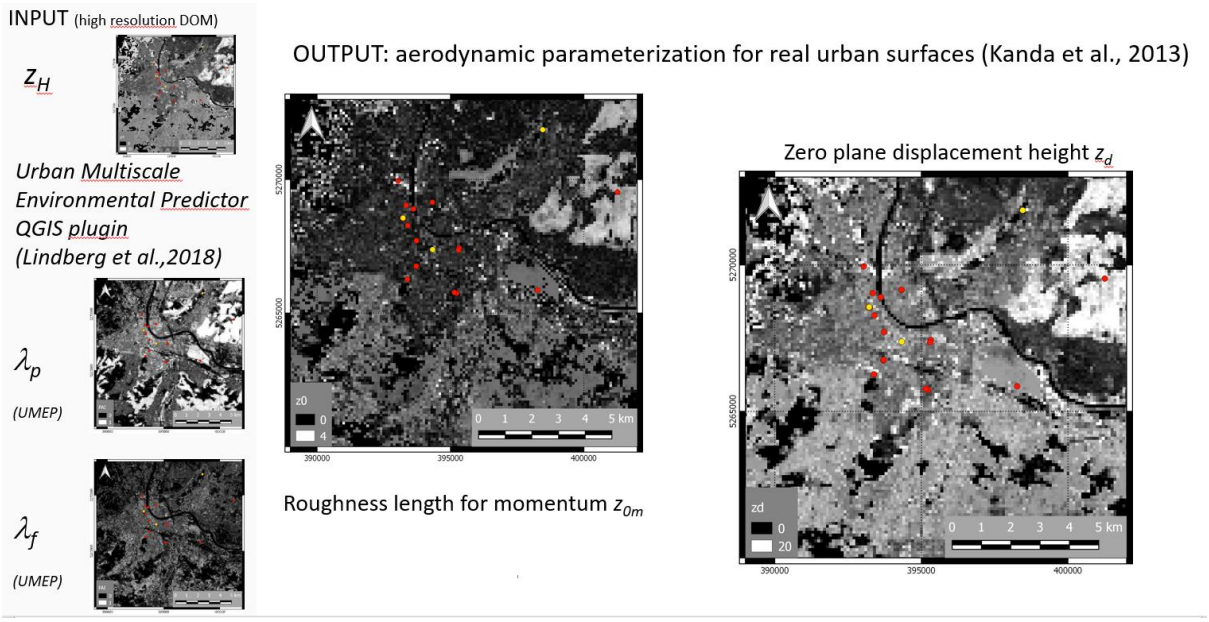

Figure 10. *UMEP input (left) and output of roughness parameters for calculation of aerodynamic resistance.*

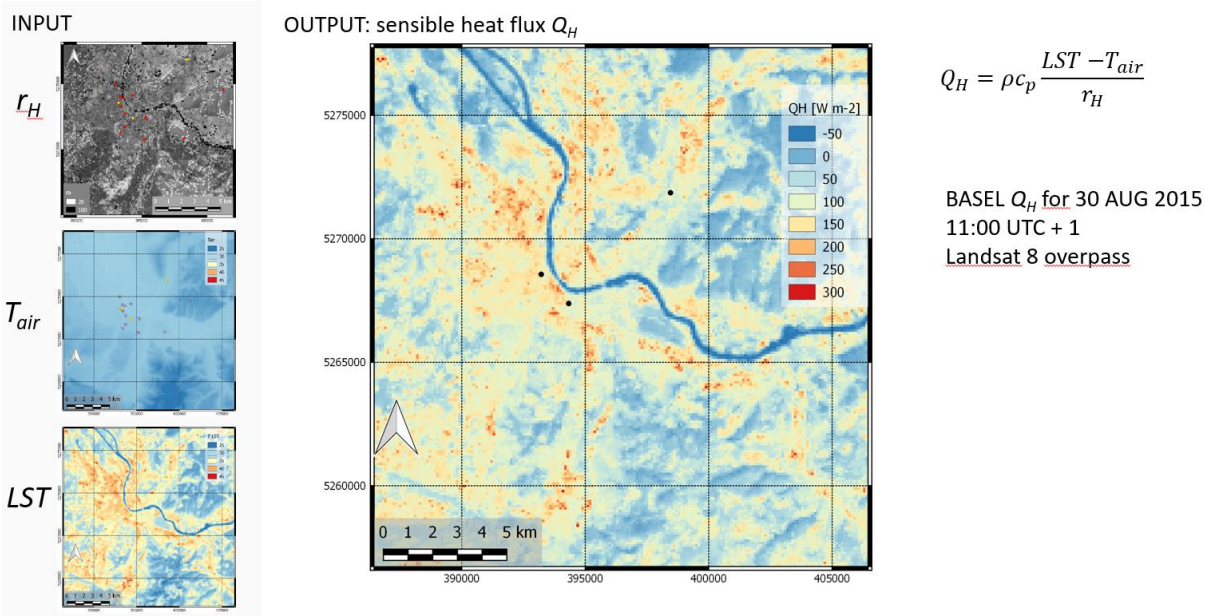

Figure 11. *Final calculation of spatial distribution of Q_H. Example from URBANFLUXES presented at JURSE, 6-8 MAR 2017, Dubai.*

4.2.3 Uncertainty, limitations and validation

A comparison of measured sensible heat fluxes with weighted modelled fluxes in the footprint of the flux towers in the frame of the URBANFLUXES project showed that measured Q_H were generally higher for all case study cities. Several reasons may lead to these differences, as discussed in Feigenwinter et al. (2018): The uncertainty inherent to EC measurements for Q_H is in the range of 10% (25% for other trace gases), the representativeness of flux tower

measurements in urban environments is reduced compared to rural areas due to the heterogeneity of urban neighbourhoods and there are large (inherent) variations in EC measurements between the averaging intervals which additionally increase the uncertainty for the time of the satellite overpass. There are also known drawbacks of the ARM method: input parameters (T_{air} , friction/wind velocity) have to be spatially derived from in-situ measurements (flux towers and/or sensor networks) and may differ from "true" values in certain areas during satellite overpass; further large uncertainties exist in the calculation of the aerodynamic resistance including $k\beta^{-1}$. Figure 12 shows the deviations between measured and modelled values of QH for two flux tower sites (adapted from the URBANFLUXES project).

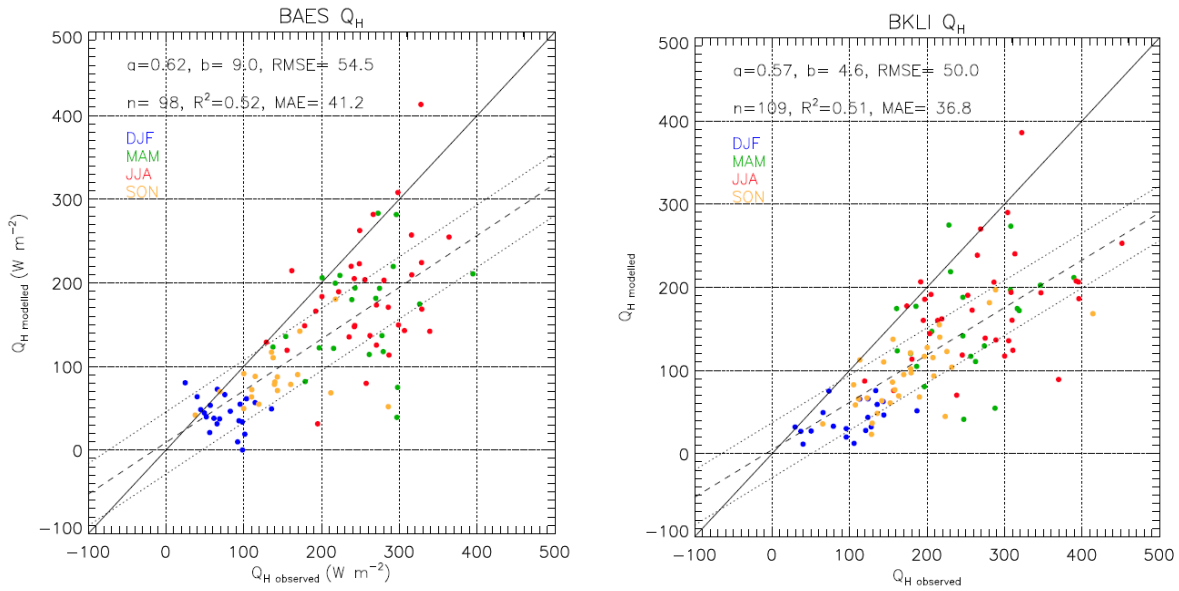

Figure 12. *Differences between measured and modelled Q_H for two flux tower sites in Basel, Switzerland.*

Since the deviations are systematic, we hypothesize that the differences are related to the anthropogenic heat flux, which may not be considered in the ARM method but is measured by the EC system. It is planned to further investigate this topic until M24 of the CURE project.

4.3 Output features & characteristics

AP03 will be applied to front-runner city Heraklion and follower city Basel. The outcome are maps with sensible heat flux distribution in the area of interest of the respective city. Maps are provided as GeoTiffs in a 100 m x 100 m resolution. The time range and time resolution depend on the frequency of the AP01 LST product. Stakeholders are able to identify hot spots of heat emissions for different times of the day in different seasons. This will support decisions that will be taken to reduce heat emissions and heat load. Figure 13 shows an example for Basel as published in Feigenwinter et al. (2018).

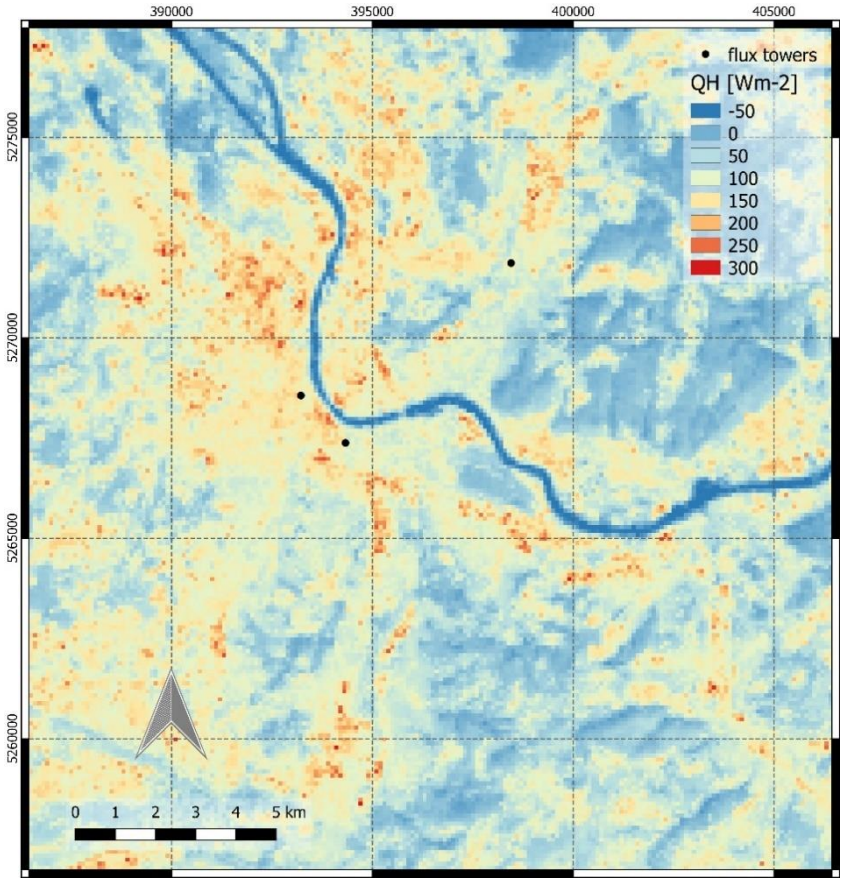

Figure 13. *Example demonstration for the urban heat emission monitoring application AP03 (adapted from Feigenwinter et al., 2018)*

4.4 Stakeholder needs addressed by the application

AP03 addresses the stakeholder needs of both local city planners, but also larger scale policy makers. It can assist urban planners to optimize their adaption strategies with regard to heat emissions. The stakeholder needs identified in D1.1 and addressed by AP03 are lined out in detail in Table 5.

Table 5. *Requirements as defined in D.1.1 with relevance to AP03 (left column) and how these requirements are met by AP03 (right column)*

G.1: CURE should use and provide access to the most recent data for different applications	AP03 relies on the LST product of AP01
G.3: CURE should provide the possibility to extract timeseries at specified coordinates through APIs	Not possible for time series based on time of the day, but for seasons

G.4: CURE should provide high resolution data and high frequency data e.g., hourly dynamics of heat emission	Not possible, because hourly LST are not available
G.5: CURE should be able to use and provide data combination of satellite-based, EU databases and local data	AP03 combines, via the output of AP01, the satellite-based thermal information with local data and Copernicus services
G.6: CURE should compare and/or validate CURE application outputs with other existing data sources such as local climate zones from wudapt database	AP03 maps are validated with in-situ flux measurements. A model comparison is out of the scope of AP03
G.7: CURE should provide data outputs including […] 2D/3D city model, building heights. LULC etc. […]	This is not application specific, but a general service. AP03 input data are provided
G.9: CURE should provide various simulations	AP03 is not designed to perform simulations
G.12: CURE should provide early warning system e.g., issuing an alert when a threshold is reached such ..., urban heat...	AP03 is not suitable for an early warning system
G.13: CURE should provide interoperability i.e. ability to interface with existing or future information systems in cities	If GeoTiffs are accepted, outputs of AP03 are ready to be integrated into cities' information systems.
G.22: CURE should provide information on day vs night peaks	AP03 provides maps for daytime and nighttime
H.1: Heraklion is interested in the following CURE applications: ... Urban Heat Emission Monitoring...	AP03 will provide heat emission monitoring in Heraklion
H.2: The scale of CURE applications, especially, heat related applications should be local to make it usable.	AP03 will be provided in a 100 m x 100 m resolution
H.3: Heraklion wants to use the most recent data, i.e. from 2019 onwards, in the CURE applications	AP03 maps are dependent on the availability of the AP01 LST product

5 AP04 URBAN CO_2 EMISSIONS MONITORING

5.1 Purpose of the Application

The total urban CO_2 emissions have a spatial dimension due to the heterogeneous nature of urban land use/land cover and urbanization. In this CURE application AP04, the CO_2 emissions are partitioned into an anthropogenic (traffic, heating/cooling) and a biogenic component (urban green space). Spatial planning strategies have an influence on the urban form, and consequently affect CO_2 emissions through changes in traffic patterns, energy consumption and location and extent of urban green areas. Knowing the portion of the anthropogenic and the biogenic part of CO_2 emissions in a high spatial resolution (neighborhood scale) will provide urban planners with an additional decision support tool for developing emission reduction strategies.

5.2 Data & Methodology

CURE AP04 will be developed for retrieving CO_2 emissions within city boundaries in neighborhood scale, combining local scale CO_2 flux measurements by Eddy Covariance (Stagakis et al., 2019) with surface parameterization based on Land Use/ Land Cover (LULC) classification derived from VHR satellite data and CLMS products through the most up-to-date turbulent flux source area model (Kljun et al. 2015). The individual processes contributing to the total CO_2 emissions will be statistically modelled and scaled up according to the associated land cover/use type and environmental controls derived from CAMS and C3S.

Note that at the time of this document submission, AP04 is in a less mature state, because the method presented in Stagakis et al. (2019) is currently being adapted and further developed for integration into the CURE cross-cutting application system and interface. Preparation activities include processing of the input data with focus on quality assessment and quality control (QA/QC) of the Eddy Covariance CO_2 fluxes.

5.2.1 Input data

AP04 is based on a mix of local data, products from ESA- and Copernicus data sources and pure Copernicus services. Key data sets are the Land Use/Land Cover (LULC) maps with extension of the road network/traffic data and the CO_2 fluxes from urban flux towers.

- LULC maps: A high resolution (1.6 m x 1.6 m) map derived from very high resolution (VHR) satellite data and provided by FORTH. This LULC will be extended with the road network from OpenStreetMap
- Turbulent fluxes of CO_2: in-situ measurements from urban flux towers equipped with Eddy Covariance systems. The core data set of AP04 to be used for assigning LULC contributions to the total flux.
- Meteorological data: Air temperature, humidity, wind velocity, wind direction, radiation from in-situ measurements. Needed for flux footprint calculation.

- Digital Object Model (DOM): A high resolution (1 m x 1 m) model of buildings and trees is the essential base for calculation of sectorial roughness parameters as input for the flux footprint model.

Table 6 provides an overview of the datasets used in AP04.

Table 6. *Input data for AP04 (local and Copernicus).*

Data	Local	Copernicus service
Land Use/Land Cover map	Available in high resolution for front-runner city Heraklion and follower-city Basel based on VHR satellite data	CLMS urban atlas
DOM	Available in high resolution for front-runner city Heraklion and follower-city Basel (buildings and trees)	CLMS building heights CLMS street tree layer
Road network and traffic data	OpenStreetMap, TomTom traffic statistics product, traffic counts (if available)	
Meteorological data	In-situ measurement network	C3S ERA5 Reanalysis data
Turbulent CO_2 flux F_C	In-situ EC flux tower	
CO_2 concentration and fluxes		CAMS Flux inversion reanalysis of global CO_2
Energy/Fossil fuel consumption	From city authorities, where available	

5.2.1.1 LULC and road network

The concept of LULC map from the former H2020 URBANFLUXES project (Chrysoulakis et al., 2018) is the base for LULC classification used in AP04. This classification is extended with the road network from OSM, because traffic is one of the main sources of CO_2 emissions in general and in the front-runner city Heraklion in detail. Figure 14 shows the LULC classification with road network.

Figure 14. *LULC map of the HERAKLION city center extended with OSM network.*

Because there are no traffic data available for the front-runner city Heraklion we are currently evaluating a trial set of the traffic statistics from the TomTom Historical Traffic Services (https://support.move.tomtom.com/ts-introduction/) and its Traffic Stats product. If the data set proves to be suitable for partitioning traffic emissions in AP04, we intend to order more data. Figure 14 shows an example of the capabilities of this data set. For each street node, "hits", i.e. the number of vehicles, are available in hourly resolution. Since the road is in the area of the main contribution to the total flux (red and yellow colors of the flux footprint), this dataset may be an adequate substitute for automatic permanent traffic count locations.

5.2.1.2 Eddy Covariance flux tower data

CO_2 fluxes from the Heraklion flux tower measured by the Eddy Covariance (EC) method are available from November 2016 to date, with a large gap due to technical problems from November 2018 to July 2019. A detailed description of the EC method in general can be found in Aubinet et al. (2012), while Feigenwinter et al. (2012) refers to the specific issues of EC measurements in urban environments. EC raw data (20 Hz) were processed with the EddyPro® Software version 7 from LI-COR Biosciences resulting in half hourly CO_2 fluxes and numerous diagnostic parameters. A very useful diagnostic parameter is the quality flag calculated after the method of Foken et al. (2004) which provides the flag "0" for high quality fluxes, "1" for intermediate quality fluxes and "2" for poor quality fluxes. This system is suitable for selecting flux results complying with international practices.

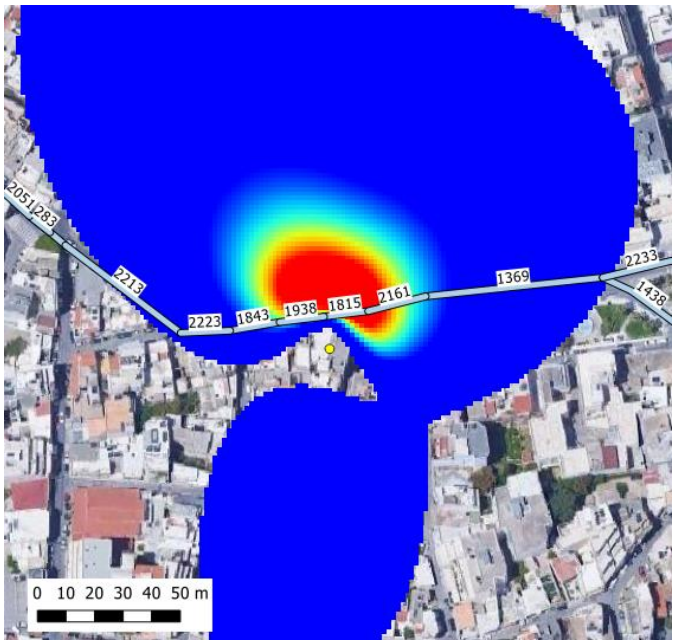

Figure 15. *TomTom road nodes (numbers) with hourly vehicle counts in the footprint of the HERAKLION flux tower (yellow dot). Colors refer to relative contributions to the total flux from high (yellow) to low (blue).*

Figure 16 exemplarily shows the data availability and the data quality of half hourly Heraklion CO_2 fluxes for the months JUL/AUG/SEP 2018. For all further processing only fluxes with flags 0 and 1 are used.

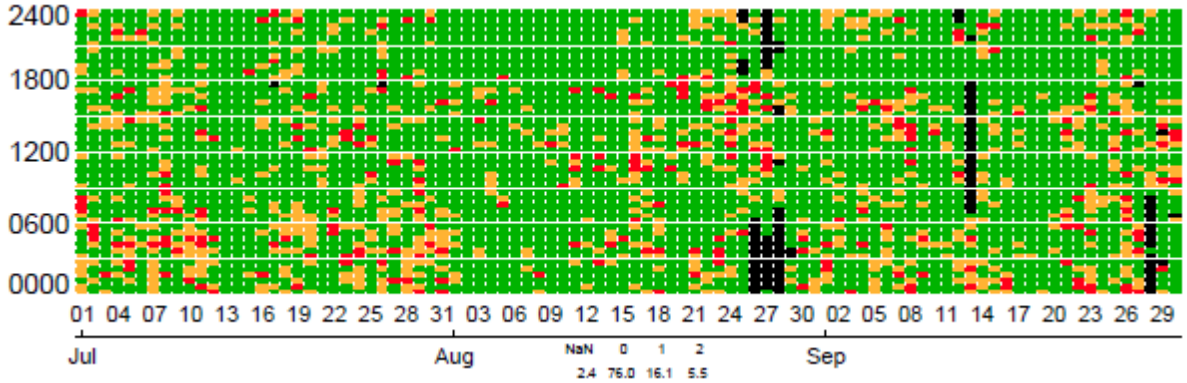

Figure 16. *Data availability for and data quality of HERAKLION CO_2 fluxes for JUL/AUG/SEP. Green, orange and red colors refer to quality flags 0,1,2 (high, intermediate, poor), respectively. Black colors refer to "no data".*

5.2.2 Methodology

The approach for estimating within urban boundaries' CO_2 emissions (excluding industrial processes) will be based on statistical modelling of all individual source and sink processes in the urban environment, according to the following equation:

$$F_C = E_V + E_b + R_H + R_S + (R_V - P_V) = E_V + E_b + R_H + F_{bio}$$

where, F_C is the net CO_2 flux, E_V concerns emissions from fossil fuel combustion by motor vehicles, E_B is emissions from combustion within buildings (e.g., for heating), R_H is the

metabolic release of CO_2 by human respiration, R_S is the below-ground soil, root, and waste microbial respiration, R_V is the above-ground vegetation respiration, and P_V is the CO_2 assimilation by photosynthesis. The term $R_S + (R_V - P_V)$ is compiled into F_{bio}, i.e. the biogenic part of the total flux F_C. The method will combine local scale CO_2 flux measurements by Eddy Covariance with geospatial information of urban form parameters through analytic source area modelling (Crawford and Christen, 2014, Stagakis et al., 2019). The turbulent flux source area model (Kljun et al., 2015) will be applied and parameterized based on detailed urban morphology indicators. The relationships between LULC classes, building morphology, population density and the measured F_C will be defined through multiple regression analyses. Traffic profiles and air temperature derived heating degree days will be auxiliary parameters for E_V and E_B modelling. R_H model will be based on spatially aggregated population statistics (Christen et al., 2011). Since the vegetation fraction in the footprint of the Heraklion flux tower is very small, the biogenic portion F_{bio} will be negligible. Therefore, a simple empirical model based on NDVI and environmental controls is proposed for estimating F_{bio} (e.g. Del Grosso et al., 2018). Individual models will be scaled up to the urban boundaries, reaching daily to monthly local scale city-wide maps, and then synthesized to net CO_2 flux products.

5.2.2.1 Mean seasonal diurnal fluxes and footprint calculation

For the final AP04 product we propose an approach based on seasonal mean diurnal fluxes and the corresponding averaged footprints, i.e. the footprint climatology. Figure 17 shows the mean diurnal course of CO_2 fluxes for the meteorological seasons winter (DJF), spring (MAM), summer (JJA) and autumn (SON) for the years 2017 to 2020. The bi-modal shape indicates that traffic (rush hours) are the main driver of CO_2 emissions in the footprint of the HERAKLION flux tower. It is therefore important to have detailed information about traffic in order to correlate the CO_2 fluxes with traffic frequencies. From Figure 17 it is also obvious, that heating in the winter plays a minor role since no increase of the mean daily total emission is observed. On the other hand, also no significant signal from F_{bio} is observed, because this would exhibit lower emissions due to photosynthesis in the vegetation period. Mean half hourly footprints are calculated by averaging the available footprints for each half hour in a similar way (not shown). The mean diurnal courses of CO_2 fluxes and the average footprints will be used for further processing as described in the previous section.

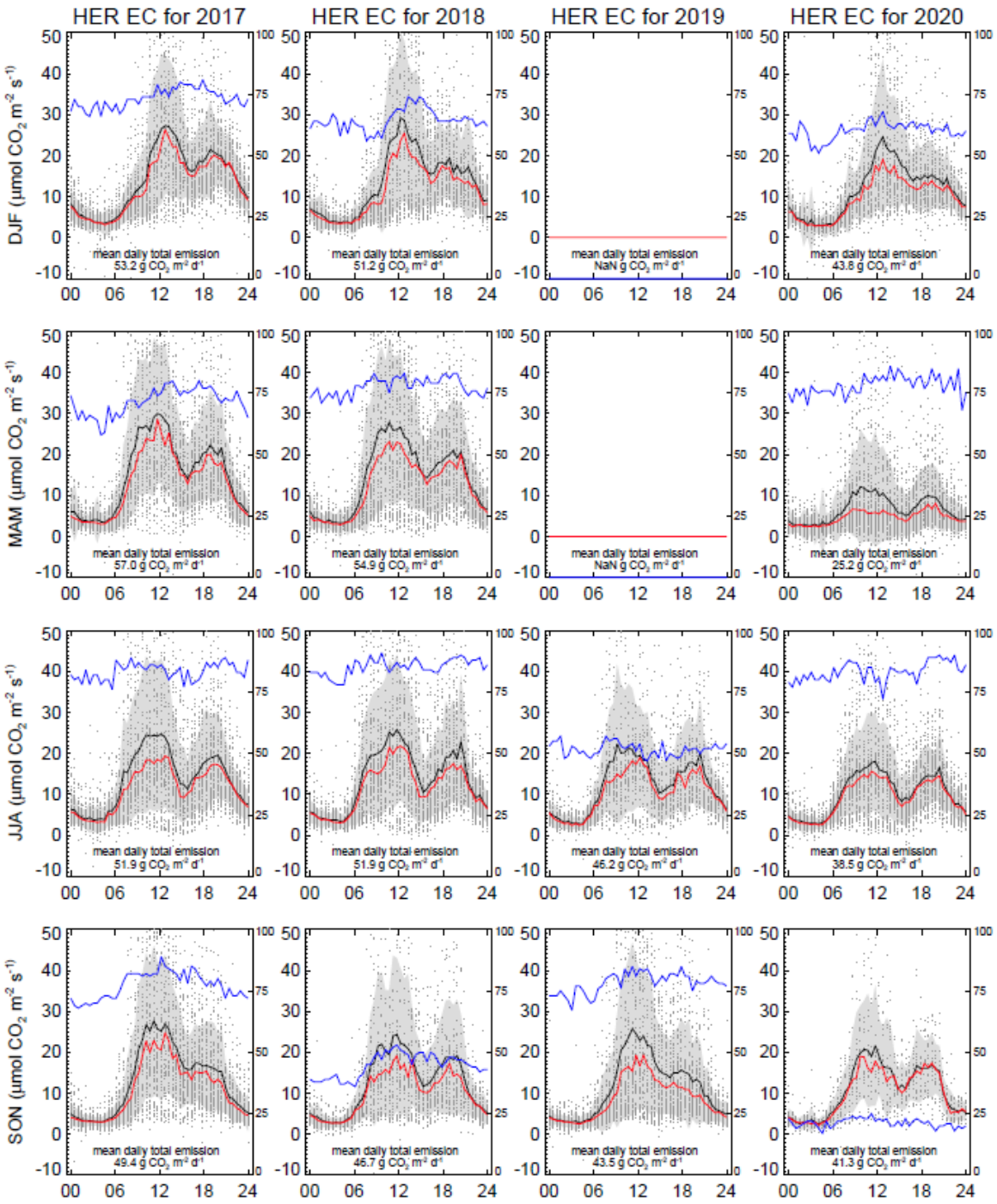

Figure 17. *Mean diurnal course of F_C for all seasons (top to bottom) and years 2017 to 2020 (left to right) with mean daily total emissions. Arithmetic mean (black), median (red), standard deviation (gray shaded) and single half hourly values (dots). The blue curve refers to the number of measurements used for averaging and scales with the right y-axis (max. number of measurements is around 90 days for a season).*

5.3 Output features & characteristics

AP04 will be applied to front-runner city Heraklion and follower city Basel. The outcome are maps with estimated CO_2 emissions in the area of interest of the respective city. Maps are provided as GeoTiffs in a 100 m x 100 m resolution. In a first step we will provide seasonal maps for the year 2018 and 2019 with a time resolution of some hours, e.g. CO_2 emissions for winter (DJF) 2018 from 0-4 h, 4-8 h, 8-12 h, 12-16 h, 16-20 h and 20-24 h. Extension to year 2020 is an option. Stakeholders are able to identify and quantify hot spots of CO_2 emissions for different times of the day in different seasons. This will support decisions that will be taken to reduce CO_2 emissions. No examples are available at the time of D3.1 publication (M12).

5.4 Stakeholder needs addressed by the application

AP04 addresses the needs of city planners and city stakeholders to optimize their adaption strategies regarding hotspots of CO_2 emissions. The stakeholder needs identified in D1.1 and addressed by AP04 are lined out in detail in Table 7.

Table 7. *Requirements as defined in D.1.1 with relevance to AP04 (left column) and how these requirements are met by AP04 (right column)*

G.1: CURE should use and provide access to the most recent data for different applications	AP04 can be updated in a 6-month interval, however it is not designed for automatic updates
G.6: CURE should compare and/or validate CURE application outputs with other existing data sources such as local climate zones from wudapt database	AP04 maps will be validated with CAMS Flux inversion reanalysis of global CO_2, if feasible
G.7: CURE should provide data outputs including […] 2D/3D city model, building heights. LULC etc. […]	This is not application specific, but a general service. AP04 input data are provided
G.9: CURE should provide various simulations	AP04 is not designed to perform simulations
G.13: CURE should provide interoperability i.e. ability to interface with existing or future information systems in cities	If GeoTiffs are accepted, outputs of AP04 are ready to be integrated into cities' information systems.
G.16: CURE should be able to use traffic monitoring in anticipation for managing urban air quality	AP04 uses traffic monitoring if available, but will not make predictions

G.22: CURE should provide information on day vs night peaks	AP04 provides up to 6 maps per day for each processed season and year covering daytime and nighttime
H.1: Heraklion is interested in the following CURE applications: ... Urban CO_2 Emission Monitoring...	AP04 will provide CO_2 emission monitoring in Heraklion
H.3: Heraklion wants to use the most recent data, i.e. from 2019 onwards, in the CURE applications	AP04 can be updated in a 6-month interval, however it is not designed for automatic updates

6 AP05 URBAN FLOOD RISK

6.1 Purpose of the Application

The flood risk relevance is increasing due to ongoing climate change and related increase in the number and intensity of extreme rainfall and related flood events. The CURE AP05 Urban Flood Risk aims to support the end-users by providing information about the exposure of urban areas and people living in them to this type of natural hazard. In particular, the app will focus on estimation of flood risk to community assets (in particular built-up units and population).

Thus, flood risk service will provide information on flood hazard exposure of urban units, their potential vulnerability and assets risks distribution. Moreover, the app will enable to model different scenarios of flooding events depending on intensity of precipitation and hydrological and terrain characteristics of that particular area. This will bring valuable information about local susceptibility to floods, expected flood frequency and inundation depth for each spot in the frame of the Area of Interest (AOI) and each urban land use unit, and each flooding scenario.

Thus, this service can not only bring rapid flood monitoring information about recent or on-going events and through this support effectivity of city response activities on these events, but also increase a long-term preparedness of the cities on potential future floods and help them to tailor climate adaptation activities (e.g. better anticipation of localization of most endangered units in the city and the inundation depths expected at those placed corresponding with different intensities of floods, which will allow for better spatial targeting of flood risk mitigation measures). Such kind of information support can significantly contribute to reduction of flood-related damages in the city in the future and through this to reduction of financial or other consequences of such events.

6.2 Data & Methodology

The method will be based on **combination of information about flood risk** depending on local terrain and hydrological characteristics and information about **spatial pattern**, **internal structure and temporal evolution of urban areas** and also about **distribution of population** in those areas.

The app will adopt a **"scenario modelling" approach** – i.e. scenarios representing different intensities of flood events will be modelled and compared as well as (potential) damage on urban assets and people in the cities caused by these events. This will be done based on reference information about flood events in the past and simulations of estimated intensities of expected floods in the future also in relation with different potential climate change scenarios.

6.2.1 Data inputs

The main type of input data will be represented by Copernicus Core Services datasets. This will secure high replicability (scalability) potential of the service. In particular, following datasets from Copernicus CSs will be used as the input data:

Table 8. *Input data to be used by AP05 Urban Flood Risk*

CCS	Dataset	Information on
CLMS	EU-DEM	Terrain characteristics/geomorphology
CLMS	European Image Mosaic - High Resolution	Reference information about land surface characteristics in very high resolution
CLMS	Urban Atlas	Distribution, typology and change of the urban land use units
CLMS	EU-Hydro - River Network Database	River network
C3S	E-OBS daily gridded meteorological data for Europe from 1950 to present derived from in-situ observations	Reference information about extreme rainfall events in the past
EMS	Flash flood indicators	Hydrological predictions/scenarios
EMS	Real-time river discharge forecasts	Hydrological predictions/scenarios
EMS	River discharge thresholds	Hydrological predictions/scenarios
EMS	Flood forecasts	Hydrological predictions/scenarios
EMS	River discharge reforecasts	Hydrological predictions/scenarios

These datasets can be also supplemented by the Copernicus HRL Imperviousness layer and with World Surface Footprint Evolution (WSFE) layer if needed in order to obtain more detailed information about the perviousness of urban land units and about their development in time (urban evolution).

These datasets will be integrated with local city information, where local data available with higher level of detail and when requested by the user. This may include following types of local city data/information:

- Detailed river geometry in vector format
- Detailed terrain model (DTM)/ Digital Surface Model (DSM) e.g. 0,4m DSM/DTM
- Local meteo and hydrological data (river network, runoff, discharge data, sea level)
- Reference data (information) on previous flood events – frequency, extent, inundation depth, incl. corresponding intensity of precipitation, damage on buildings, infrastructure, agricultural land etc.

- Geomorphology/Geology/Infiltration properties of local terrain/landscape
- City plans/urban planning maps - location of buildings, infrastructure, flood-vulnerable units etc.

6.2.2 Methodology

6.2.2.1 Information about flood hazard

First part of the method will be dedicated to obtaining information about flood itself. Information about flood hazard will be achieved by combination of various means:

- flood inundation extent and frequency from historical EO data
- geomorphic analysis using DEM/DSM for estimation of flood susceptibility
- modelling inundation extent and depth using runoff and discharge patterns, morphology and land cover.

For the first type of analysis, the historical Earth Observation (EO) data will serve as the input, in particular dataset from Copernicus programme. This will not only allow for evaluation of the extent and impact of past flood events, but also the Near Real Time (NRT) imageries from Copernicus service will help to include a service with a "rapid response" character, serving for monitoring and evaluation of potential ongoing flood events.

Second, the geomorphic analysis approach leading to quantification of flood susceptibility will use in particular the digital surface models in combination with the river network data, and information about basic hydrological characteristics of that area – in particular quantification of runoff representing different precipitation intensities.

The third, most advanced types of analysis will be based on sophisticated hydrologic and hydro-dynamic modelling approaches leading not only to modelling inundation extent and depth using runoff and discharge patterns, morphology and land cover, but also other advanced hydro-dynamic analysis, e.g. to compute water surface profiles for steady and unsteady flow models. For this type of analysis, the already existing hydro-dynamic modelling SWs will be exploited. At this moment, HEC-RAS[1]/GeoHECRAS[2], Telemac 2D[3] and Flo-2D[4] are considered to be used for this purpose; the pros and contras of each of these modelling suits will be assessed during the app implementation and the SW suiting best to the purposes of final application will be selected.

As a result of this first part of the analysis, raster maps representing flood susceptibility, frequency or flood extent and inundation depth for different flooding scenarios, will be generated, which can either be used on their own or combined with datasets describing urban

[1] https://www.hec.usace.army.mil/software/hec-ras/
[2] https://www.civilgeo.com/products/geo-hec-ras/
[3] http://www.opentelemac.org/index.php/presentation?id=17
[4] https://flo-2d.com/

areas in the next step, to obtain meaningful information about flood risk exposure of urban units.

The app will be able to generate results for different flooding scenarios, corresponding with different intensities of rainfall, which can then be compared by the user. The user should be able to modify this parameter to generate flood masks for his own scenarios.

6.2.2.2 Urban flood risk exposure evaluation and modelling

In this second step, the information about (potential) flood intensity will be combined with information about the land use, in particular about distribution, typology and changes of urban areas. Maps of flood susceptibility or frequency and estimations of inundation extent and depth for different flood intensities in the future will be integrated with the Copernicus Urban Atlas layer (or local land use maps if requested by the user) to get information about flood hazard to urban assets. Zonal statistics will be applied to evaluate flood risk level for each particular land use block from the Urban Atlas. This will be combined with the classification of the Urban Atlas block, to derive information about typology of the endangered urban units (residential, commercial, transportation etc. units). Moreover, data on temporal evolution of urban areas (from Urban Atlas or WSF-Evolution layer) will be combined with those about flood risk in order to gather (early-warning) information about new constructions in flood-prone areas.

6.2.2.3 Presentation of results

Information about flood hazard exposure of urban assets will be visualised in an attractive manner in a proprietary web-based platform (by GISAT), which is built on open-source components and programming languages. The basis for this platform will be common with the platform developed for the CURE AP06 – exploiting the open-source based modular framework owned by GISAT allowing to build tailor-made interactive web-based applications focusing different end-user needs for different types of thematic applications (but still with overlapping character to certain extent, coming from similar types of data presented – geo-data - and end-users targeted – administrations at different levels of city-related decision making). This platform will allow for interactive analysis of the results. The GIS layers generated by automated processes implemented in the frame of the AP05 will be exposed via WMS and presented in an interactive web map in 2D or 3D mode, allowing the user to follow the geomorphic properties of the terrain in the AOI and distribution of urban areas endangered by floods. Appropriate symbology will be used to show the quantitative and qualitative characteristics of the local flood risk.

6.2.2.4 Universal character of the application

The app will be implemented in maximally universal and automated manner, maximally exploiting the Copernicus data which are harmonized for all (larger) European cities. Thanks to this, the application will be replicable for most of the European cities (there could be some specificities which may limit replicability potential for some of the European cities, like specific

terrain characteristics etc. Second, the main added value of the application will consist in combination of the hydrological modelling (dealing with terrain morphology, river network characteristics, intensity of precipitation) with the (harmonized, for all European cities) information about spatial distribution (incl. typology as by distinguished in Copernicus Urban Atlas) and temporal evolution (UA and WSF-Evolution) of urban units.

Some general statistics (e.g. area of residential/commercial units endangered by flood risk per city) can be calculated and compared for different cities. However, taking into consideration sensitive character of such information, it should be carefully assessed which information will be presented and how it will be published (the access to such information may be restricted to several users, recruited either from administrations of particular cities for which the modelling is performed, or from European institutions). Same is fact is valid for the AP06 dedicated to urban land movements monitoring.

6.2.2.5 Link between flood risk (AP05) and land subsidence (AP06)

For effective urban planning, the integration approach is crucial. Therefore, also for the CURE project, it is important to combine information acquired by means of different applications in a meaningful way. Moreover, in case of two applications to be developed by GISAT (AP05 and 06), there can be direct link between these two types of natural hazards. The urban (or sub-urban) land subsidence can occur or intensify as a consequence of previous urban flood. On the other hand, the flood risk to particular areas in the city can increase in time, in case a land subsidence process is present at that spot.

Therefore, we aim to combine information acquired from the AP05 and 06, to enable the end-users to follow potential link (consequences) between floods and terrain subsidence. This integration is planned at least at two levels/in two different ways/:

- First, for each land use block of Copernicus Urban Atlas layer, information about both subsidence and flood risk exposure will be evaluated and presented.
- Second, we plan to visualise the results of these two apps in the same interactive web-based map application (see 6.2.2.3), so the user can easily follow and evaluate potential links between these two types of hazards.

6.3 Output features & characteristics

The outputs of this app will be represented by the GIS data on floods (frequency, extent, inundation depth, flood susceptibility, flood hazards to urban assets), which can be shared as they stand (in a form of GIS layers), or presented in a form of maps, charts (when translated to statistics) or interactive web-based visualisations. Raster layers will be used to store information about the flood extent, inundation depth, flood frequency or susceptibility. Vector layers (polygons) will be used to shore information about the vulnerability by flood risk at the level of meaningful urban units, typically Urban Atlas blocks. Examples of such analytical results are presented below.

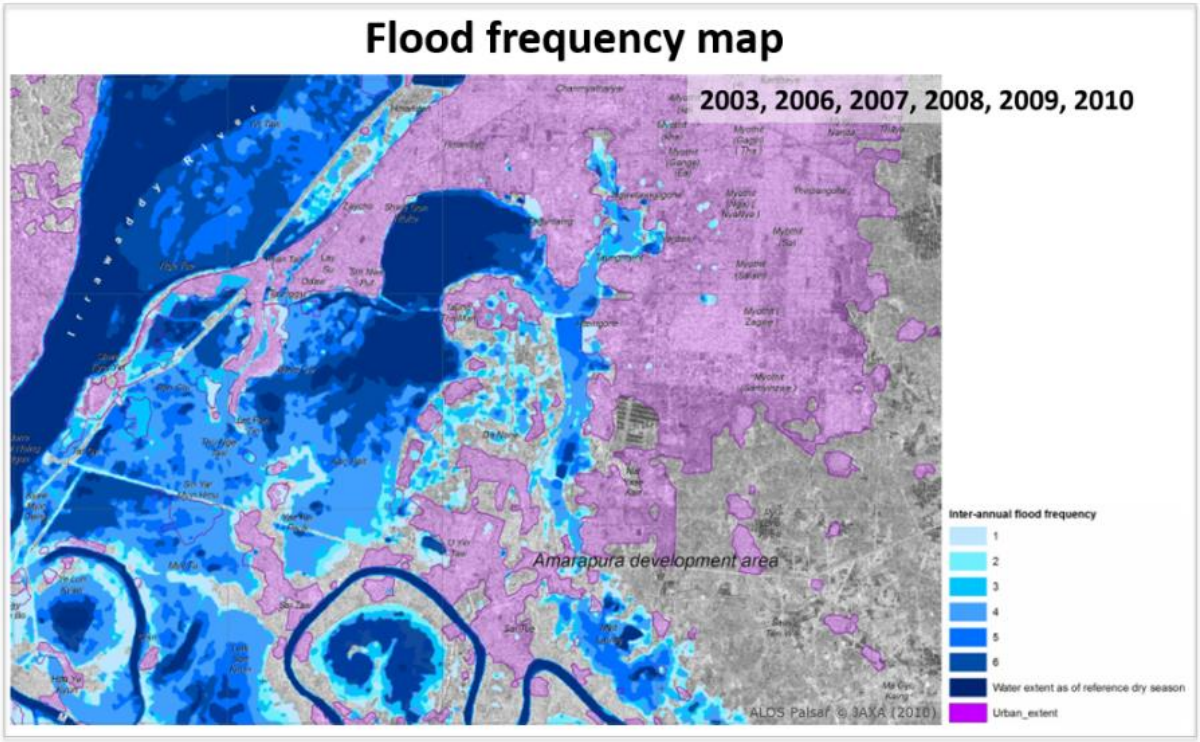

Figure 18. *Example of results of the AP05 Flood risk assessment - "Flood frequency" presented in a form of map.*

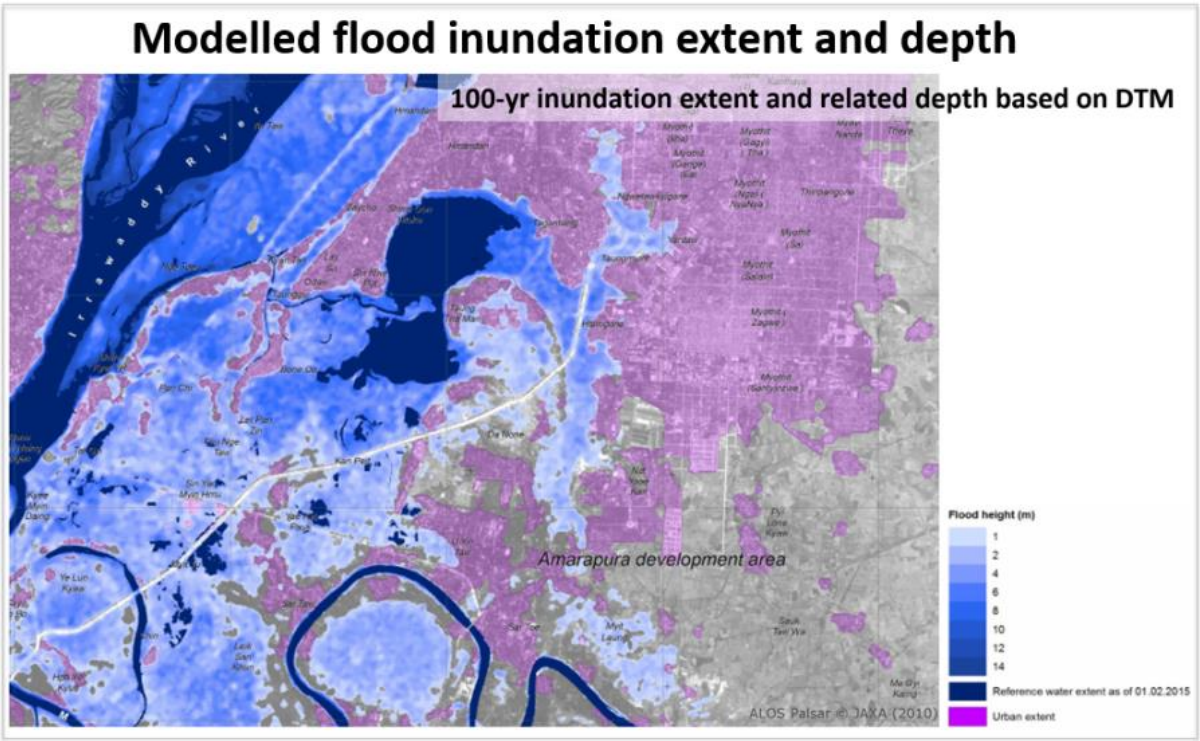

Figure 19. *Example of results of the AP05 Flood risk assessment - "Modelled flood inundation extent and depth" presented in a form of map.*

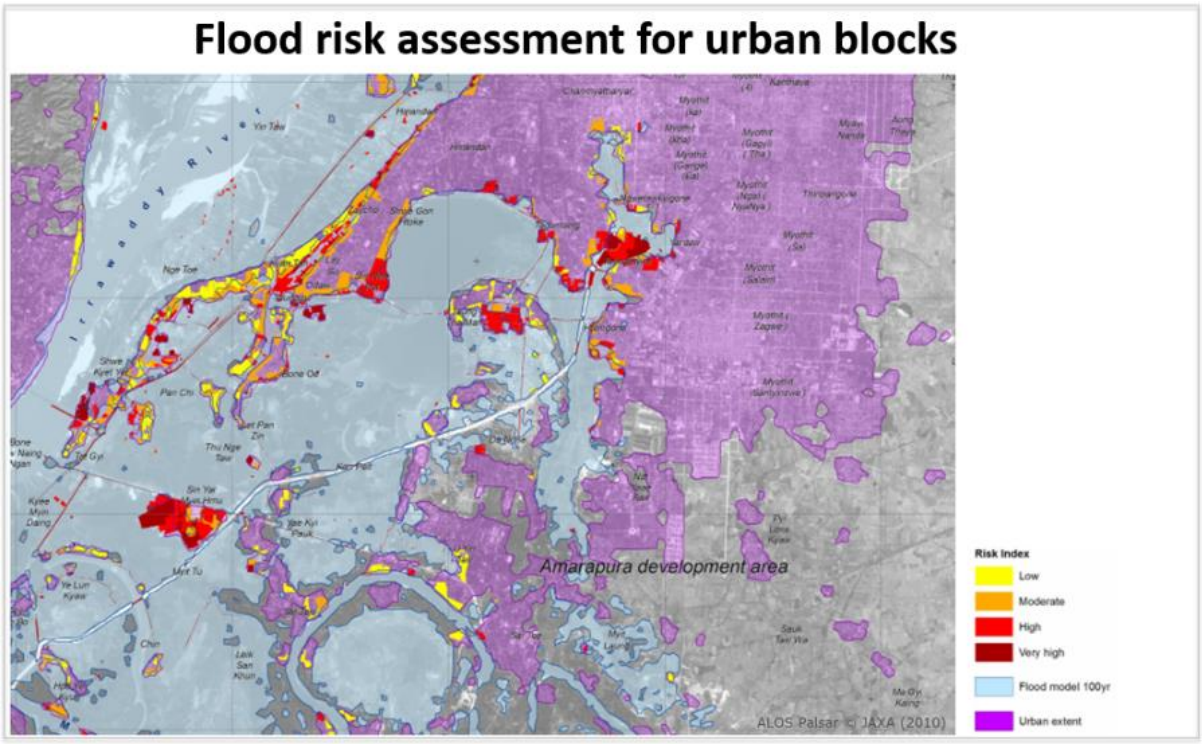

Figure 20. Example of advanced analytical results of the AP05 Flood risk assessment coming from combination of information about flood extent and inundation depth with information about distribution of urban blocks - presented in a form of map.

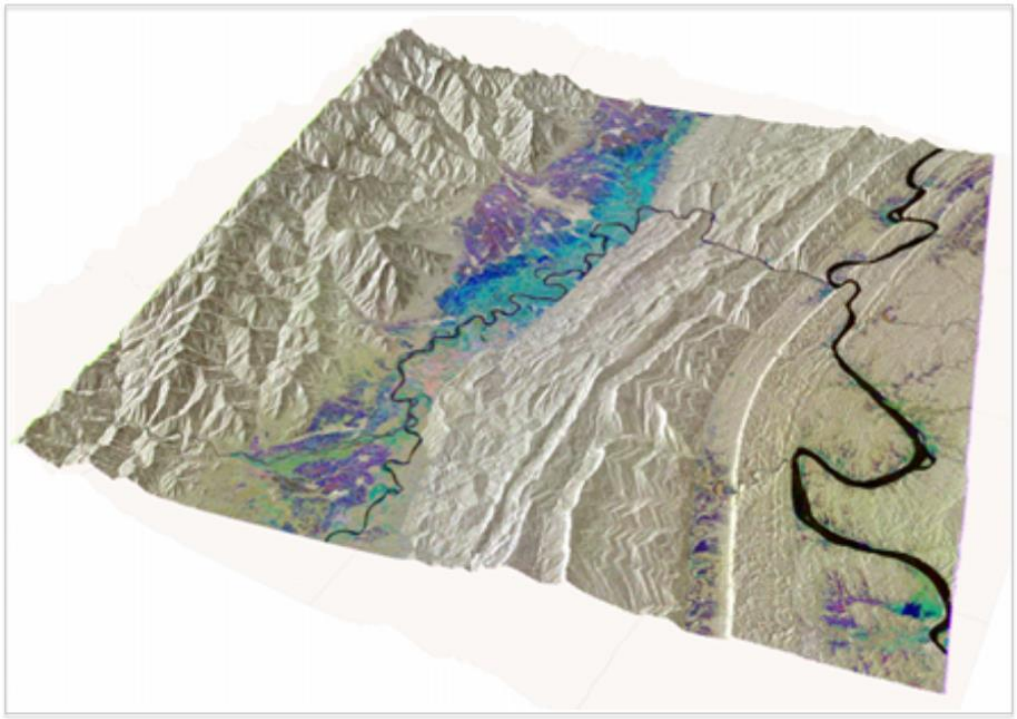

Figure 21. Visualization of the AP05 results – inundation extent and depth – in 3D mode, with DSM on the background. Our aim is to allow such 3D visualizations in dedicated web-based application.

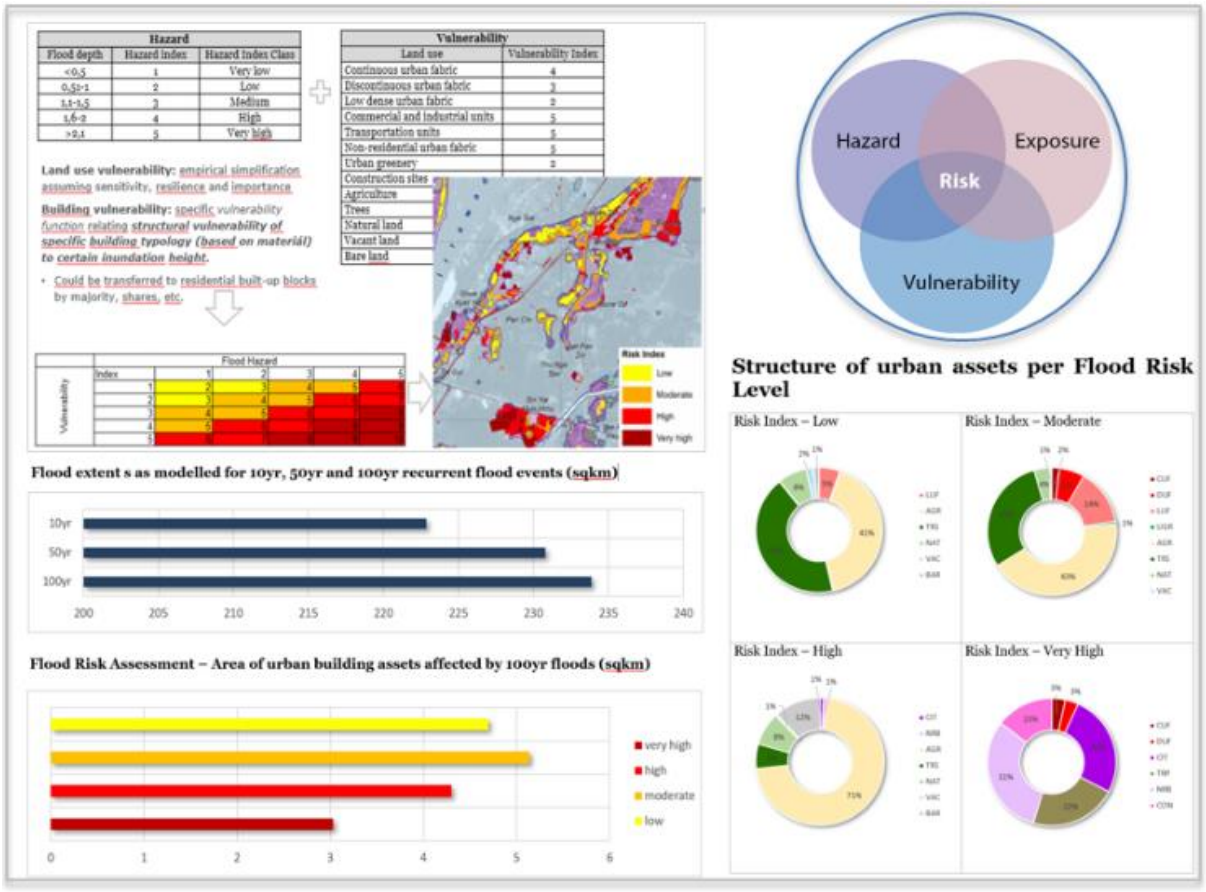

Figure 22. Example of advanced analytical results of the AP05 Flood risk assessment – quantitative and qualitative evaluation of the flood extent and flood risk to urban assets. Selected types of statistics will be automatically calculated for each flood scenario and visualized in analytical charts.

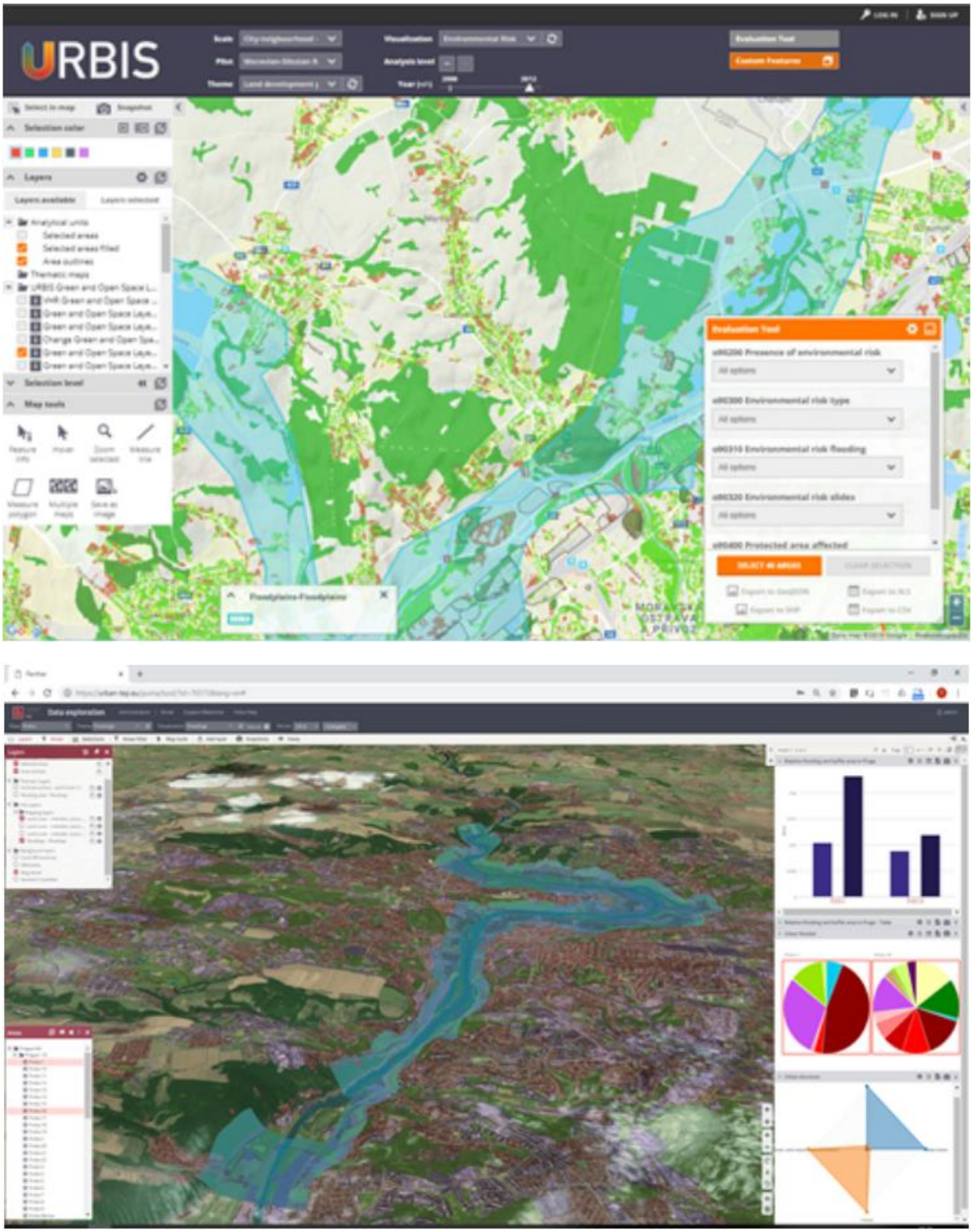

***Figure 23**. Example of interactive web-based visualization presenting flood risk assessment results. Here, the flood risk is put into relation with distribution of different types of urban units (potential development sites – up, land use blocks as classified by Urban Atlas – bottom). The application combines the map layers with statistical evaluation per administrative units and interactive analytical functionalities allowing in particular benchmarking of units of interest – by presence and level of flood hazard in combination with other relevant properties)*

6.4 Stakeholder needs addressed by the application

AP05 addresses the stakeholder needs of both local city planners but also larger scale policy makers. It can assist urban planners to optimize their adaption strategies with regard to flood risk hazard, early warning or emergency response systems. The requirements on very detailed spatial level of analysis cannot be fulfilled, due to character of application and limited spatial resolution of input data leading to limited spatial level of results (10-100meters, not in 1m). This demonstrator app will be implemented for Heraklion city (as a front-runner) in the frame of CURE project. The stakeholder needs identified in D1.1 and addressed by AP05 are lined out in detail in Table 10.

Table 9. *Stakeholder needs related to the Urban Flood Risk App 05 and our response to them.*

Stakeholder	*Requirement*	*Response*
General (G.1)	CURE should use and provide access to the most recent data.	This application will be built on the most recent input data sets that are available from both Copernicus and third-party sources, the results will be provided for most recent years 2019/2020.
General (G.1)	CURE should provide single point of access for various datasets of different applications through one map	This should be fulfilled for the two apps (AP05 and AP06) for which GISAT is responsible. It will be realized via interactive web application developed by GISAT, dedicated to visualization of the results of these two apps which will also facilitate integration of relevant additional data (e.g. local city plans)
General (G.5)	CURE should be able to use and provide data combination of satellite based, EU databases (e.g., risk behind natural events – earthquakes or other adverse events caused by climate change) and local data (i.e., sensors data, transport data including transport conditions, social activity data	This App will integrate satellite based information (NRT VHR imagery) and EU datasets (Urban Atlas, EU-DEM) and local data (hydrological information) also with third-party data with global coverage (WSF-Evolution)

	such as walkability, etc.), smart city	
General (G.6)	CURE should compare and/or validate CURE application outputs with other existing data sources such as local climate zones from wudapt database	Local data/information on torrential rains, flood events and caused damage on urban assets may be used as reference data for validation, if available
General (G.12)	CURE should provide early warning system	The app will bring information highly relevant for early warning systems of the cities on potential flood risk in future in relation with expected city-development.
General (G.13)	CURE should provide interoperability i.e. ability to interface with existing or future information systems in cities	Output formats of the results will ensure interoperability with information systems of the cities.
General (G.14)	CURE should be able to use open data from cities, National (statistics, meteorology and mapping) agencies and EU databases and other applications but this requires careful mapping to access data through APIs – few data source examples from different EU states (Portugal, Netherland, Italy, Germany etc) and Pan-European cities (Antwerp, Berlin, etc) are provided.	The app should allow for integration of local open data – in particular urban planning materials and hydrological/flood-related data, which could complement the Copernicus Urban Atlas information

General (G.18)	Other datasets which CURE should use are: CORINE land cover and land use data, Open street map data, Eurostat data, World Urban Database, Citizen science data	App uses the Urban Atlas land use data
General (G.27)	CURE applications should be easy/comfortable to use, reachable (accessibility)	Results of the AP06 will be presented in a web-based app, which will make them easily accessible and usable
General (G.31)	CURE should consider ground motion service by EEA as input to USMDR application	The EGMS will serve as a crucial input for CURE AP06 when the service will become operational
General (G.34)	CURE should consider application on Moravian Silesian region to prepare an adaptation strategy	The app will be applied for MS region in the second “follower-city” stage
Heraklion (H.1)	Heraklion is interested in the following CURE applications: Surface Urban Heat Island, Urban Heat Emission Monitoring, Urban CO2 Emission Monitoring, Urban Flood Risk and Urban Subsidence Deformation and Movement Risk.	The AP06 Urban Subsidence Deformation and Movement Risk will be implemented for Heraklion
Heraklion (H.2)	The scale of CURE applications, especially, heat related applications	He AP06 will provide information at local level, showing Subsidence Risk for urban land use blocks

	should be local to make it usable.	
Heraklion (H.3)	Heraklion wants to use the most recent data i.e. from 2019 onwards, in the CURE applications.	We plan to implement the AP06 for the most recent years, from 2019 onwards.

7 AP06 URBAN SUBSIDENCE, MOVEMENT AND DEFORMATION RISK

7.1 Purpose of the Application

The CURE Land Subsidence App aims to support cities with enriched information about land subsidence and related dangers. It should provide the responsible authorities with both synoptic and detailed knowledge about localization, extent and magnitude of exposure to terrain slow motions due to subsidence or slope instability (landslide risk), and building or infrastructure deformations (due to terrain motions or maintenance failure) both in **urban and sub-urban** areas.

The information about terrain movements and subsidence in urbanized areas obtained using the PS InSAR techniques (either extracted by GISAT based on multi-temporal analysis of Sentinel-1 SAR imageries or later coming directly from the Copernicus EGMS service https://land.copernicus.eu/pan-european/european-ground-motion-service) will be combined with information about distribution, typology and chronology of evolution of urban areas (coming from Copernicus Urban Atlas or World Settlement Footprint-Evolution layers).

These methods applied are suitable in particular for identification and monitoring of **slow terrain movements**, which may indicate potential hazards not only for urban assets, like buildings, transportation networks´ infrastructure incl. railway tracks, highway crossings, bridges etc. or underground infrastructures like pipelines but also as for the inhabitants living in the residential areas of the city or people moving around the city in general. The application to be developed can identify those dangers in time and thus to serve as an effective early warning system for the cities and city-regions.

Moreover, the combination of the information about localization and velocity of subsidence with information about chronology of building blocks´ construction in the city can be very valuable for the end-users. It can detect potential deviations from standard multi-temporal subsidence profiles in the particular city/region which may indicate issues in particular urban block. Moreover, this will allow to detect potential correlations between the construction period of urban blocks and their inclination to subsidence, which may indicate systematic issues in constructions.

On the other hand, timely information about subsidence in specific areas intended for city-development in near future (including brownfields or patches of land without current use which are crucial for the city re-development) may help to predict and thus to prevent potential issues related to increased susceptibility of the areas to subsidence. Such use case have been already identified as one of interest of the Ostrava/Moravian-Silesian Region end-users (acting as follower user) in the Czech Republic. Also, focus will be put on areas of former coal mining activity in this region.

Emphasis will also be put on **integration of results of this application with results from CURE AP05 targeting Urban Flood Risk**. It shall support assessment of potential links between land subsidence and increase of the flood risk or spatial association between floods occurrence and land subsidence patterns.

7.2 Data & Methodology

Analysis of spatial patterns of subsidence phenomena brings insights into hazard distribution and its magnitude. Essential is identification of clusters of subsiding measurement points attributed to similar behaviour and outlying points or clusters dissimilar to behaviour of points in surroundings. Furthermore, given complex nature of potential drivers and size of observable objects in the urban environment multi-scale approach will be adopted.

To understand drivers and impacts of land subsidence at city and sub-city level the intensity of terrain deformation hazard derived by means of MT InSAR technology needs to be integrated with additional supportive information. Distribution and chronology of urban evolution (expansion, densification) may affect (among other factors) both spatial and temporal patterns of land subsidence and should be assessed in relation to observed deformation rate. The module will consist of series of Python scripts responsible for spatial-temporal analytics and data fusion. Spatial associations will be analysed within results from Copernicus EGMS, or from custom MT InSAR processing chain deployed on DIAS infrastructure. Next, the results will be integrated with temporal patterns derived from pan-European and global open datasets describing urban structure and height (Copernicus Urban Atlas with 3D component) and long-term built-up evolution (DLR's World Settlements Footprint-Evolution, JRC's GHSL). Output from module will be represented by standardized analytics providing added value derived from fusion of scalable inputs.

7.2.1 Data inputs

There will be two main types of information needed for this app. First, the **information about the subsidence** measured at stable points (permanent scatterers) distributed over the city and city-region needs to be obtained. For this purpose, the **Sentinel-1 SAR imageries** from Copernicus programme will be exploited, allowing to identify potential movements at those points and to follow the pattern of their velocity and direction in time. This is allowed by comparison of the situation with a help of dense time-series of Sentinel-1 imageries. This input data source will – in near future – be replaced by the outcomes of the **Copernicus European Ground Motion Service (EMGS)** (https://land.copernicus.eu/pan-european/european-ground-motion-service) , which should become operational next year.

The second type of information needed by the AP06 is the **information about the spatial pattern of urbanized areas and their development in time**. The first – spatial pattern of urbanized areas - will be derived in particular from the **Copernicus Urban Atlas**, which brings highly accurate

information about internal structure of the cities - distribution of different types of land use in the cities. If not available, this dataset can be replaced by local city planning maps with Urban Atlas-like nomenclature. This could be relevant in particular in case of potential replications of the service in outside-European cities. The information about the chronology and spatial pattern of the city development will be obtained primarily from the **World Settlements Footprint-Evolution** dataset.

7.2.2 Methodology

7.2.2.1 Measuring terrain movements by means of MT InSAR

The first step in methodology focuses on **acquisition of information about the subsidence itself.** For this purpose, the **Synthetic Aperture Radar Interferometry** (**InSAR**) method is exploited. For over than 20 years, this method has been providing ground deformation data at centimeter precision. In the past decade, new ways of processing satellite radar images have been developed using **Persistent Scatterer Interferometry** (**PSI**) that allow ground movements over wide areas to be detected and monitored with even greater sensitivity. Free and routinely-available SAR data collected by Sentinel-1 sensors' constellation within Copernicus programme represent a unique opportunity for applying these methods on operational level on a global scale (Pepe and Calò 2017). The technique is based on processing of time series of high or very-high resolution satellite SAR imagery which enable detection of up to millimetre displacements. This method has been demonstrated in number of national (Hlavacova et al. 2016; Lazecky et al. 2010) and global EMS related activations and also used for recently awarded state-of-the-art service (TACR Governance Award 2018, CZ) developed by GISAT (Kolomaznik et al. 2016).

By applying multi-temporal InSAR techniques to a series of satellite SAR images over the same region, it is possible to detect movements of the structure systems on the ground in the millimeter/centimeter range and, therefore, to identify abnormal or excessive movement indicating potential problems requiring detailed ground investigation. (Lazecky et al. 2015)

Principles of InSAR measurement techniques and their use for monitoring of deformations in urban areas are illustrated by the two figures below.

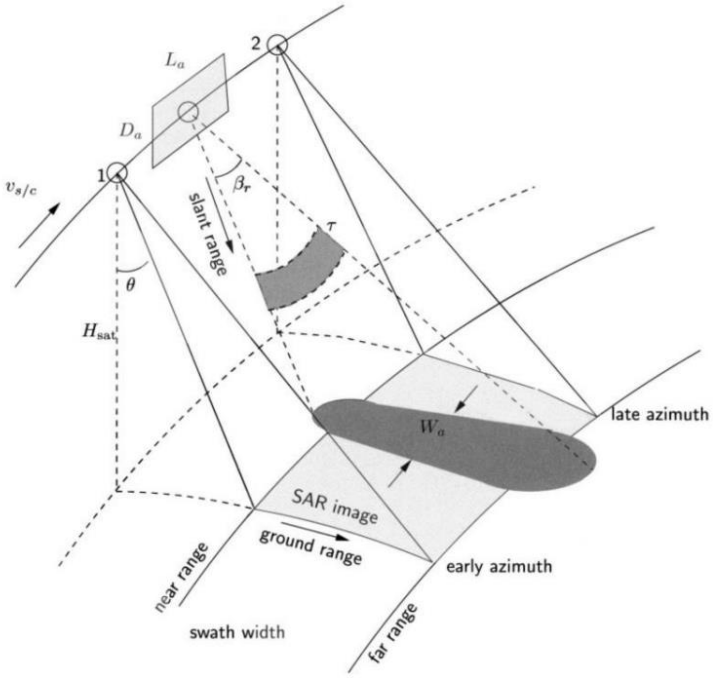

***Figure 24**. Side-looking image geometry of a spaceborne SAR acquisition. The satellite velocity vs is approximately 7 km/s. The dark gray area indicates the footprint of a single pulse. The total coverage of a SAR scene, between early and late azimuth direction, and near and far range, is depicted in light gray source: EGMS specification and Implementation EEA 2020*https://land.copernicus.eu/user-corner/technical-library/egms-specification-and-implementation-plan*)*

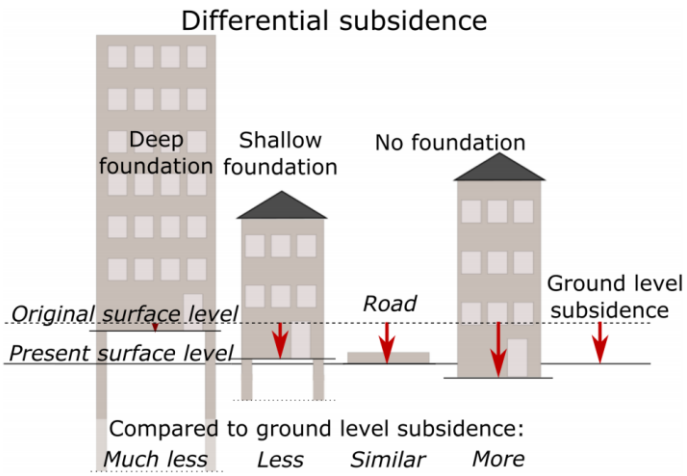

***Figure 25**. Differential subsidence of individual objects and their relation between foundation depth and weight. Combining this relation with the PSI-estimated subsidence rates can be used to investigate and quantify depth-dependent subsidence rates. . (source: Minderhoud et al. 2020)*

The subsidence processes are identified and monitored in a multi-temporal manner. The dense time-serie of SAR images (Sentinel-1) allows to follow displacements of selected coherent

targets - permanent scatterers points by measuring phase differences between time-series of acquisitions and to estimate average displacement rate.

***Figure 26**. Stable points with terrain/surface movements subsidence measurements, classified by velocity of movements in urban area.*

For each of measurement points the temporal profile is generated, showing the trend of displacements over the observation period as detected in satellite's line-of-sight direction, or as converted into vertical or horizantal (East-West) planes.

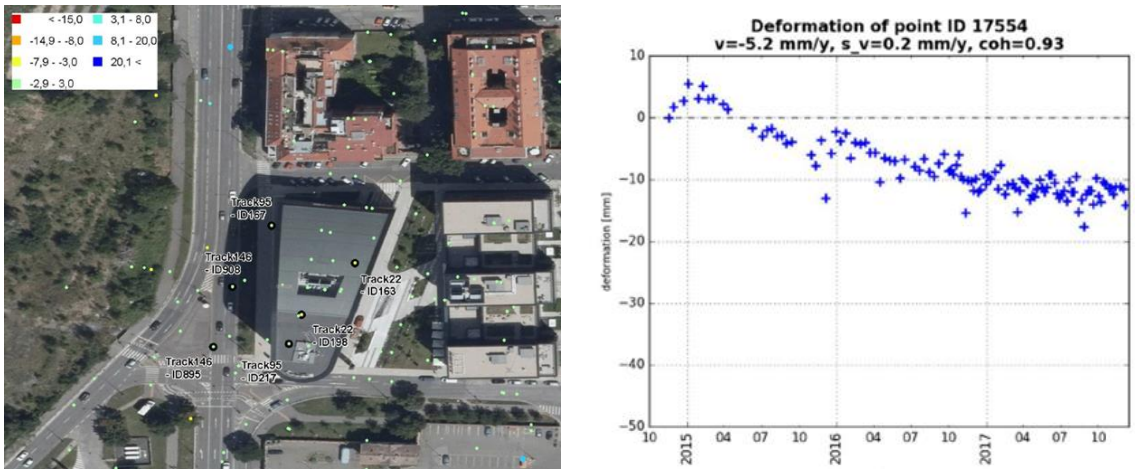

***Figure 27.** Subsidence measurements for selected stable points in the city area classified by velocity of movements (left), temporal profile of subsidence for selected point.*

With a help of these techniques, the displacement rate (average annual velocity) is estimated for each point. Using this method, the points with ongoing subsidence (or other types of surface movements) can be detected. The points are categorized based on velocity of ongoing subsidence to be able to identify the most intensive subsidence processes in the city.

7.2.2.2 Integration with information on urban land structure and evolution

The second step of the methodology consists of **integration of the information about the subsidence with relevant additional data and information** in order to derive meaningful intelligence and understanding about the ongoing subsidence-related processes in the city and surrounding areas. This will include clustering of stable points with subsidence information and spatial overlay analysis (in particular zonal statistics) with the layers representing the structure and development of the city structure.

First, the information about the subsidence will be converted to the level of meaningful (functional) urban units using primarily the geometry of the Urban Atlas layer, applying the zonal statistics, in order to obtain information about potential subsidence per each particular land use block. In this step, the Urban Atlas layer can be complemented by custom layers, representing different types of functional urban units, for which the information about subsidence should be derived (e.g. in the Moravian-Silesian region, this analysis can be done for brownfields or undermined areas). Also, similar type of analysis can be done with linear data representing street segments or underground infrastructure like pipelines.

Next, the subsidence information will be combined with the WSF-Evolution dataset representing chronology of urban expansion of the cities (example in Figure 28). Based on this, temporal profiles of subsidence processes showing their timing (after the building block construction) can be prepared for each of the newly constructed units in the city area.

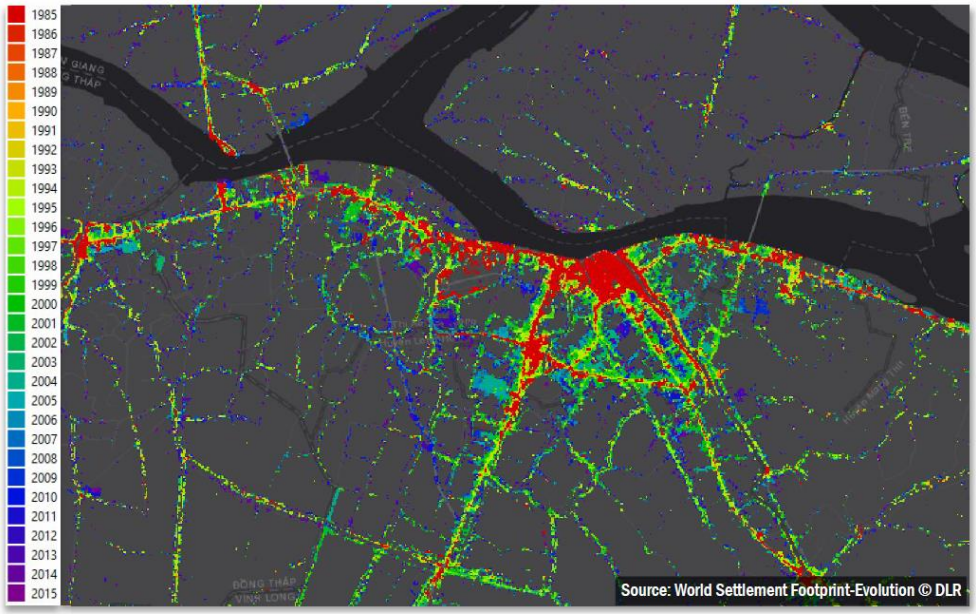

Figure 28. *Spatial-temporal pattern of built-up expansion for selected city as depicted by World Settlement Footprint-Evolution (Marconcini et al. 2018). Colors represent year when built-up was detected for the first time in time series of satellite data. ((Source: EO4SD report, 2020)*

Last, but not least, the presentation of the results of these analysis to the end-users will be secured by integration of the data-results into an interactive web-based analytical platform and visualised in an attractive and easy-to-understand manner. The app is based on open-source components and programming languages. Custom GIS layers can be integrated into this application as WMS or WFS, in order to combine these analytical results of the AP06 with the local-city data and information also in sense of visualisation.

7.3 Output features & characteristics

The outputs of this analysis will be represented mostly by GIS layers – point, polygon or line features containing information about ongoing subsidence trends and their intensities in form of attributes. Such data can be shared with the city users simply as GIS layers, which can be integrated into local city GIS platforms if needed and also these results will be visualized in a dedicated interactive web-based visualization and analytical platform.

The first result of the analysis in the frame of this application will be the quantification of terrain subsidence per each of measurement points in the city area. A temporal profile will be generated for each of those points, representing changes of velocity of subsidence in time on that particular point. The measurement points will be grouped in spatial clusters, in order to obtain better overview about significant subsidence processes in the city.

Next, the result of integration of the information about the subsidence with relevant additional data (Urban Atlas, WSF) and information will be generated, representing already meaningful intelligence about the ongoing subsidence-related processes in the city and surrounding areas.

The information about the subsidence will be translated to the level of the units from the Urban Atlas layer. This brings information about the subsidence level for each of the functional urban units (e.g. building blocks or commercial/industrial units). This helps to identify units currently endangered by too intensive subsidence in the city in combination with the type of the unit.

Then, the subsidence information will be overlayed with the data from WSF-Evolution and temporal profiles of subsidence processes and their timing (after the building (block) construction) will be prepared for each of the newly constructed units in the city area.

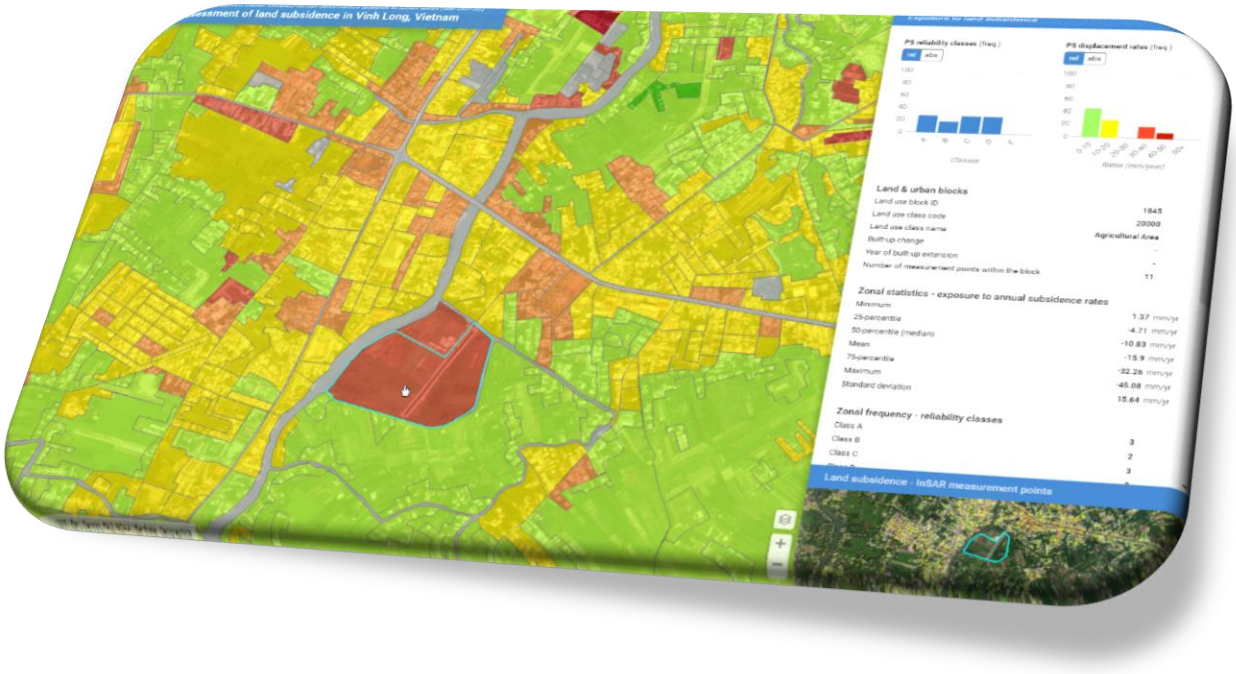

Figure 29. *Front end GUI of interactive web-app presenting results of surface movements analysis (in this case per land use block) in interactive map and interactive analytical charts.*

7.4 Stakeholder needs addressed by the application

The stakeholder requirements are identified and documented in Deliverable 1.1 of the CURE project. The ones related to the Urban Subsidence, Movement, Deformation Risk App 06 are listed and addressed in Table 10 below.

Table 10. *Stakeholder needs related to the Urban Subsidence, Movement, Deformation Risk App 06 and our response to them.*

Stakeholder	*Requirement*	*Response*
General (G.1)	CURE should use and provide access to the most recent data.	This application will be built on the most recent input data sets that are available (Sentinel-1, Urban Atlas 2018, WSF-Evolution, EGMS data when the monitoring will be operational) and the results will be provided for most recent years 2019/2020.

General (G.1)	CURE should provide single point of access for various datasets of different applications through one map	This should be fulfilled for the two apps (AP05 and AP06) for which GISAT is responsible. It will be realized via interactive web application developed by GISAT, dedicated to visualization of the results of these two apps which will also facilitate integration of relevant additional data (e.g. local city plans)
General (G.4)	CURE should provide high resolution data and high frequency data.	This App will be able to produce high resolution results at the level of Urban Atlas Blocks. High frequency of data for temporal profiles of subsidence velocity on each point, with S-1 temporal resolution.
General (G.5)	CURE should be able to use and provide data combination of satellite based, EU databases (e.g., risk behind natural events – earthquakes or other adverse events caused by climate change) and local data (i.e., sensors data, transport data including transport conditions, social activity data such as walkability, etc.), smart city	This App will integrate satellite based information (S-1, Urban Atlas), EU datasets (Urban Atlas, EGMS data) and local data (local city plans and other relevant information) also with third-party data with global coverage (WSF-Evolution)
General (G.6)	CURE should compare and/or validate CURE application outputs with other existing data sources such as local climate zones from wudapt database	Local data/information on urban subsidence, movement, deformation may be used as reference data for validation, if available
General (G.7)	CURE should provide data outputs including soil (impervious soil	Not absolute data, but data on relative movements and deformations of surface elevation in time

	detection / soil permeability (sub-surface zone)), land conditions, 2D/3D city model, cultural heritage data, nature protection data, building heights, surface elevation data, land cover, land use, energy performance data, traffic flow (multi-modal), cartographic maps (buildings, streets), digital elevation maps, albedo of urban surface, imperviousness and percentage of green areas, wind, temperature and emissions, NO2, PM10, PM2.5 particulate measurements, green areas (and proximity to green areas) and blue corridors, noise, social data	
General (G.12)	CURE should provide early warning system	The app will bring information highly relevant for early warning systems of the cities.
General (G.13)	CURE should provide interoperability i.e. ability to interface with existing or future information systems in cities	Output formats of the results will ensure interoperability with information systems of the cities.
General (G.14)	CURE should be able to use open data from cities, National (statistics, meteorology and mapping) agencies and EU databases	The app should allow for integration of local open data – in particular urban planning materials, which could complement the Copernicus Urban Atlas information

	and other applications but this requires careful mapping to access data through APIs – few data source examples from different EU states (Portugal, Netherland, Italy, Germany etc) and Pan-European cities (Antwerp, Berlin, etc) are provided.	
General (G.15)	CURE should be able to use local urban heat islands (data) with satellite data	No
General (G.16)	CURE should be able to use traffic monitoring in anticipation for managing urban air quality	No
General (G.17)	CURE should be able to use socio-economic and energy related data to understand usage/data patterns	No
General (G.18)	Other datasets which CURE should use are: CORINE land cover and land use data, Open street map data, Eurostat data, World Urban Database, Citizen science data	App usese the Urban Atlas land use data
General (G.27)	CURE applications should be easy/comfortable to use, reachable	Results of the AP06 will be presented in a web-based app, which will make them easily accessible and usable

	(accessibility)	
General (G.31)	CURE should consider ground motion service by EEA as input to USMDR application	The EGMS will serve as a crucial input for CURE AP06 when the service will become operational
General (G.34)	CURE should consider application on Moravian Silesian region to prepare an adaptation strategy	The app will be applied for MS region in the second “follower-city” stage
Heraklion (H.1)	Heraklion is interested in the following CURE applications: Surface Urban Heat Island, Urban Heat Emission Monitoring, Urban CO2 Emission Monitoring, Urban Flood Risk and Urban Subsidence Deformation and Movement Risk.	The AP06 Urban Subsidence Deformation and Movement Risk will be implemented for Heraklion
Heraklion (H.2)	The scale of CURE applications, especially, heat related applications should be local to make it usable.	He AP06 will provide information at local level, showing Subsidence Risk for urban land use blocks
Heraklion (H.3)	Heraklion wants to use the most recent data i.e. from 2019 onwards, in the CURE applications.	We plan to implement the AP06 for the most recent years, from 2019 onwards.

8 AP07 URBAN AIR QUALITY

8.1 Purpose of the Application

Ambient air pollution is one of the key environmental problems in Europe. Exposure to air pollution is associated with acute health impacts caused by short-term exposure as well as chronic diseases following long-term exposure (WHO 2016). According to the European Environmental Agency, each year more than 450.000 deaths in the EU-28 are related to air pollution (EEA 2019). Because of the severe health impacts, air pollution also has considerable economic impacts, increasing medical costs and reducing productivity through lost working days across various economic sectors.

Exposure to outdoor air pollution is predominantly an urban issue. The EEA estimates that currently approximately 50% of the European urban population is exposed to concentrations exceeding the limit values put forward by the World Health Organization (EEA 2019). We consider two pollutants which play a key role in urban air pollution in Europe: nitrogen dioxide (NO_2) and particulate matter (PM).

Nitrogen dioxide is a gaseous air pollutant which is strongly linked to road traffic emissions. High exposure is therefore expected near traffic sources. An important aspect of NO_2 pollution in urban areas concerns the spatial heterogeneity of the concentrations. Because of the variation of the traffic emissions over short distances, the urban NO_2-concentrations vary strongly over short distances (Cyrys et al. 2012). Particulate matter is the sum of all solid and liquid particles suspended in air, including organic and inorganic particles, such as dust, pollen, soot, smoke, and liquid droplets. These particles vary in size and therefore two types of particulate matter are considered: PM_{10} and $PM_{2.5}$ (the former measuring the weight of all particles with a diameter smaller than 10 micrometres, the latter measuring the weight of the particles with a diameter smaller than 2.5 micrometres). The dominating source of PM pollution varies across Europe. Atmospheric processes that lead to the formation of particles as a result of traffic, domestic heating and agriculture emissions are the most considerable in Western Europe, while domestic fuel burning dominates the contributions to particulate matter in Eastern Europe (Karagulian et al. 2015).

8.2 Data & Methodology

8.2.1 Urban air quality

Urban air quality is a multi-scale problem. Pollutant concentrations on a street-level scale are influenced by regional background concentrations, urban increments due to local industrial, traffic and residential heating sources, and an additional contribution coming from recirculation in narrow streets with high rise buildings adjacent to it (the so-called street-canyons). Only when the contribution of all three scales is taken into account, the urban air

quality exposure can be correctly determined. As illustrated in Figure 30, monitoring the compliancy of limit values also requires the combination of the three scales, as otherwise local exceedances could be overlooked.

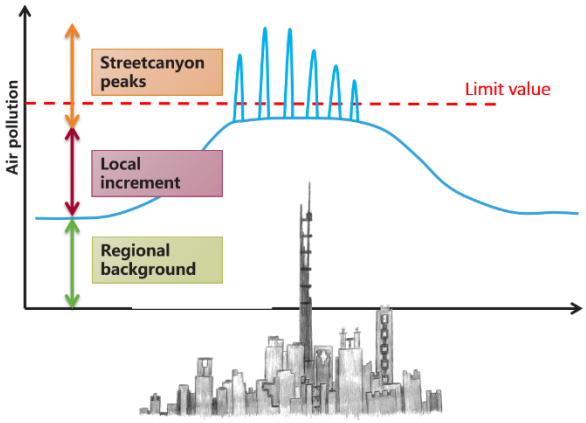

Figure 30. *Illustration of the different scales involved in urban air quality assessment.*

8.2.2 ATMO-Street model chain

CURE Application 07 assesses the urban air quality using the ATMO-Street application. ATMO-Street is an integrated air quality model chain (Lefebvre et al. 2013a), designed to correctly assess and combine the different scales of urban air quality. The model chain relies on several underlying models and input datasets to compute the air pollution at street-level scale (10m) for an urban area. The flowchart of the model chain is provided in Figure 31. In the next paragraph, we provide a general description of the model chain. Section 8.2.3 describes the model components and their interlinkage more in detail.

The ATMO-Street model chain starts from datasets describing the most important local emissions in the domain under consideration. For urban areas in Europe, road traffic, industrial and residential heating emissions are generally considered. Preferably, all three emission datasets are provided at a high resolution: residential and industrial sources are typically represented by a point source for each company / house with stove, while line sources (i.e. one value per road segment) are used for road traffic emissions. If industrial and residential sources are not available at this high resolution, surface sources with a somewhat lower resolution (e.g. 5 by 5 km) can be used as an alternative. Based on the high-resolution emissions data, two core models compute the local contribution to the air pollution at a resolution of 10m: the bi-gaussian plume dispersion model IFDM accounts for the impact of local emissions from traffic and industry (Lefebvre et al. 2013b), while the street-canyon module OSPM calculates the in-street increment resulting from street-canyon effects (Berkowicz et al. 1997). To correctly assess the local contribution, these models require two additional datasets. Meteorological data (vectorial wind speed and temperature) is required to correctly assess the dispersion, while a detailed 3D building dataset (relying on building

layouts using polygons) is required to correctly assess the recirculation in street canyons. In a final step, the total air pollution is computed by combining the local contribution with the regional background concentrations. These background concentrations contain the pollution caused by all the sources outside the model domain, and the sources that are not explicitly considered in the emission data (e.g. emissions for other sectors, such as shipping and non-road transport). This data is either based on results of regional background models or measurements (possibly combined with spatial interpolation using e.g. land use regression models).

The ATMO-Street model chain is the official air quality model chain in Flanders. It is used by the Flemish Environmental Agency for the assessment of current and future air quality, and its output is reported to the European Commission. The model chain has recently also been used in many other countries, including Poland, Slovakia, Hungary, Croatia and China. The model chain has been validated using several measurement campaigns, focusing on spatial patterns and time series alike (Lefebvre et al. 2011, Lefebvre et al. 2013a). Most of these validation campaigns focused on a relatively small number of sampling locations, with at most a few dozens of locations distributed among a single urban region. Recently, however, the Curieuzeneuzen Citizen Science air quality measurements have been used to validate the model using measurements for 20.000 sampling locations in Flanders (Hooyberghs et al. 2020). The validation highlights the capability of the model chain to correctly assess the spatial variation of the air pollution in Flanders.

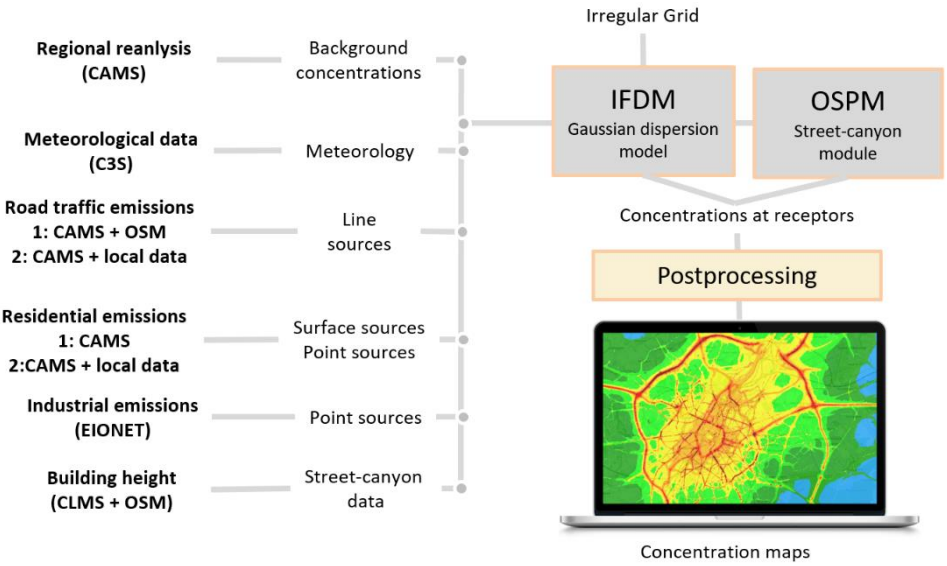

Figure 31. Flowchart of the ATMO-Street model. The numbers refer to the two options for downscaling used in the current project (fully Copernicus or Copernicus combined with local data for downscaling). More details: see text.

In CURE, the (raw) input data for the ATMO-Streets model chain stems as much as possible from Copernicus datasets. Emissions are retrieved from the Copernicus Atmosphere Monitoring Services (CAMS), meteorological data from the Copernicus Climate Change Service (C3S), and building information from the Copernicus Land Monitoring Service (CLMS). Additionally, industrial emissions of the European Environment Information and Observation Network (EIONET) have been used.

Although the resolution of the CAMS emission inventories for Europe has increased in recent years, there is still a significant gap between the resolution of the inventories and the resolution required in street-level scale urban air quality modelling. The emission data has therefore been combined with higher resolution proxy data to downscale the CAMS emissions to the requested resolutions (point sources / surface sources for residential emissions, and line sources for traffic emissions). Two options for the downscaling are considered. In the first set-up, we have relied on the global open-source roadmap OpenStreetMaps (www.openstreetmaps.org) to downscale the emissions to line sources, and used the residential emissions of CAMS at their native resolution (0.05 by 0.1 degrees). This first option is therefore transferable to any location in the European Union. In the second setup, a local bottom-up roadmap (with information on the road capacity) and a local dataset describing the location of heaters are as well considered. We expect that the final downscaled emissions of this second method are more in line with the real-life situation, but the method is no longer transferable to other cities.

Table 11 provides an overview of the datasets used in the urban air application. Section 8.2.4 describes the input datasets and the downscaling of the emissions for both set-ups in more detail.

Table 11. *Overview of the input datasets.*

Copernicus service	*Dataset*	*Type*	*Usage*
CAMS	Regional air quality reanalyis	Air quality data	Background concentrations
CAMS	Regional Emissions for Air Pollutants (REG-AP), v3.1	Emissions	Road traffic and residential emissions
C3S	ERA5	Meteorological data	Meteorological data
CLMS	Urban Atlas	Building Height	Building height
-	OpenStreetMaps	Building layout	Building layout

-	OpenStreetMaps	Road map	Downscaling traffic emissions
-	Road map Sofia	Road map	Downscaling traffic Emissions
-	EIONET Large Point Source data	Point source data	Industrial emissions
-	Inventory of wood and coal burning heaters in Sofia	Location of heaters	Downscaling residential emissions

8.2.3 Building blocks of the ATMO-Street model chain

Local open-street concentrations due to traffic emissions and point sources are modelled by the bi-Gaussian plume model IFDM (Immission Frequency Distribution Model) (Lefebvre et al. 2013b). IFDM is a receptor grid model: air pollutant concentrations are computed for an abundance of receptor locations. Instead of a regular grid, we use a pointsource- and road-following grid. This approach ensures that more receptor points are available where the largest concentration gradients are expected (Lefebvre et al. 2011). The chemical equilibrium in the NOx-O3 reaction is determined on the basis of temperature and solar height and is based on the fast-ozone-chemistry scheme (Berkowicz et al. 2008).

To take the effect of buildings on the street level concentrations into account, the IFDM model is coupled to the Operational Street Pollution Model (OSPM) (Jensen et al. 2017). OSPM models street level concentrations due to traffic emissions using a combination of a plume model for the direct contribution and a box model for the recirculating part of the pollutants in the street. In the current set-up for OSPM, a receptor location is placed every 20m on each road with a row of buildings adjacent to the road (i.e. at a maximum distance of 50m to the middle of the road).

The concentrations at the receptor locations of the IFDM and OSPM model are combined and gridded in a three-step postprocessing module. At first, IFDM results are gridded using Delaunay triangulation to obtain gridded open street concentrations. Secondly, we grid the OSPM results using nearest-neighbour interpolation. In the last step, both gridded maps are combined into a map with a 10m resolution, by using the OSPM results at locations where buildings are adjacent to the road, and the IFDM results at all other locations.

8.2.4 Input data

Table 11 provides an overview of the datasets used in the urban air quality application. In the following paragraph the datasets and the required processing are described in more detail.

8.2.4.1 Meteorological data

ATMO-Street requires hourly (vectorial) wind speed and temperature data. Both parameters are taken from the ERA5 reanalysis dataset of the Copernicus Climate Change Service (C3S). ERA5 provides surface temperature and wind speed with a resolution of 30 kilometre. We interpolate the data to the centre of the domain using bilinear interpolation.

8.2.4.2 3D building model

To correctly assess the street-canyon contributions, ATMO-Street requires a 3D model of the city under consideration. The 3D model requires at least the following two parameters:

- Building height
- Ground plan of the building, preferably described using a polygon (sub-meter resolution is required).

Building heights are available in the CLMS Urban Atlas for all European capitals. Although the dataset is already a few years old (dating from 2012), we assume that the urban fabric has not changed too much in the European capitals.

The Urban Atlas provides building heights at a resolution of 10m, but it does not provide a building layout. Since the façade-to-façade distance is one of the most important parameters in street-canyon models, an additional dataset is required to build a full 3D model of a city. We make use of the open-source OpenStreetMaps dataset, which includes a polygon layer with the exact location of the buildings. Figure 32 further visualizes the gridded CLMS data and the polygon of OpenStreetMaps.

Figure 32. *Illustrations of the two datasets used for the 3d building model. The blue lines indicate the ground plan of the buildings according to OpenStreetMaps data, while the yellow-to-red colors indicate the building height according to the 10m resolution UrbanAtlas dataset. Background image: OpenStreetMaps.org.*

As OpenStreetMaps is a crowd-sourced project, the quality and completeness of the data varies greatly between different areas. We have controlled the completeness for Sofia using a

visual comparison with satellite data, and with the (lower resolution) building height of Urban Atlas. Most buildings in the inner-city are correctly represented, and only some residential neighbourhoods in the outskirts are missing a considerable number of buildings. These locations are however not important for the air quality applications, as the highest concentrations are expected in the inner-city.

The CLMS and OpenStreetMaps data are combined using geospatial tools. For each building polygon in OpenStreetMaps, we determine the mean height of the overlapping grid cells from the CLMS Building Height layer.

8.2.4.3 Background concentrations

ATMO-Street's components IFDM and OSPM only explicitly take the concentrations due to traffic, residential and industrial emissions in the city into account. Concentrations due to other emissions in the city (e.g. rail transport, trade and services etc) and emissions outside the city are not taken into account. These 'background' concentrations vary over a longer spatial scale (order of kilometres rather than order of metres), and are therefore not explicitly modelled in the urban air quality applications. They are, however, added to the final concentrations field using a regional background concentration from CAMS.

CAMS provides hourly regional background concentrations for Europe in the 'Regional reanalysis datasets.' This dataset assimilates the output of regional air quality models (so-called chemical transport models, CTMs) with measurements of the official measurement networks of the EU-countries. The resulting dataset comprises gridded hourly concentrations for Europe with a resolution of 0.1 degree, for nitrogen dioxide, ozone, and particulate matter. The most recent dataset contains concentrations for 2018.

Directly coupling the background concentrations to the local concentrations field would give rise to sharp gradients at the edges of the CAMS grid cells. Therefore, the CAMS data are resampled to a concentration field with a 2000m resolution using bilinear interpolation.

8.2.4.4 Emissions

ATMO-Street requires high resolution emission data for road traffic, industry (including powerplants), and residential heating. In the following paragraphs, these three sectors are discussed in detail.

Industrial emissions

For industrial emissions, we rely on the figures reported by the member states of the European Union to the Central Data Repository (CDR) of the European Environment Information and Observation Network (EIONET). According to directive 2016/2284/EU the member states must every four years report the air pollutant emissions of large point sources (LPS), which the EU subsequently reports to the United Nations Economic Commission for Europe (UNECE) Environment and Human Settlements Division under the Convention on Long-range Transboundary Air Pollution (CLRTAP).

The data for Bulgaria is publicly available on http://cdr.eionet.europa.eu/bg/un/clrtap/lps/envwqsyda/. We use the data reported in 2017 (which refers to the situation in 2015). For Sofia, the dataset contains emissions for four powerplants and one industrial plant. In all five cases, a high stack is present (ranging from 70 to over 130m high), and it is therefore expected that the influence of these industrial emissions on the ground concentrations is rather limited.

Road traffic emissions

Several global and regional emissions datasets have recently been developed under the CAMS umbrella (CAMS 2019). In the current set-up, we use the CAMS regional anthropogenic emissions for Europe, using the CAMS–REG-v3.1 dataset developed by TNO. This dataset provides gridded emissions on a 0.1 by 0.05 degree resolution for several sectors (including road traffic and residential combustion) and several air pollutants (including NO2 and PM10). Version 3.1 of the dataset provides total annual emissions for 2016. Monthly profiles are provided by the CAMS-TEMPO dataset.

ATMO-Street requires emission data for all the line segments in the domain. The total CAMS emissions in Sofia have therefore been combined with higher resolution proxy data to downscale the CAMS emissions to the requested resolutions. As mentioned above, two options have been considered: a first option relying on pan-European datasets, and a second option relying on local datasets. More in detail, the downscaling uses the following proxy data:

1. In the pan-European methodology, the road map of OpenStreetMaps is used. The emissions are spread over all the roads in the domain according to the number of lanes for each road (thus assuming that more vehicles are using roads with a larger number of lanes). Moreover, we assume that the emissions on a highway segment (roadtype trunk or motorway in OSM) are twice as large as the emissions on other types of roads, because vehicle speeds and vehicle numbers are in general larger on highways. Note that is method is rather crude, and does not use any local knowledge.
2. The local method uses a bottom-up dataset of the Sofia municipality. The dataset indicates for each road the maximal capacity of the road. We assume that the emissions can be spread over all the roads according to their maximal hourly capacity. Note that this method is less crude than the pan-European methodology, but it is still far from perfect. In an ideal situation, the CAMS emissions are either spread over the domain according to realistic traffic flows, which consider the morphology of the city (e.g. some roads link residential and office areas, and are therefore much more used during rush hours etc). Alternatively, the road traffic emissions could by calculated using a traffic emission model, which combines the traffic flows with the traffic fleet and bottom-up emission factors.

Residential emissions

For the residential emissions, we anew start from the CAMS REG-AP-v3.1 dataset, but this time we use the data for the residential combustion sector. The rest of the processing differs for both set-ups:

1. When only using pan-European datasets, there is no decent proxy data to further downscale the emissions to individual houses or wood / coal burning devices. We therefore use the emissions on a 0.05 by 0.1 degree resolution. The emissions are therefore spread over the entire urban area, and we will certainly miss some important PM hotspots in neighbourhoods with a large share of wood and coal burning.
2. The Sofia municipality has compiled a large dataset containing the location of all coal and wood burning heaters. In the second method, we spread the total emissions in Sofia uniformly over all these devices. Note that this entails an important assumption, and will cause some uncertainty. After all, in real-life, the emissions of individual heaters strongly depend on the characteristics of the heater (type, age, maintenance...), and the way in which the heaters are used. This type of data is, however, not available at the level of individual heaters in the entire city.

8.2.5 Limitations and validation

As mentioned in the earlier paragraphs, there are several limitations and uncertainties related to the methodology applied for the urban air quality application. Most of the uncertainties are related to the Copernicus datasets and the downscaling of these data to the required resolution, but there is an additional uncertainty related to the model core (IFDM-OSPM). We for instance observe the following limitations:

- The background concentrations are based on the CAMS regional reanalysis data, which are the result of an air quality model on a regional scale. Although the results have been assimilated with measurements, we have observed underestimations of the background concentrations by CAMS in other cities (e.g. Bratislava).
- Similarly, wind and temperature input data are an assimilation of model data and measurements. Although the quality of these type of reanalysis products has been greatly improved recently (e.g. with the update from ERA-Interim to ERA5), there could be some deviations from the actual local data.
- Downscaling the emissions to individual point sources and road segments comes with an important uncertainty. The quality of the downscaling greatly depends on the quality of the proxy data that have been used. We thus expect better results if we rely on a combination of local data and pan-European / gloabl proxy datasets. Note, however, that although the local datasets are the best available proxy data, they are not the ideal proxy data (e.g. capacity instead of traffic volumes / no information on wood / coal burning heaters).
- The model has initially been developed to model the air quality in Flanders, and therefore relies on a stability scheme based on measurements in Flanders.

To quantify the uncertainties related to these limitations, we validate the model results using the measurements of the official network of Bulgaria. We rely on the official time series data reported to the EEA (https://discomap.eea.europa.eu/map/fme/AirQualityExport.htm), and focus both on the spatial pattern and the time series.

8.3 Output features & characteristics

8.3.1 Output features

The urban air quality application will initially be applied to Sofia. The outcome of the applications are air quality maps describing the yearly mean concentrations of nitrogen dioxide and particulate matter (PM10) in the city on a resolution of 10 by 10 meters. We focus on the year 2018, as it is the most recent year for which background concentrations are available. More recent years can easily be added if background concentrations are released by CAMS.

Figure 33 shows preliminary results for nitrogen dioxide and particulate matter in Sofia. These results are not yet validated, and should only be considered as a demonstration of the final maps. The maps show how the air quality in Sofia varies strongly over short distances. For NO_2, the highest concentrations are observed near the most important roads, with the highest concentrations occurring in busy street canyons in the city centre. For particulate matter, the highest concentrations are observed in the neighbourhoods with an abundance of coal and wood burning heaters. Note, however, that these results are preliminary and that there is a significant uncertainty in the PM results related to the downscaling, as mentioned in section 8.2.5.

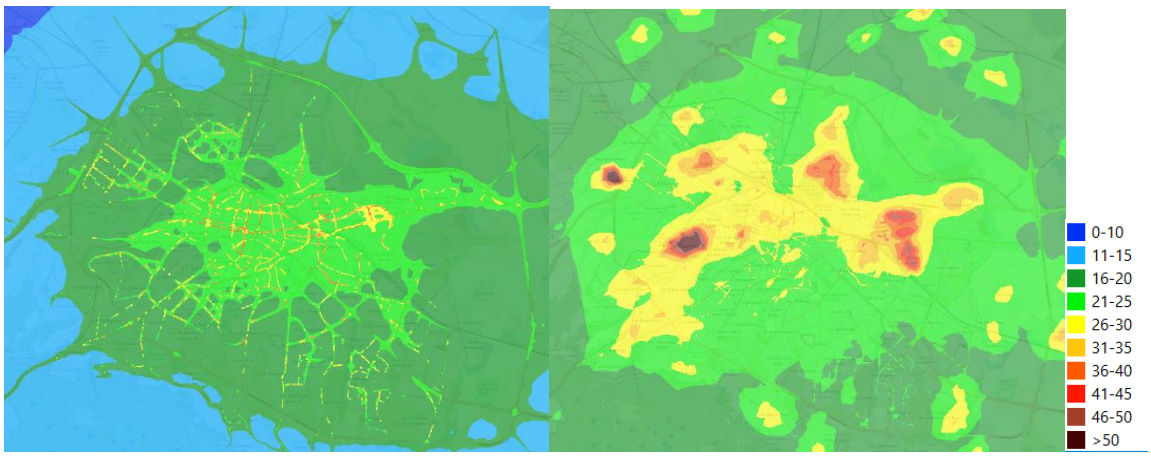

Figure 33. Preliminary (and unvalidated) demonstration results for the urban air quality applications. The figures show the annual mean NO2 (left) and PM (right) concentration in 2018 in Sofia in ug/m^3. Values highlighted in read are in exceedance of the annual limit values put forward by the EU legislation.

The maps allow stakeholders to identify the neighbourhoods and districts with the worst air quality, and to decide in an informed manner for which areas action should be prioritized. Moreover, the maps can be used for compliance checking. The EU guidelines set a threshold

of 40 ug/m^3 for the yearly mean PM_{10}- and NO_2-concentrations. All locations shown in red on the figure are thus in exceedance of the limit values put forward by the EU legislation. By combining the results with population data, the exposure of the population can be determined, and one can for instance report the percentage of the population exposed to a chosen concentration interval, or the percentage of the population living at values exceeding the EU-threshold. Population exposure for Sofia is not yet available, but a similar analysis for the city of Antwerp in Belgium has been conducted. Figure 34 shows the results of this analysis. Based on such a population exposure histogram, the health impact (e.g. number of premature deaths or attributed incidence of diseases) of the air pollution in a city can be computed, as shown in the health impact application (AP11).

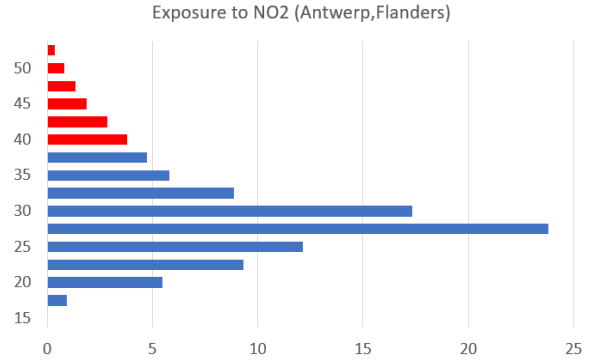

Figure 34. *Population exposure in Antwerp. The figure shows the percentage of the inhabitants in Antwerp as a function of the NO_2-pollution they are exposed to (in ug/m^3). All inhabitants marked in red are living at locations exceeding the EU limit value (approximately 11% of the inhabitants).*

A second output of the urban air application concerns the sector contribution. For each of the sectors that are explicitly considered in the local modelling (road traffic, industry and residential heating), also the approximate contribution of the individual sector to the total concentration is provided[5]. Using these results, stakeholders can identify key sectors for which measures are prioritized. The sector contribution also provides a rough estimate for the (theoretical) maximal pollution reduction related to local measures for the sector under consideration. Indeed, the sector contribution of the specific sector is the gain one can achieve if all the emissions of the sector are mitigated (e.g. if all traffic emissions disappear). Such a scenario is of course theoretical, as it is nearly impossible to remove all the emissions of a specific sector (e.g. even with electric vehicles, there are significant non-exhaust particulate matter emissions), but it indicates the order of magnitude of the maximal gain that can be achieved using local measures. Demonstration results for Sofia are not yet available, but Figure 35 shows the results of a sector contribution analysis for Ghent, Belgium, as visualized in a VITO visualization tool.

[5] For particulate matter, the sector contribution is the exact contribution. For nitrogen dioxide, providing an exact contribution is impossible because of the chemical interaction with ozone.

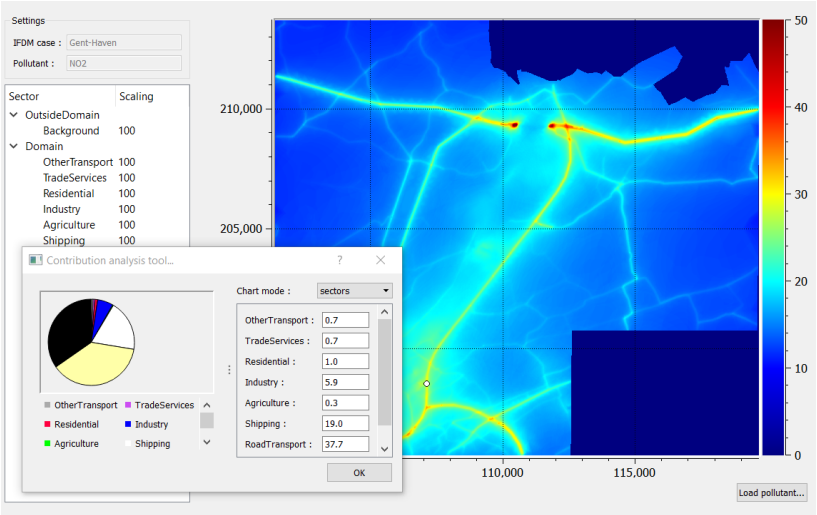

Figure 35. *Results of a sector contribution analysis for Ghent, Belgium. The pie chart shows the sector contribution for the location of the white dot. Clearly, the local contribution is dominated by road traffic (yellow) and shipping (white), while also the background concentrations (black) contributes an important share of the total air pollution.*

Finally, in addition to the annual mean concentrations, hourly time series of pollutant concentrations will be saved for some selected locations. These time series results are important for scientific users of the results, as they can directly be used for model validation (and improvement).

Technically, the annual average maps and the sector contribution data is provided as GeoTIFFs. All data is presented in the European Terrestrial Reference System 1989 (EPSG:3035). This information is also stored in the header of the GeoTIFF files. The time series results are provided as CSV-files.

8.4 Stakeholder needs addressed by the application

The following stakeholder requirements in Deliverable 1.1 are specifically mentioning air quality. For each of these requirements, we discuss whether or not they are considered in CURE.

- Requirement G.12: CURE should provide early warning system
  - There will be no early warning system and air quality forecasting application provided. This requirement was not foreseen at the budget stage, and an air quality forecasting application already exists within CAMS (see https://atmosphere.copernicus.eu/)
- Requirement G.16: CURE should be able to use traffic monitoring in anticipation for managing urban air quality

    - If local traffic data covering the entire urban area are available, CAMS emission data are downscaled to road segments using these datasets. Unfortunately, for Sofia
- Requirement G.25: CURE should consider medium sized and small towns
    - The application will be developed for frontrunner city Sofia, and afterwards set-up for Ostrava, hence covering a large city and a medium-sized town
- Requirement B.1: Interest of Berlin in Air quality modelling
    - Because recent high resolution air quality maps already exist for Berlin, the AQ application will not be applied for Berlin.
- Requirement C.3: CURE applications should assess the environmental (e.g. air quality […]) impact of tree plantation in Copenhagen
    - Because recent high resolution air quality maps already exist for Copenhagen, the AQ application will not be applied for Copenhagen. Moreover, the impact of added urban green (trees etc.) on urban air quality is negligible if no other abatement strategies are considered (e.g. introducing an additional pedestrian zone at the location of the new urban green)
- Requirement S.1: Sofia is interested in […] Urban Air quality
    - The AQ application will be developed for Sofia.
- Requirement S.3, S.5, S.6 and S.8: Technical demands of Sofia municipality concerning resolution, output format and geographical coverage.
    - All these demands will be met by the AQ application.
- Requirement S.9: CURE applications should provide projections i.e. what is the current state and how can it be improved in the future?
    - Because of budgetary reasons, only the current air quality will be mapped. The sector contribution results will, however, provide an insight in the maximal improvements related to the reduction in local road traffic and residential emissions.

9 AP08 URBAN THERMAL COMFORT

9.1 Purpose of the Application

Heat stress is an increasing problem in many European cities, having a negative impact on sleep, productivity, health and mortality of urban residents. Citizens experience higher levels of heat stress than people in rural areas due to higher air temperatures (Urban Heat Island effect), lower wind speeds and higher levels of solar and thermal radiation coming from building materials. Due to the ever-increasing climate warming, this problem is expected to get only worse in the future.

The Urban Thermal Comfort application will quantify and map human thermal comfort for a typical hot day at a very high resolution (1-2m) for entire urban areas. This will allow stakeholders (e.g. urban planners and city administrations) to identify hotspots and give them insight in the local variation of heat stress. Furthermore, the application will allow users to upload different land use scenarios and assess the effectiveness of e.g. green-blue adaptation measures to impact local heat stress problems. As a result, the stakeholders will be able to assess and justify their adaptation strategies, in the sense of providing evidence of their climate-friendliness. Also, they will be enabled to assess the impact of specific intentions of developers on the local thermal comfort conditions in the city, which can help them to decide which intentions should be realized and which not, from the environmental point of view.

9.2 Data & Methodology

To study the urban microclimate, VITO has developed the urban boundary layer climate model “UrbClim”, designed to cover individual cities and their nearby surroundings at a very high spatial resolution (De Ridder et al., 2015). UrbClim consists of a land surface scheme, coupled to a 3-D atmospheric boundary layer module. The land surface scheme is based on the soil–vegetation–atmosphere transfer scheme of De Ridder and Schayes (1997), but is extended to account for urban surface physics. The model has been applied to and validated for over 10 cities worldwide (De Ridder et al., 2015 ; Garcia-Diez et al., 2016 ; Lauwaet et al., 2015 ; Lauwaet et al., 2016 ; Zhou et al., 2016). The model operates at a typical horizontal resolution of 100m, and provides the local meteorological input variables for the high resolution thermal comfort module.

To set up the 100m resolution model simulations, several Copernicus input datasets are needed (Table 12). The spatial distribution of land cover types, needed for the specification of required land surface parameters, is taken from Urban Atlas (2018), and converted to relevant classes for the UrbClim model. Terrain height is specified by the EU-DEM map. The UrbClim model needs also information on the soil sealing and vegetation cover fraction in each grid cell. The percentage urban land cover is specified using the Imperviousness data from CLMS, and the vegetation cover fraction from the NDVI data set. More details about these data sets can

be found in D2.1 of the CURE project. The model is driven by large-scale meteorological data from the C3S ERA5-reanalysis. The model output consists of hourly 2m air temperature, humidity and wind speed fields, as well as land surface temperatures.

Table 12. *Overview of the input datasets for the 100m resolution background UrbClim simulations.*

Copernicus service	*Dataset*	*Usage*
CLMS	Urban Atlas	Specification of land use classes
CLMS	EU-DEM	Specification of terrain height
CLMS	Imperviousness	Specification of soil sealing % in grid cell
CLMS	NDVI	Specification of vegetation % in grid cell
C3S	ERA5	Large-scale meteorological input data

These data give a good overview of the spatial distribution of air temperatures (which don't vary much over short distances) and the Urban Heat Island effect of a city. However, air temperatures don't tell the complete story of heat stress experienced by citizens. Also the radiation load (both shortwave and longwave), humidity and wind speed are important factors to quantify human thermal comfort. An indicator that takes all these variables into account is the Wet Bulb Globe Temperature (WBGT), which is calculated as follows:

$$WBGT=0.7\times Tw+0.2\times Tg+0.1\times Ta$$

with Tw = the wet bulb temperature, Tg = the black globe temperature and Ta= the air temperature.

The Wet Bulb Globe Temperature has a long tradition of being used as a thermal comfort index and is the ISO standard for quantifying thermal comfort (ISO, 1989). It is currently in use by a number of bodies including the US and UK Military, civil engineers, sports associations and the Australian Bureau of Meteorology (Willett and Sherwood, 2012). It is the only heat index to have known thresholds based on a large number of observations, developed by the U.S. Army (2003) (Table 13).

Table 13. *Heat stress category limits of the U.S. Army (2003).*

Heat Stress Category	WBGT [°C]
1	≤ 25.6-27.7
2	27.8-29.4

3	29.4-31.0
4	31.1-32.1
5	≥ 32.2

By combining the standard output of VITO's UrbClim model with detailed radiation calculations based on 3D building and vegetation data, it is possible to calculate the WBGT with a very high spatial resolution (Lauwaet et al. 2020). The methodology used by VITO is adopted from the paper by Liljegren et al. (2008), the recommended method to calculate outdoor WBGT values (Lemke and Kjellstrom 2012). As input for these calculations, additional Copernicus data sets are needed, which are listed in Table 14.

***Table 14**. Overview of the input datasets for the high resolution WBGT module.*

Copernicus service	*Dataset*	*Usage*
CLMS	Urban Atlas Building Height	Specification of building heights
CLMS	Urban Atlas Street Tree layer	Specification of tree locations in cities
Copernicus Data Warehouse	Very High Resolution land cover map	Specification of land use classes

When assessing WBGT values, it is best to focus on typical hot summer days, because it is during these type of days that people will suffer from heat stress issues. The CURE Thermal Comfort App will deliver heat stress maps for a selected hot summer day. Users will be able to download the basic VHR land cover map, modify it according to their needs and upload it again to the Application, which will automatically calculate new heat stress maps.

A complete overview of the whole modelling chain is shown in Figure 36.

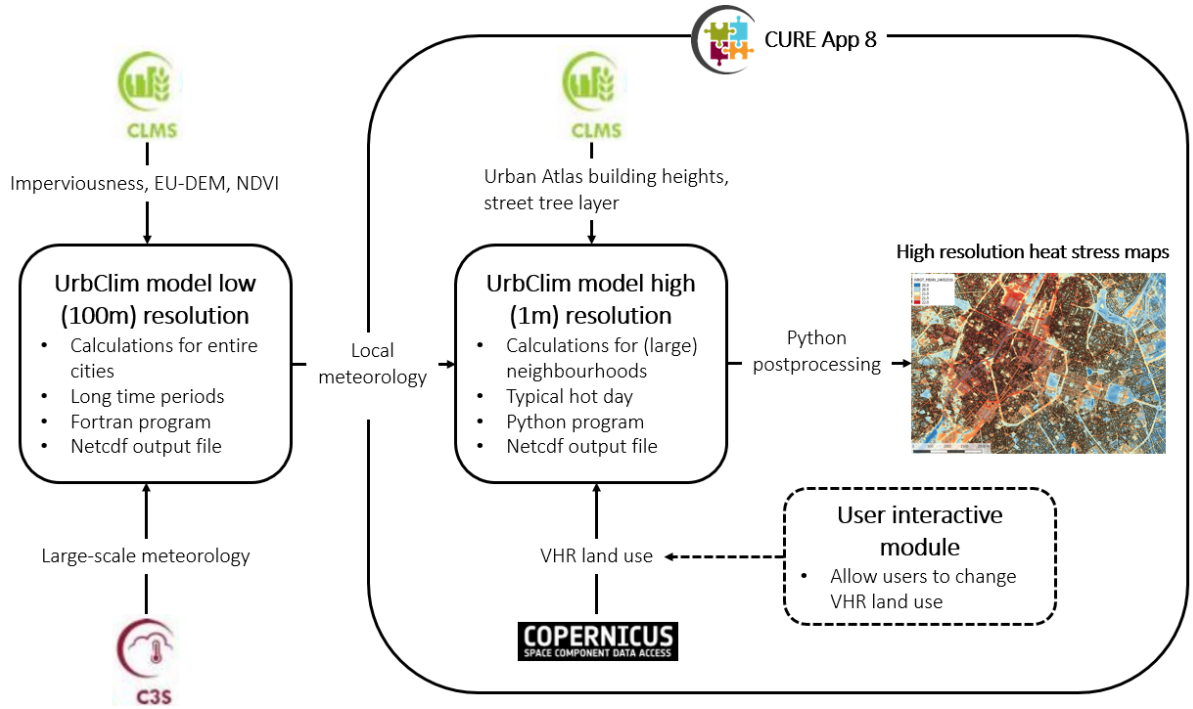

Figure 36. Overview of the Thermal Comfort Application.

9.3 Output features & characteristics

As indicated in the section above, one of the results of this Application are the 100m resolution meteorological variables (air temperature, humidity, wind speed and land surface temperature) that are calculated by the UrbClim model (Netcdf format). These are only intermediate results, needed as input for the thermal comfort module, but they could be provided to the users and stakeholders if they are interested. An example for the city of Copenhagen, one of the front-runner cities in this project, is shown in Figure 37. The map shows the average air temperature for a specific hot day during the summer of 2019. The city and harbour areas are clearly a few degrees warmer than the surrounding water and vegetated areas. It should be kept in mind that the UHI is not constant in time, it builds up gradually during the day and reaches its peak in the late evening. During sunny days with low wind speeds like this one, the UHI can reach over 5°C for a city as Copenhagen, whereas the intensity will be much lower (only 1°C or less) during cloudy, windy or rainy days.

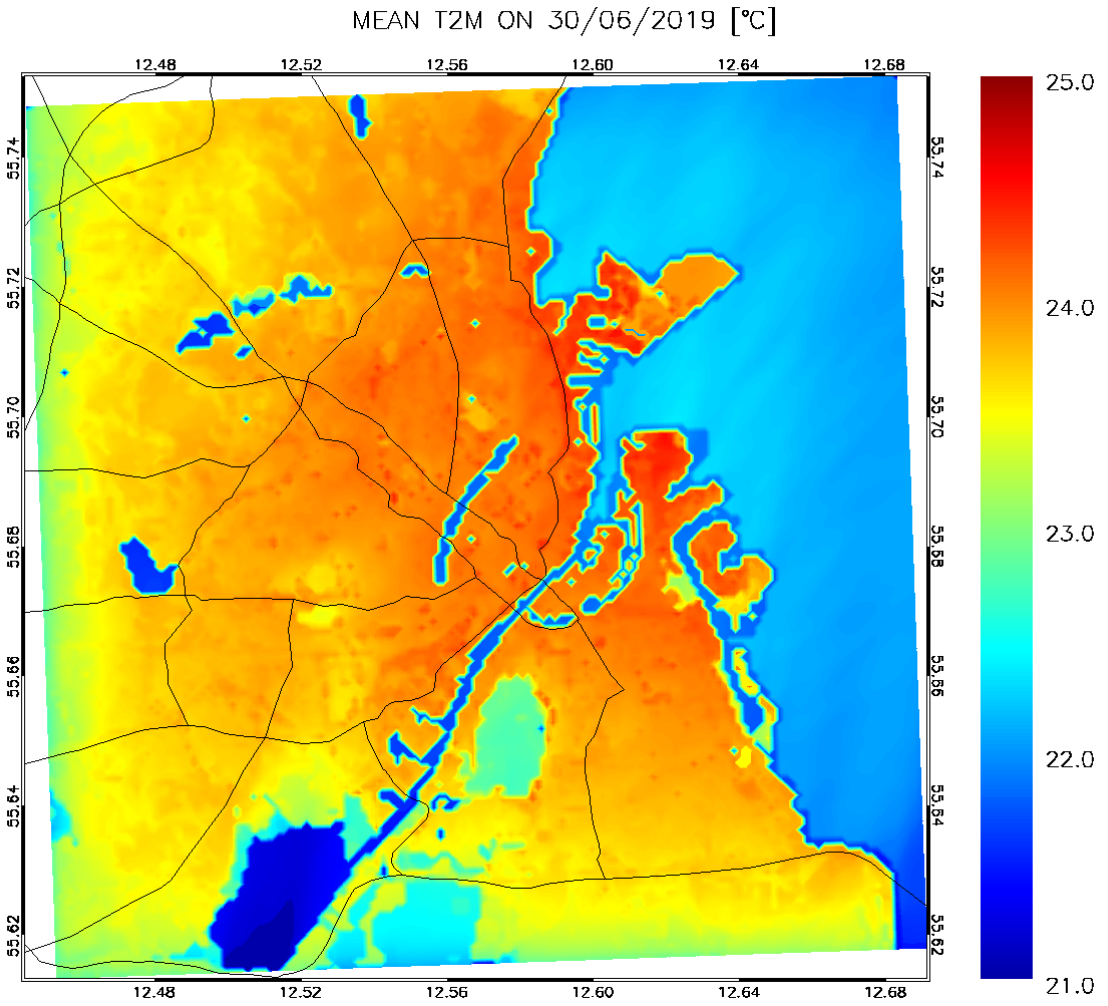

Figure 37. *The mean 2m air temperature map on 30 June 2019 in and around the city of Copenhagen.*

The dedicated results from the Thermal Comfort App will be high-resolution (1-2m) heat stress (WBGT) maps for a selected area of the city center (geotiff format). Several maps can be provided (e.g. daily mean, maximum and minimum values) that can be used to assess the heat stress situation in a city. An example for the city of Copenhagen is shown in Figure 38. Clearly, water areas and forested areas where trees provide shade are the coolest locations in the city. Open, sealed areas without shade from trees or buildings are the hottest locations. From these maps, overview statistics can be calculated (e.g. City quarter averages, area above/below defined threshold values) that can be used to compare different land use/adaptation scenarios.

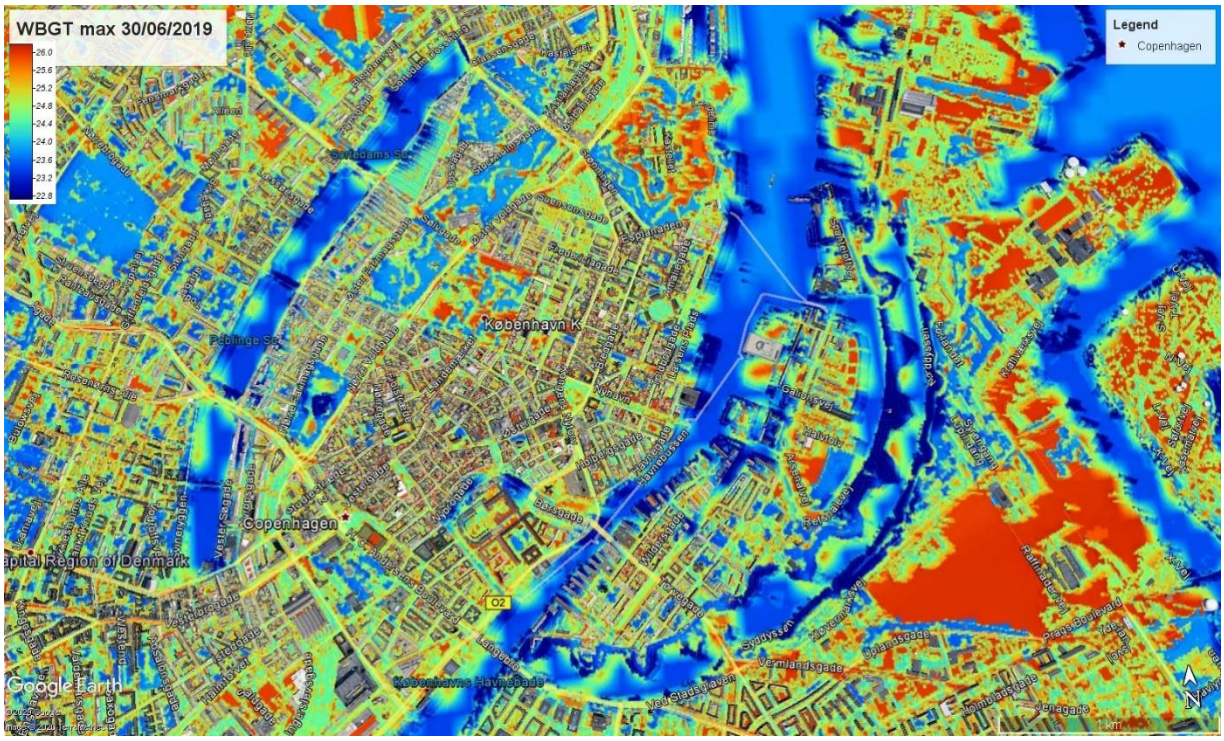

Figure 38. *Maximum Wet Bulb Globe Temperature map on 30 June 2019 for the city center of Copenhagen (overlay in Google Earth).*

Finally, we will produce validation results for the front-runner and follower cities of the CURE project, by comparing our results to available weather observation and remote sensing data. These results will be shared to the stakeholders and reported in the project Deliverables.

9.4 Stakeholder needs addressed by the application

The stakeholder requirements are identified and documented in Deliverable 1.1 of the CURE project. The ones related to the Thermal Comfort App are listed and addressed in Table 15 below. For the city-specific requirements, we focus on the two front-runner cities (Copenhagen and Sofia) for which the application will be developed.

Table 15. *Stakeholder needs related to the Thermal Comfort App and our response to them.*

Stakeholder	*Requirement*	*Response*
General (G.1)	CURE should use and provide access to the most recent data.	This application will be built on the most recent input data sets that are available and the maps will be made for a selected hot day from the past 2 years (2018-2019).

General (G.3)	CURE should provide the possibility to extract timeseries at specified coordinates through APIs.	The data produced by this App allows to do this, but it remains to be seen if this is technically and budget-wise feasible within the CURE project.
General (G.4)	CURE should provide high resolution data and high frequency data.	This App will produce hourly data at a resolution of 1-2m.
General (G.8)	CURE should do coupling of different applications	We will investigate during the CURE project if it is possible to couple this application to the NBS App.
General (G.12)	CURE should provide early warning system	This is out of scope in this project. VITO does provide a heat stress early warning system for the city of Antwerp in a commercial project.
Copenhagen (C.3)	CURE applications should assess the environmental impact of tree plantation in Copenhagen	The impact of tree plantation can be assessed with this App. It will have a significant impact on local heat stress in the city.
Copenhagen (C.5)	CURE applications could investigate the correlation with health.	This is not planned in the CURE project, but could perhaps be looked at if the time and budget allows it (and the necessary data is available).
Sofia (S.3)	The geographical coverage should be for the whole territory of the municipality to identify areas for interventions with specific measures.	We will see if this is possible. It depends on the extent of the VHR input map and computational limitations.
Sofia (S.5)	The spatial scale should be at least 10x10m.	The output maps have a spatial resolution of 1-2m.
Sofia (S.6)	Output should be in vector or raster tiff format.	The output maps are in raster geotiff format.

Sofia (S.9)	CURE applications should provide futuristic analysis or projections i.e. what is the current state and how can it be improved in the future?	The users of the application will be able to upload their own future land use scenario to assess the heat stress impact.
Sofia (S.10)	Developing a model linking to parametric planning – with all indicators in the model - seeking balance between different parameters would be useful.	This is not very clear. We will set up a follow-up discussion with the stakeholders from Sofia.
Sofia (S.11)	A number of UHI and modelling studies have been performed in the past and these studies should be used for developing and cross-comparing with the specific CURE applications.	We will have a look at these studies and will try to compare our results against these.

10 AP09 URBAN HEAT STORAGE MONITORING

10.1 Purpose of the Application

Observations of global temperature evolution indicate a pronounced air temperature warming, since an increase in the occurrence of heat waves and the Urban Heat Island (UHI) effects tends to exacerbate such warming. Among all the effects caused by the substitution of natural ecosystems for urban land-use, the most pronounced is the increase in the amount of energy stored in the urban canopy (especially in buildings), which is approximately 2-6 times larger than in non-urban canopies. The slow release of this energy, stored mainly in the buildings and paved surfaces of cities, causes the UHI effect and it is therefore related to the energy efficiency and consumption in cities. In this framework, the CURE application will deploy various earth observation and in-situ urban data, such as land cover, geometry, radiation and air/surface temperature, towards monitoring urban heat storage.

10.2 Data & Methodology

10.2.1 Data

AP09 will be implemented for Heraklion (front-runner) and Basel (follower) cities. Table 16 lists the data that are used for the AP09. AP09 is using data from two of the Copernicus Services (CLMS and CAMS), very high resolution optical third-party data from the Copernicus Contributing missions Data Warehouse (Copernicus, 2020) and data products from AP01.

Table 16. *Summary of data used for AP09.*

Data Source	Description of the Product
CAMS	Clear-sky surface solar irradiation
CLMS	Urban Atlas
CLMS	Urban Atlas: Building Heights
CLMS	EU-DEM
CLMS	High Resolution Vegetation Phenology and Productivity (Under Development)
Copernicus Satellite	Sentinel-2, Level-2A Bottom Of Atmosphere (BOA) reflectance images
Third-party	Baseline Land Cover from VHR (from the DWH)
Third-party	Material maps from URBANFLUXES project (Chrysoulakis et al., 2018)
Third-party	Buildings and Trees Height from URBANFLUXES project (Chrysoulakis et al., 2018)
Third-party	In-situ air temperature from local city data

10.2.2 Methodology

is the net flow of heat stored in urban canopy and represents all the mechanisms of storage of energy within the volume, i.e., the air, on trees, in buildings constructed in the ground, etc.

(Offerle et al. 2005). An updated version of the Objective Hysteresis Model (OHM) that has been recently released (Lindberg et al. 2018) will be used in CURE to estimate heat storage at local scale. The method will be adapted to Copernicus Core Services. The hysteresis effect on energy flux storage indicates how quickly the urban surface responds to the input of energy and its association with the diurnal evolution of the boundary layer, varying according to latitude, cloud cover, soil characteristics, wetness and vegetation cover. OHM is based on the following expression (Grimmond and Oke, 1999):

$$\Delta Q_S = \sum_{i}^{N}(f_i a_{1i})Q^* + \sum_{i}^{N}(f_i a_{2i})\frac{\partial Q^*}{\partial t} + \sum_{i}^{N}(f_i a_{3i})$$

where Q^* is the net all-wave radiation, $\vartheta Q^*/\vartheta t$ is the time rate of change for net all-wave radiation at the surface and f_i the fraction of each of the N surface components within each grid cell and a_1, a_2 and a_3 are coefficients associated to response of the surface cover due the energy input. Coefficient a_1 indicates the intensity of the relationship between the stored energy flux and the net all-wave radiation. Coefficient a_2 quantifies the magnitude of hysteresis, indicating the direction and degree of the phase relationship between stored energy flux and net all-wave radiation. Coefficient a_3 is an intercept term and indicates the extent to which a negative storage energy flux occurs before the net all-wave radiation starts to become negative. In CURE, Q^* will be estimated as per (Chrysoulakis, 2003), using CAMS products to calculate the incoming shortwave and longwave radiation, the CURE downscaled LST product, to estimate the outgoing longwave radiation, whereas the outgoing shortwave radiation will be calculated at local scale by combining Sentinel 2 reflectance with lower resolution albedo products (Chrysoulakis et al., 2018). Moreover, the coefficients a_1, a_2 and a_3 will be determined from CLMS, based on the land cover as per Grimmond and Oke (1999) and the parameter $\partial Q^*/\partial t$ will be calculated as per Xu et al. (2008), based on CAMS products and *in-situ* air temperature observations. The method will be evaluated in Heraklion (front runner city), based on cross-comparisons with the respective URBANFLUXES products (Chrysoulakis et al., 2018), which are based on the more detailed Element Surface Temperature Method (Offerle et al., 2005). It will be transferred to Basel (follower city).

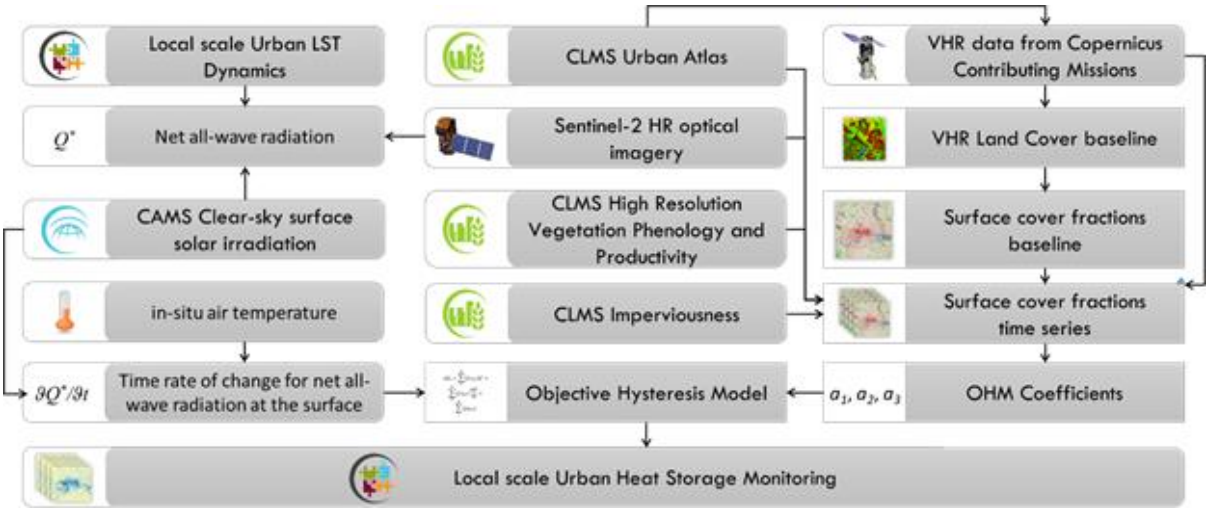

Figure 39. Methodology for the estimation of Urban Heat Storage at local scale.

10.3 Output features & characteristics

The CURE Urban Heat Storage Monitoring application (AP09) is developing time series (4 times per day, depending on the cloud cover) of urban heat storage change flux maps of 100 m x 100 m spatial resolution (local scale). This refers to the heat storage change flux of the urban surface (W/m^2) at the time of the satellite acquisition.

The output maps will be made available as one GeoTiff (image files with geographic information) per Sentinel-3 acquisition.

10.4 Stakeholder needs addressed by the application

Requirement G.1: AP09 will use and provide access to past data only, because of limitation in the methodology.

Requirement G.3: Time series data would be available from AP09.

Requirement G.4: In terms of spatial and temporal resolution, AP09 is products from AP01 to achieve 100 m for 4 times per day time series. More enhanced spatial and temporal resolutions, would require the respective products from AP01.

Requirement G.5: Local air temperature data will be necessary for the development of AP09.

Requirement G.6: The AP09 will be compared to urban heat storage maps of the URBANFLUXES project (Chrysoulakis et al., 2018) which are derived using a different method.

Requirement G.7: AP09 is using transitional products, such as percentage of green areas and land cover change, but these are not made available as CURE products.

Requirement G.8: No coupling of AP09 products is foreseen within CURE, but these products can be coupled with data products from AP03 for the assessment of urban energy budget as per (Chrysoulakis et al., 2018).

Requirement G.11: Similarly to G.7, AP09 is using transitional products, such as percentage of green areas and land cover change, but these are not made available as CURE products.

Requirement G.18: AP09 is using the Open Street Maps to complement the VHR land cover maps as in AP01.

Requirement G.19: The spatial resolution of AP09 is dependent on the spatial resolution of AP01 products. Therefore, see the respective answer in Section 2.4.

Requirement G.21: The temporal resolution of AP09 is dependent on the spatial resolution of AP01 products. Therefore, see the respective answer in Section 2.4.

Requirement G.22: AP09 does provide day and night data.

Requirement G.28: AP09 cannot provide hourly data. See also Requirement G.4 and G.21 above and the respective ones in Section 2.4.

Requirement G.29: AP09 provides 24/7 geo-referenced data.

Requirement G.30: All CURE data will be accompanied by metadata. Details are provided in Deliverable D7.4 (Poursanidis et al., 2020).

Requirement G.33: AP09 does provide time series of data.

Requirement G.34: AP09 will be not implemented for part of the Moravian Silesian region (Ostrava).

Requirement H.2: AP09 will provide data at local scale.

Requirement H.3: AP09 will provide data for 2018-2019 for Heraklion and there is the possibility to extend this to present data.

11 AP10 NATURE BASED SOLUTIONS

11.1 Purpose of the Application

"Nature-based solutions" (NBS) are actions **inspired by nature which use the features and complex system processes of nature, such as its ability to store carbon and regulate water flows,** in order to **help societies address a variety of environmental, social and economic challenges in sustainable ways**. Nature based solutions examples are green roofs, green walls, urban farms, etc. Specifically, green roofs provide multiple benefits as reducing the risk of flooding by collecting rainwater, reduce the ambient temperature, improve energy efficiency in buildings and offer many social benefits associated with urban agriculture, well-being, noise reduction, healing, environmental and air quality, among others. Knowing the capacity of a city to host these types of nature based solutions allows defining which areas have the highest potential to accommodate these solutions and provide decision-makers with different scenarios on green roof potential deployment.

The AP10 of Nature Based Solutions will allow to identify and map already existing green roofs and will enable identifying areas with high roof retrofitting potential by quantifying potential green roof installation according to specific installation conditions. To accurately quantify the urban assets capabilities, it is crucial to identify firstly which buildings have flat or quasi-flat roofs and which ones present an already vegetated surface, in order to identify the maximum green roof potential. Following a zoning approach and in order to prioritize areas with highest potential, albedo and imperviousness are also considered. Furthermore, buildings with highest potential of being retrofitted are identified, considering a set of suitability criteria, such as buildings with low protection level, year of construction and solar radiation.

After applying these thresholding, prioritization and suitability criteria, the outputs of estimated green-roof potential will be coupled with the thermal comfort application. This will allow to spatially explicitly assess the potential improvement in thermal performance of public spaces of the city if massively installing green roofs. Furthermore, alternative scenarios for green roof installation could be benchmarked assessing thermal comfort benefits in each of the cases.

In summary, the development of the NBS application will contribute to advance beyond the state of the art in the following terms: I) identifying inexpensive alternatives to LiDAR information from Copernicus sources; ii) improve prioritization and suitability criteria for quantification of maximum green roof potential; iii) analyze potential effectiveness of alternative scenarios of green roof installation as additional decision-making information.

11.2 Data & Methodology

In urban areas, contribution of green roofs is a valid alternative to increase the green area, especially where available land for greening is limited. The methodology proposed aims to

estimate the potential for green coverage at rooftop level by identifying suitable locations for green roof deployment and supporting decision-making towards broader sustainable urban development.

With the objective of comparing the results of the analysis and their accuracy, three inputs for object detection will be considered:

- LiDAR: From LIDAR data digital surface model is derived, which includes elevation data of the urban environment, including the elevations of urban elements such as buildings, vegetation or roads, among others. The number of points and point density improves data accuracy, which is crucial.
- Stereo Imagery DSM: Out of the granted VHR WorldView-1 and WorldView-3 images acquired at different time steps with different viewing angles, we generate a sub-meter (i.e., 50 cm) spatial resolution DSM. In particular, the DLR "Catena" operational infrastructure is used. Here, the standard chain generates orthorectified images using a worldwide reference image database. For this task, ground control points are automatically extracted from the satellite and reference images, which are used to correct attitude and ephemeris data. Next, the original satellite image is orthorectified using a high-resolution digital elevation model. Finally, automatic atmospheric correction is performed and concurrently the DSM is generated.
- Euro-Maps 3D DSM: Euro-Maps 3D products developed by GAF are DEMs semi-automatically derived from 2.5 m in-flight stereo data provided by IRS-P5 Cartosat-1 and. Among these, the Euro-Maps 3D DSM layer is a homogeneous 5m spaced DSM product including detailed flanking information consisting of several pixel-based quality and traceability layers. A sophisticated and tailored algorithm based on semi-global matching is applied and the reliability of the information is increased by using multiple overlapping stereo pairs. Since 2020, Euro-Maps 3D products are available from ESA as Third Party Mission data for on demand ordering upon submission of a Project Proposal subject to evaluation and acceptance. In this regard, the CORE consortium is going to submit a dedicated proposal in early 2021.

Buildings outlines are derived from cadastral map in form of vector file.

The methodological process for the calculation as described below:

Identification of the maximum green roof potential

As flat or quasi flat roofs are the ones more suitable to host a green cover, slope computation is performed (step 1). For each unit (building), an analysis of the slope is performed on the basis of each DSM by measuring the actual slope at each point/pixel of the roof. The slope map of the building is analyzed using a statistical algorithm that gives us the estimation of the real slope and the flat area available. Buildings with a suitable flat surface are labeled as flat roof by noting their flat zone percentage. The threshold for the slope computation is adjusted on a case by case, considering local regulations and policies. Consequently, for each building, the

percentage of flat surface is calculated (step 2), considering roofs whose flat surface percentage is greater than 10% if their size is lower than 100 m² or greater than 5% if their size is greater than 100 m², which are those considered as suitable for hosting a green roof (Marconcini et al. 2016). Furthermore, NDVI is used to compute vegetated surfaces, considering as existing green roofs the ones whose percentage vegetation cover is greater than 10% (step 3). This process allows for determining the maximum green roof potential.

Prioritization of areas with highest potential/benefit

Benefits of green roofs are larger if these solutions are installed in areas characterized by impervious surface and low albedo (step 4), contributing also to reduce the Urban Heat Island effect. Average percentage imperviousness (step 5) is considered by establishing a buffer area around the potential green roofs, while reflectance parameters of each roof are analyzed to catalog them according to their energy efficiency (roof tile, dark roof, clear roof).

Identification of buildings with highest potential

CityGML data model with buildings in Level of Detail (LoD) 2, which has differentiated roof structures and thematically differentiated surfaces will be used for this phase. The CityGML model will be generated extruding buildings outlines with height values using LIDAR digital surface and terrain maps, even if the possibility of using Copernicus Building Height layer will be further explored. The input CityGML data model needs to be completed with all the available semantic information (step 6 and 7). Cadastral information will be used to include the year of construction and the protection degree of buildings. In addition, information on which buildings have flat or quasi-flat roof and its flat surface percentage is also stored. Furthermore, using solar radiation raster file, the average solar radiation value is stored (step 8). For this purpose, a raster file which indicates the values of the solar radiation per pixel has been calculated based on LIDAR digital surface model.

The following graph shows the overall approach and methodological steps for the development of the NBS App:

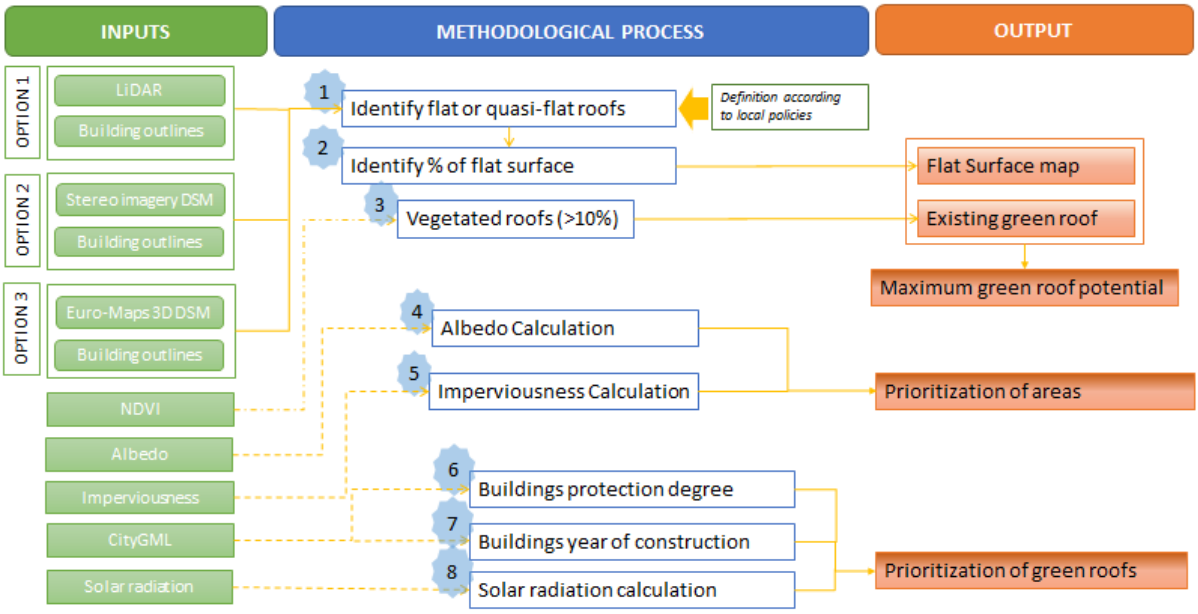

Figure 40. Overview of the Nature Based Solution App

Table 17. Overview of the input datasets for the prioritization of green roofs

INPUT	*Copernicus service*	*Dataset*	*Usage*
LIDAR (option 1)			Identify flat surface of the roofs
Stereo imagery DSM (option 2)			Identify flat surface of the roofs
Euro-Maps 3D DSM (option 3)			Identify flat surface of the roofs
Building outlines			Identify flat surface of the roofs
NDVI	CLMS	NDVI	Identify already existing green roofs (with vegetation >10%)
Albedo	CLMS	Albedo	Prioritize intervention areas
Imperviousness	CLMS	Imperviousness	Prioritize intervention areas
CityGML			Inclusion of cadastral semantic information (step 6 and 7) and solar radiation (step 8) and storage of previous results
Solar Radiation		LIDAR DSM	Solar radiation calculation for building (Step 8)

11.3 Output features & characteristics

The output of the NBS App will be a raster file identifying the buildings with highest potential of being retrofitted. The following Figures show examples of the flat surface map of the city of Donostia- San Sebastian

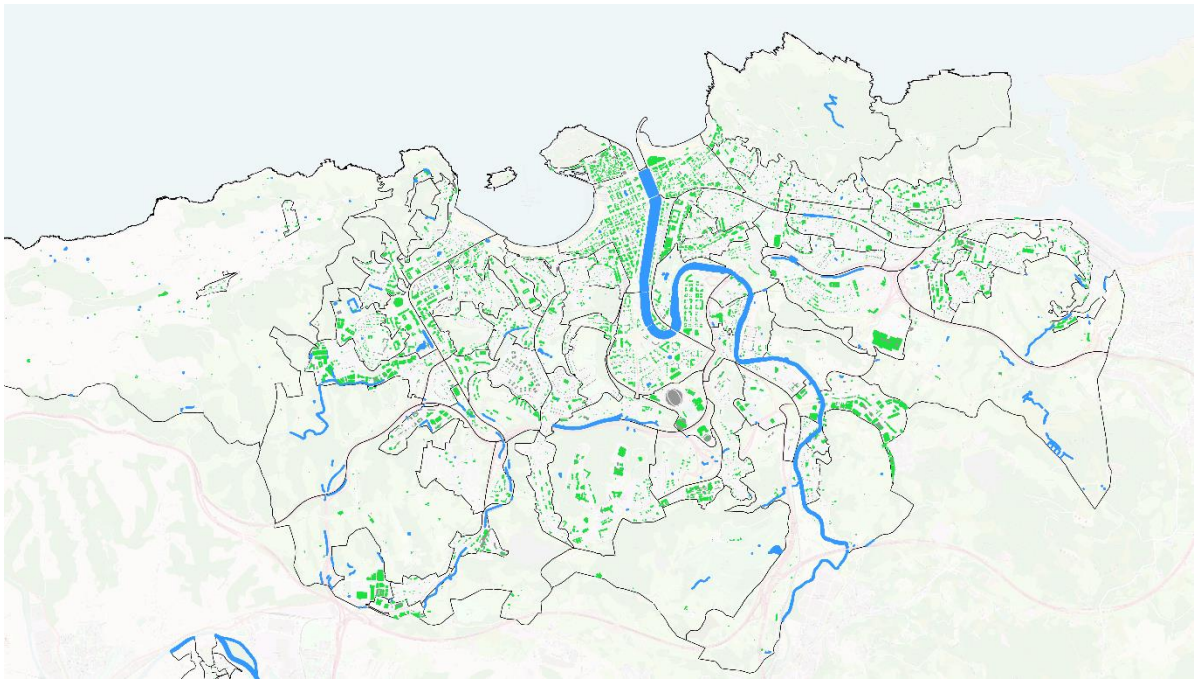

Figure 41. *Flat Surface Map for the city of Donostia/San Sebastián*

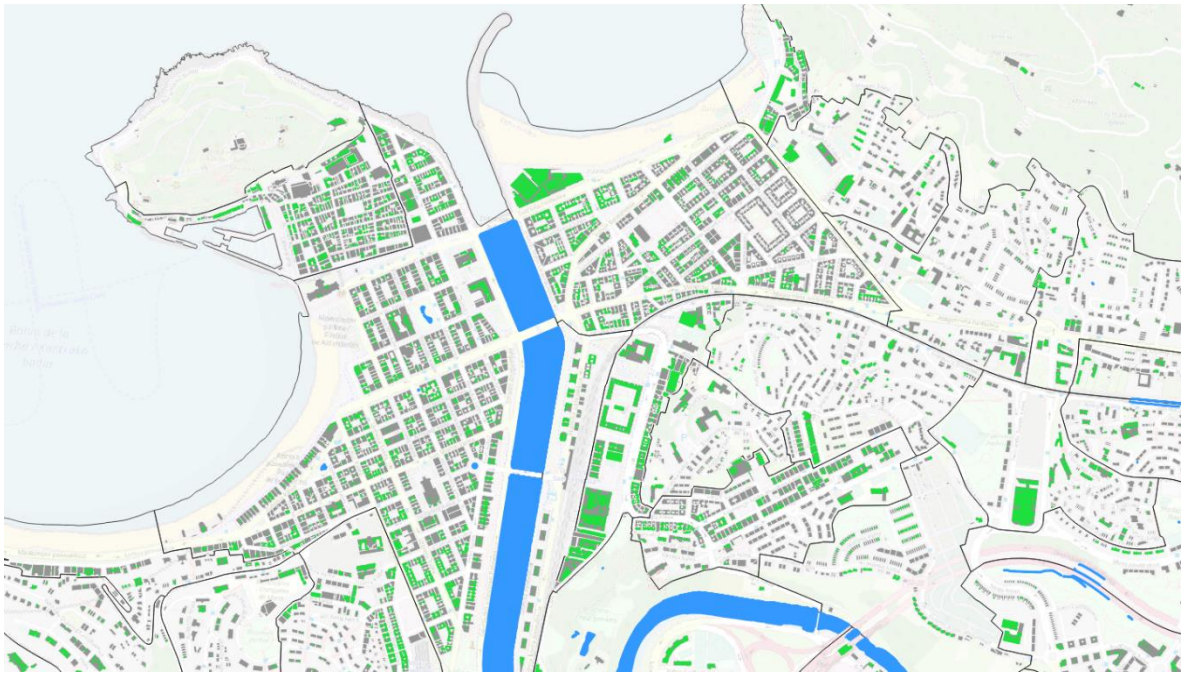

Figure 42. *Flat Surface Map for the city center of Donostia/San Sebastián*

11.4 Stakeholder needs addressed by the application

The stakeholders' requirements identified in Deliverable 1.1 and related to NBS App are listed in Table 18 below. Both general requirements as well as Sofia specific requirements, for which the app will be developed, are addressed.

Table 18. Stakeholder needs related to the NBS App and our response to them.

Stakeholder	*Requirement*	*Response*
General (G.1)	CURE should use and provide access to the most recent data.	The app will use most recent data, considering the availability of the dataset required.
General (G.4)	CURE should provide high resolution data and high frequency data.	This App will produce high resolution output (between 0.5 - 5 m). The purpose of the App does not require for high frequency data.
General (G.5)	CURE should be able to use and provide data combination of satellite based, EU databases and local data	The App will be based mainly on satellite imagery and cadastral information, both geometric and semantic.
General (G.6)	CURE should compare and/or validate CURE application outputs with other existing data sources	3 different input data sources will be compared, furthermore in the follower city of San Sebastian the analysis will be compared with already existing information
General (G.7)	CURE should provide data outputs including soil, land, 2D/3D city model, cultural heritage, building heights, surface elevation data, and cover, land use, cartographic maps (buildings, streets), digital elevation maps, albedo of urban surface, imperviousness, etc.	The App will be based on the integration of different information, by means of the creation of a 3D model that will combine urban and building information.
General (G.8)	CURE should do coupling of different applications	We will investigate if it is possible to couple this application to the Thermal Comfort App.

General (G.9)	CURE should provide various simulations including climate protection and adaptation measures	The App will provide different scenarios for the implementation of green roofs
General (G.13)	CURE should provide interoperability	The 3D model ensures operability as it is built on standards and the output will be a raster file
General (G.30)	There must be integrated and harmonized metadata (considering INSPIRE directive) and interpretation	The model will explore the INSPIRE directive for different elements
Sofia (S.3)	The geographical coverage should be for the whole territory of the municipality to identify areas for interventions with specific measures.	The App will analyze the Municipal territory and will identify areas and buildings most suitable for the installation of green roofs
Sofia (S.5)	The spatial scale should be at least 10x10m.	Different outputs will be compared, considering resolutions from 0.5 to 5 m.
Sofia (S.6)	Output should be in vector or raster tiff format.	The output maps are in raster format.
Sofia (S.8)	CURE applications should use historical data to perform retrospective analysis where it helps in projections/futuristic analysis contributing to evidence based planning and policy making challenges	For the NBS app, retrospective analysis would not provide useful information, but outputs will provide scenarios for evidence based decision making
Sofia (S.9)	CURE applications should provide futuristic analysis or projections i.e. what is the current state and how can it be improved in the future?	The App will analyze the current state and will perform different scenarios of green roof potential

12 AP11 HEALTH IMPACTS

12.1 Purpose of the Application

Application 11 Health impacts (socioeconomic perspective) will look at the health impacts and costs of air pollution and heat stress in urban settings. The main focus of the application will be on the topic of air pollution, where the EVA (Economic Valuation of Air pollution) model will be used on two frontrunner cities. The heat stress topic will be covered by a literature search focusing on heat stress impact on health costs for Europe.

12.1.1 Air pollution

The health impacts of air pollution will be analysed using the EVA model (Economic Valuation of Air Pollution) developed by Aarhus University, and will be performed on the two frontrunner cities Copenhagen (Denmark) and Sofia (Bulgaria). The integrated model system is based on the impact-pathway chain and is used for assessment of health impacts from air pollution, including both health effects and related external costs (sometimes also referred to as "indirect costs") which can be attributed to air pollution exposure.

The EVA model system describes the health effects of air pollution related to:

- Bronchitis in adults
- Bronchitis and asthma in children
- Sick days
- Hospital admissions for respiratory and cardiovascular diseases
- Lung cancer
- Acute deaths (caused by short term exposure)
- Years of Life Lost (caused by long-term exposure)
- Total amount of deaths (=chronic years lost/10,6* + acute deaths)

The EVA system has the capability of giving useful insights to the planning and prioritization of the regulation policies and instruments. The related external costs found can be used to directly compare the contributions from different emission sectors, as a basis for decision-making on regulation and emission reduction.

12.1.2 Heat stress

The health impacts of heat stress will be based on available information on heat stress in urban settings in Europe and how this affects the morbidity and mortality of citizens. Available research forecasting temperature rises can help decision-makers understand the economic implications of a drastic changing climate and why they should prepare for such scenarios now.

12.2 Data & Methodology

12.2.1 The EVA model

The integrated model system is based on the impact-pathway chain and is used for assessment of health impacts from air pollution, including both health effects and related external costs (sometimes also referred to as "indirect costs") which can be attributed to air pollution exposure.

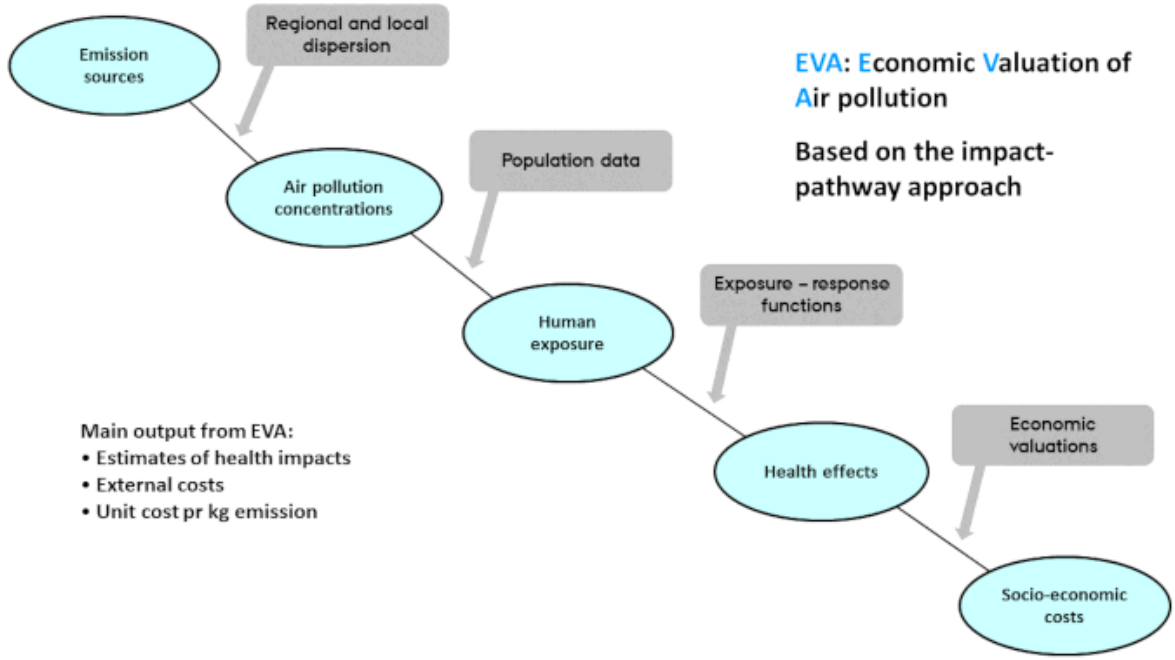

Figure 43. *A schematic diagram of the impact-pathway methodology. The site-specific emissions result (via atmospheric transport and chemistry) in a concentration distribution, which together with detailed population data, can be used to estimate the population-level exposure. Using exposure-response functions and economic valuations, the exposure can be transformed into impacts on human health and related external costs.*

Chemical components important for health impacts and included in the EVA system are: nitrogen dioxide (NO2), sulphur dioxide (SO2), ozone (O3) and particulate matter (PM2.5), where the individual constituents of PM2.5 are: mineral dust, black carbon (BC), organic matter (OM), secondary inorganic aerosols (SIA – i.e. nitrate, sulphate and ammonia), secondary organic aerosols (SOA) and sea salt.

The EVA model is coupled to the air pollution models DEHM (Danish Eulerian Hemispheric Model) and UBM (Urban Background Model) for regional-scale and local-scale health impact assessments, respectively. EVA includes gridded population data, exposure-response functions for health impacts in terms of morbidity and mortality, and economic valuation of the health impacts from air pollution.

The EVA system uses comprehensive and thoroughly tested chemistry-transport models when calculating air pollution levels in general as well as scenarios describing how specific changes in emissions of pollutants to the air affect air pollution levels at regional and local scale.

Modelling of air quality is based on the regional air pollution model DEHM and the urban background model UBM resulting in calculations performed on a 1 km x 1 km grid resolution. Urban background concentrations are the general air pollution in the city and reflect the concentrations in a park, a backyard or the roof of buildings. Urban background concentrations differ from street concentrations, which represent the concentrations in the height of 2 m at the facade of buildings. Street concentrations are calculated using air quality model OSPM.

To estimate the effect of a specific emission source or emission sector, emission inventories for the specific sources are implemented in DEHM, together with all other relevant anthropogenic and natural emission sources, see Table 19 for description of emission sources.

Table 19. *Definition of the SNAP categories and a short description of the emissions of interest.*

Region	SNAP	Emission scenario (or the "tag")
EU/DK	1	Combustion in energy and transformation industries
	2	Non-industrial combustion plants, including private wood combustion
	3	Combustion in manufacturing industry
	4	Production processes
	5	Extraction and distribution of fossil fuels and geothermal energy
	6	Solvents and other product use
	7	Road transport
	8	Other mobile sources and machinery (excl. international ship traffic)
	9	Waste treatment and disposal
	10	Agriculture
	Sum 1–10	Sum of the above 10 SNAP categories
	All	All anthropogenic emissions (SNAP 1–SNAP 10)

To calculate the impacts of the total air pollution levels or of emissions from a specific source or sector, concentrations and address-level population data are combined to estimate human exposure, and then the response is calculated using an exposure-response function (ERF) of the following form: $R = A \cdot C \cdot P$, where R is the response (e.g. in cases, days, or episodes), C the concentration (i.e. the total concentration or additional concentration resulting from emissions of a particular emission source), P the affected share of the population, and A is an empirically determined constant for the particular health outcome, typically obtained from published cohort studies, see Table 20 for exposure-response functions.

Table 20. Example of health effects, exposure-response functions and economic valuation (applicable for Danish/European conditions) included in the EVA model system (note, prices are from 2006). (PM is particulate matter, including primary PM2.5,NO−3and SO2−4. YOLL is years of life lost. SOMO3 (Sum of Ozone Means Over 35 ppb) is the sum of means over 35 ppb for the daily maximum 8-hour values of ozone.

Health effects (compounds)	Exposure-response coefficient (α)	Valuation, euros (2006 prices)
	Morbidity	
Chronic bronchitis (PM)	8.2×10^{-5} cases/$\mu g m^{-3}$ (adults)	52 962 per case
Restricted activity days (PM)	$= 8.4 \times 10^{-4}$ days/$\mu g\, m^{-3}$ (adults) -3.46×10^{-5} days/$\mu g\, m^{-3}$ (adults) -2.47×10^{-4} days/$\mu g\, m^{-3}$ (adults > 65) -8.42×10^{-5} days/$\mu g\, m^{-3}$ (adults)	131 per day
Congestive heart failure (PM) Congestive heart failure (CO)	3.09×10^{-5} cases/$\mu g\, m^{-3}$ 5.64×10^{-7} cases/$\mu g\, m^{-3}$	16 409 per case
Lung cancer (PM)	1.26×10^{-5} cases/$\mu g\, m^{-3}$	21 152 per case
	Hospital admissions	
Respiratory (PM) Respiratory (SO_2)	3.46×10^{-6} cases/$\mu g\, m^{-3}$ 2.04×10^{-6} cases/$\mu g\, m^{-3}$	7931 per case
Cerebrovascular (PM)	8.42×10^{-6} cases/$\mu g\, m^{-3}$	10 047 per case
	Asthma, children (7.6 % <16 yr)	
Bronchodilator use (PM) Cough (PM) Lower respiratory symptoms (PM)	1.29×10^{-1} cases/$\mu g\, m^{-3}$ 4.46×10^{-1} days/$\mu g\, m^{-3}$ 1.72×10^{-1} days/$\mu g\, m^{-3}$	23 per case 59 per day 16 per day
	Asthma, adults (5.9 % >15 yr)	
Bronchodilator use (PM) Cough (PM) Lower respiratory symptoms (PM)	2.72×10^{-1} cases/$\mu g\, m^{-3}$ 2.8×10^{-1} days/$\mu g m^{-3}$ 1.01×10^{-1} days/$\mu g\, m^{-3}$	23 per case 59 per day 16 per day
	Loss of IQ	
Lead (Pb) (<3 year)* Mercury (Hg) (foetus)*	1.3 points/$\mu g\, m^{-3}$ 0.33 points/$\mu g\, m^{-3}$	24 967 per point 24 967 per point
	Mortality	
Acute mortality (SO_2) Acute mortality (O_3)	7.85×10^{-6} cases/$\mu g\, m^{-3}$ 3.27×10^{-6}*SOMO35 cases/$\mu g\, m^{-3}$	2 111 888 per case
Chronic mortality, YOLL (PM) Infant mortality (PM)	1.138×10^{-3} YOLL/$\mu g\, m^{-3}$ (>30 yr) 6.68×10^{-6} cases/$\mu g\, m^{-3}$ (>9 months)	77 199 per YOLL 3 167 832 per case

EVA calculates and uses the annual mean concentrations of CO, SO2 and PM2.5, while for O3 , it uses the SOMO35 metric that is defined as the yearly sum of the daily maximum of 8 h running average over 35 ppb, following WHO (2013) and EEA (2017).

In EVA, the number of lost life years for a Danish population cohort with normal age distribution, when applying the ERF of Pope et al. (2002) for all-cause mortality (relative risk, RR of 1.062 (1.040–1.083) on a 95 % confidence interval), and the latency period indicated, sums to 1138 years of life lost (YOLL) per 100.000 individuals for annual PM2.5 increase of 10 µg m−3 (Andersen et al., 2008). EVA uses a counterfactual PM2.5 concentration of 0 µgm−3 following the EEA methodology, meaning that the impacts have been estimated for the full range of modelled concentrations from 0 µg m−3 upwards.

If we take Copenhagen as a study example, the procedure for obtaining the results will look like this:

1. *Air Quality Assessment*

An air quality assessment is carried out that describes the spatial distribution of background concentrations with a resolution of 1 km x 1 km, as well as street concentrations at address level in the Capital Region. This description is based on data from a national data set, which is called Air Quality at Your Street (http://luftenpaadinvej.au.dk). For our second frontrunner city, Sofia, we will rely on a local air pollution data set. Furthermore, a summary of the results from the fixed measuring stations in the Capital Region is carried out and compared with EU limit values for air quality and WHO air quality guidelines.

2. *Source apportionment*

A source apportionment is carried out for the Capital Region. It includes an emission inventory which describes total emissions and the distribution of emissions on different sources, and how they are distributed geographically.

In addition, a source attribution that estimates the source contribution to the urban background concentrations thereby providing an overview of how many micro per cubic meter the different sources contribute to urban background concentrations seen as an average over all 1 km x 1 km grid cells in the Capital Region.

Furthermore, a source attribution for 98 streets in Copenhagen is also given providing information about how much different vehicle categories contribute to street concentrations. This will not be possible for Sofia, as we do not have these kinds of data.

3. *Health impacts and related external costs*

Health effects and related external costs are calculated for the total air pollution in the Capital Region. The total air pollution includes all sources from the Capital Region, and all other sources in Denmark and abroad. This also describes how much of total air pollution originates from local sources and how much is from sources outside the Capital Region. Moreover, calculations are carried out for each type of emission source in the Capital Region to quantify the contribution of the different sources. In principle, the Capital Region is able to regulate these sources.

Then we add calculations on the health impacts and related external costs based on information about the sources of pollution and their location, the dispersion of air pollution as well as exposure of the population, the dose-response relationship between exposure and health effects, and the valuation of health effects, also referred to as external costs related to health effects from air pollution. The EVA system includes population data with a spatial resolution of 1 km x 1 km.

12.2.2 Heat stress analysis on health costs

We will conduct a literature review of available resources on cases in Europe, where extreme heat events have occurred in the past ten to 20 years and studies which have looked at forecasting heat events, and where morbidity and mortality numbers can be found for cities and/or regions. By collecting available information and what factors account for the biggest effect on morbidity and mortality we can illustrate the severity of such effects on health in the past and in the future, and how it influences or will influence the socioeconomic circumstances in the future.

12.3 Output features & characteristics

12.3.1 Air quality and health costs

The main objective is to identify health and environmental effects for the two frontrunner cities, Copenhagen and Sofia, by seeking to answer the following questions:

- How is the air quality in Copenhagen and Sofia today (=from most recent air pollution measurements)?
- How is the air quality in relation to limit values for air quality as well as the World Health Organization's guidelines for air quality?
- What sources contribute to air quality, and how much originates from the city and outside the region?
- What are the health effects of air pollution and the associated external costs?
- What are the environmental effects of air pollution?

This will be done through the following activities:

- An air quality assessment, which describes the concentration distribution of background concentrations, as well as street concentrations and compare this with current limit values for air quality as well as the World Health Organization's guidelines for air quality
- A source apportionment which describes the distribution of total emissions on different sources, and how they are distributed geographically. In addition, a source attribution that estimates the source contributions to the urban background concentrations.
- Estimation of the health effects and external costs related to air pollution in the two cities. The external costs are the social costs.
- Description of the environmental effects of ozone, deposition of nitrogen and sulphur as well as levels of heavy metals, and compare this with critical loads and levels.

The output will be formatted as tables, see below for examples:

Table 21. *Example of total number of cases of the different impacts related to all Danish anthropogenic emissions for the year 2000.*

Health impact	Number of cases in Europe	Number of cases in Denmark
Chronic bronchitis	4350	802
Restricted activity days	4 440 000	820 000
Respiratory hospital admissions	234	44
Cerebrovascular hospital admissions	556	101
Congestive heart failure	324	69
Lung cancer	666	123
Bronchodilator use, children	128 000	21 600
Bronchodilator use, adults	851 000	157 000
Cough, children	441 000	74 600
Cough, adults	876 000	162 000
Lower respiratory symptoms, children	170 000	52 800
Lower respiratory symptoms, adults	316 000	58 300
Acute mortality	85	−9
Chronic mortality (YOLL)	49 000	8520
Infant mortality	5	1

Table 22. *Example of total health-related external costs for Europe (billion euros) and Denmark (million euros) from the 10 major individual emission SNAP categories in Europe (DEHM domain 2) for the emission year 2000 as well as their contributions in % to the total external cost in Europe and Denmark (all costs are in 2006 prices).*

European emission sector	Europe		Denmark	
	bn euros	% of cost in Europe	Mio euros	% of cost in Denmark
EU/1 Combustion in energy and transf. industries	185	24.1	698	18.6
EU/2 Non-indus. combustion plants/wood	73	9.5	362	9.7
EU/3 Combustion in manufacturing industry	60	7.9	258	6.9
EU/4 Production processes	50	6.5	193	5.2
EU/5 Extr. and distr. of fossil fuels/geoth. energy	10	1.3	50	1.3
EU/6 Solvents and other product use	13	1.7	84	2.2
EU/7 Road transport	138	18.0	857	22.9
EU/8 Other mobile sources and machinery	50	6.5	255	6.8
EU/9 Waste treatment and disposal	7.8	1.0	29	0.8
EU/10 Agriculture	180	23.5	957	25.6
Sum EU/1–10	766	100.0	3740	100.0

Calculations are carried out for the latest year for which there are updated emissions for on 1 km x 1 km resolution.

12.3.2 Heat stress output

The output will include an overview of past events, showing number of e.g. premature deaths, sick days and other factors that contribute to health and wellbeing. It will also include temperature thresholds for different regions and how the length, frequency and intensity of heat waves will influence e.g. mortality, number of hospital admissions in the coming decades, and what the total costs of such events have or will amount to.

12.4 Stakeholder needs addressed by the application

Stakeholder requirements from Deliverable 1.1 related to Application 11, have been included below, to give an indication of whether or not the requirement will be addressed by the application and if not, why so.

General requirements (only one identified as being related to App11):

Requirement G.8: CURE should do coupling of different applications e.g., NBS combating climate change risks,AQ/NBS and HI–with cause effect analysis, etc.

Answer: Air quality and health impacts with cause effect analysis will be tackled by the EVA model which is part of the service put forward as App11.

City specific requirements for Copenhagen and Sofia (only Copenhagen requirements included as requirements from Sofia were not related to App11):

'Requirement C.1: 'CURE applications should investigate the co-relation between air quality, heat island and health/economic impact for short term as well as long term illnesses.

Answer: The EVA model which will be used to analyse the relationship between air pollution and health impacts and costs includes illnesses such as:

- Chronic bronchitis
- Hospital admissions
    - respiratory
    - cerebrovascular
    - congestive heart failure - lung cancer
- Asthma children (7,6%<15years)
    - bronchodilator use
    - cough
    - lower resp. symptoms
- Asthma adults (5,9%>15years)
    - bronchodilator use
    - cough
    - lower resp. symptoms

For heat island effects, we will rely on existing studies to analyse the impacts of heat stress on morbidity and mortality.

Requirement C.2: 'CURE applications should investigate the impact of COVID lockdown from a satellite data perspective and find out what is required to implement the WHO guidelines? What are the associated socioeconomic impacts? What are the impacts on congestion levels?

Answer: Out of scope of this project.

Requirement C.3: 'CURE applications should assess the environmental (e.g., CO2 emissions, air quality) and health (socio-economic) impact of tree plantation in Copenhagen'.

Answer: Out of scope of this project.

Requirement C.5: 'for CURE applications could investigate through satellite and local data the correlation of urban heat, heat island assessment, noise with health as it can provide useful insights for planning and decision making.'

Answer: As previously stated, we will be looking at heat island effects in terms of relying on existing studies to analyse the impacts of heat stress on morbidity and mortality. Further in-depth research, which is out of scope for this project, would be needed to expand on this subject.

13 CONCLUSION

This is the first deliverable of WP3 of the CURE project, which focusses on the individual applications development. The CURE applications described in this deliverable form the basis for the development of an umbrella cross-cutting CURE service on urban resilience (WP4) and feed into the demonstration phase (WP5), in which users will give feedback on the resulting service through two demonstration workshops. After two iterations, a final set of cross-cutting applications related to urban resilience, with high automation and upscaling potential, is the expected outcome of WP3.

Among others, this deliverables explains how each application contributes to the concept of urban resilience and how different Copernicus Core Services products are used in order to build the cross-cutting service. The methodological framework of each application is explained in detail, along with details on the necessary input information, arising from the interaction with WP2.

Interactions between application developers and the users of the project in the framework of WP1 not only helped to shape the applications in terms of applicability and usability, but also revealed needs that cannot be met within the CURE project and/or require further research. This was addressed in detail for each application. These unmet needs give important hints for future development and design of urban services beyond the CURE project.

REFERENCES

Andersen MS, Frohn LM, Nielsen JS, Nielsen M, Jensen SS, Christensen JH, Brandt J. A Non-linear Eulerian Approach for Assessment of Health-cost Externalities of Air Pollution. Proceedings of the European Association of Environmental and Resource Economists 16th Annual Conference; Gothenburg, Sweden. 25–28 June 2008; 2008. p. 23.

Aubinet, M., Vesala, T., Papale, D., 2012. Eddy Covariance – A Practical Guide to Measurement and Data Analysis. Springer Atmospheric Sciences

Berkowicz, R., Hertel, O., Larsen, S., Sørensen, N., Nielsen, M., 1997. Modelling traffic pollution in streets. URL: https://orbit.dtu.dk/files/128001317/Modelling_traffic_pollution_in_streets.pdf

Berkowicz, R., Ketzel. M., Lofstrom, P., Rordam, H., 2008. NO2 chemisty scheme in OSPM and other Danish models. URL: https://www2.dmu.dk/AtmosphericEnvironment/Docs/NO2scheme.pdf

Brutsaert, W., 1982. Evaporation into the Atmosphere. Springer Netherlands. ISBN: 978-90-481-8365-4

CAMS, 2019. The Copernicus Atmosphere Monitoring Service global and regional emissions (April 2019 version). https://doi.org/10.24380/d0bn-kx16

Christen, A., Coops, N.C., Crawford, B.R., Kellett, R., Liss, K.N., Olchovski, I., Tooke, T.R., Van Der Laan, M., Voogt, J.A., 2011. Validation of modeled carbon-dioxide emissions from an urban neighborhood with direct eddy-covariance measurements. *Atmos. Environ.* 45, 6057–6069. https://doi.org/10.1016/j.atmosenv.2011.07.040

Chrysoulakis, N., Grimmond, S., Feigenwinter, C., Lindberg, F., Gastellu-Etchegorry, J.-P., Marconcini, M., Mitraka, Z., Stagakis, S., Crawford, B., Olofson, F., Landier, L., Morrison, W., Parlow, E., 2018. Urban energy exchanges monitoring from space. *Sci. Rep.* 8, 11498. https://doi.org/10.1038/s41598-018-29873-x

Copernicus, 2020. Copernicus Space Component Data Access system (CSCDA) [WWW Document]. URL https://spacedata.copernicus.eu/ (accessed 12.9.20).

Crawford, B., Grimmond, C.S.B., Gabey, A., Marconcini, M., Ward, H.C., Kent, C.W., 2018. Variability of urban surface temperatures and implications for aerodynamic energy exchange in unstable conditions. *Q. J. Royal Meteorol. Soc.* 144, 1719-1741.

Cyrys J, Eeftens M, Heinrich J, Ampe C, Armengaud A, Beelen R, Bellander T, Beregszaszi T, Birk M, Cesaroni G, Cirach M, de Hoogh K, De Nazelle A, de Vocht F, Declercq C, Dedele A, Dimakopoulou K, Eriksen K, Galassi C, Graulevičiene R, Grivas G, Gruzieva O, Gustafsson

AH, Hoffmann B, Iakovides M, Ineichen A, Krämer U, Lanki T, Lozano P, Madsen C, Meliefste K, Modig L, Mölter A, Mosler G, Nieuwenhuijsen M, Nonnemacher M, Oldenwening M, Peters A, Pontet S, Probst-Hensch N, Quass U, Raaschou-Nielsen O, Ranzi A, Sugiri D, Stephanou EG, Taimisto P, Tsai MY, Vaskövi É, Villani S, Wang M, Brunekreef B, Hoek G (2012) Variation of NO2 and NOx concentrations between and within 36 European study areas: Results from the ESCAPE study. Atmos Environ 62:374–390 . doi: 10.1016/j.atmosenv.2012.07.080

De Ridder K., Lauwaet D., Maiheu B. 2015. UrbClim - a fast urban boundary layer climate model. Urban Climate 12, 21-48.

De Ridder K., Schayes G., 1997. The IAGL Land Surface Model, Journal of Applied Meteorology 36, 167–182.

Del Grosso, S.J., Parton, W.J., Derner, J.D., Chen, M., Tucker, C.J., 2018. Simple models to predict grassland ecosystem C exchange and actual evapotranspiration using NDVI and environmental variables. *Agric. Forest Meteorol.*, 249, 1-10.

EEA Report No 13/2017 Air Quality in Europe - 2017 report https://www.eea.europa.eu/publications/air-quality-in-europe-2017

EEA, 2019. Air quality in Europe 2019]. URL https://www.eea.europa.eu/publications/air-quality-in-europe-2019

ESA, 2019. Copernicus High Priority Candidate Missions [WWW Document]. URL https://www.esa.int/Applications/Observing_the_Earth/Copernicus/Candidate_missions (accessed 10.25.19).

European Ground Motion Service: Service Implementation Plan and Product Specification Document (2020), EEA https://land.copernicus.eu/user-corner/technical-library/egms-specification-and-implementation-plan

Feigenwinter, C., Vogt, R., Christen, A., 2012. Eddy Covariance Measurements Over Urban Areas, in: Eddy Covariance. Springer Netherlands, Dordrecht, pp. 377–397. https://doi.org/10.1007/978-94-007-2351-1_16

Foken, T., 2006. 50 Years of the Monin–Obukhov Similarity Theory. *Boundary-Layer Meteorol* 119, 431–447. https://doi.org/10.1007/s10546-006-9048-6

García-Díez M., Lauwaet D., Hooyberghs H., Ballester J., De Ridder K., Rodó X., 2016. Advantages of using a fast urban boundary layer model as compared to a full mesoscale model to simulate the urban heat island of Barcelona. Geoscientific Model Development 9, 4439–4450.

Grimmond, C.S.B., Oke, T.R., 1999. Heat Storage in Urban Areas: Local-Scale Observations and Evaluation of a Simple Model. J. Appl. Meteorol. 38, 922–940. https://doi.org/10.1175/1520-0450(1999)038<0922:hsiual>2.0.co;2

Hlavacova, I., Halounova, L., Stanislav, P.: Sentinel-1 INSAR processing of corner reflector information in the northern-bohemian coal basin. The International Archives of the Photogrammetry, Remote Sensing and Spatial Information Sciences, Volume XLI-B7, 2016 XXIII ISPRS Congress, 12–19 July 2016, Prague, Czech Republic.

Hooyberhs H, De Craemer S, Lefebvre W, Vranckx S, Maiheu B, Trimpeneers Em Vanpoucke C, Janssen S, Meysman F, Fierens F. 2020. Validation and optimization of the ATMO-Street model chain by means of a large-scale citizen-science dataset. In review

ISO (1989), Hot Environments - Estimation of the heat stress on working man, based on the WBGT-index (wet bulb globe temperature). ISO Standard 7243. Geneva: International Standards Organization.

Jensen, S.S., Ketzel, M., Becker, T., Christensen, J., Brandt, J., Plejdrup, M., Winther, M., Nielsen, O.K., Hertel, O., Ellermann, T., 2017. High resolution multi-scale air quality modelling for all streets in Denmark. Transp. Res. Part D Transp. Environ. 52, 322–339. https://doi.org/10.1016/j.trd.2017.02.019

Kanda, M., Inagaki, A., Miyamoto, T., Gryschka, M., Raasch, S., 2013. A new aerodynamic parametrization for real urban surfaces. *Boundary-Layer Meteorol.* 148, 357–377. https://doi.org/10.1007/s10546-013-9818-x.

Kanda, M., Kanega, M., Kawai, T., Moriwaki, R., Sugawara, H., 2007. Roughness Lengths for Momentum and Heat Derived from Outdoor Urban Scale Models. *J. Appl. Meteor. Climatol.*, 46, 1067 - 1079

Karagulian, F., Belis, C.A., Dora, C.F.C., Prüss-Ustün, A.M., Bonjour, S., Adair-Rohani, H., Amann, M., 2015. Contributions to cities' ambient particulate matter (PM): A systematic review of local source contributions at global level. Atmos. Environ. 120, 475–483. https://doi.org/10.1016/j.atmosenv.2015.08.087

Kato, S., Yamaguchi, Y., Liu, C. C., Sun C. Y., 2008. Surface Heat Balance Analysis of Tainan City on March 6, 2001 Using ASTER and Formosat-2 Data. *Sensors*, 8, 6026 - 6044

Khan, Z., Ludlow, D., Mitraka, Z., Chrysoulakis, N., Feigenwinter, C., Marconcini, M., Lauwaet, D., Hooyberghs, H., Soukup, T., Jupova, K., Torres, E.F., Kjær-Hansen, L., 2020. CURE Project Deliverable D1.1 Summary of User Requirements.

Kljun, N., Calanca, P., Rotach, M.W., Schmid, H.P., 2015. A simple two-dimensional parameterisation for Flux Footprint Prediction (FFP). *Geosci. Model Dev.* 8, 3695–3713. https://doi.org/10.5194/gmd-8-3695-2015

Kohsiek W., De Bruin H.A.R., The H., van den Hurk B.J.J.M., 1993. Estimation of the sensible heat flux of a semi-arid area using surface radiative temperature measurements. *Boundary-Layer Meteorol*, 63, 213–230

Kolomaznik, J., Hlavacova, I., Lazecky, M., Pelant, M. (2016) TACR CZ Certified method for terrain movements and deformation monitoring on transport infrastructure by means of SAR Interferometry http://www.gisat.cz/download/projekt/TACR/GST-TB0400MD003_D3_v1-1.pdf, Technological Agency CZ (TACR)

Kolomaznik, J., Hlavacova, I., Stonacek, V., Lorenzo, A. (2020) Earth Observation for Sustainable development: Detailed terrain deformation analysis in urban areas, EO4SD Service Technical Report.

Kotthaus, S., Smith, T.E.L., Wooster, M.J., Grimmond, C.S.B., 2014. Derivation of an urban materials spectral library through emittance and reflectance spectroscopy. ISPRS J. Photogramm. Remote Sens. 94, 194–212. https://doi.org/10.1016/j.isprsjprs.2014.05.005

Lauwaet D., De Ridder K., Saeed S., Brisson E., Chatterjee F., van Lipzig N.P.M., Maiheu B., Hooyberghs H., 2016. Assessing the current and future urban heat island of Brussels. Urban Climate, 15, 1-15.

Lauwaet D., Hooyberghs H., Maiheu B., Lefebvre W., Driesen G., Van Looy S., De Ridder K., 2015. Detailed Urban Heat Island projections for cities worldwide: dynamical downscaling CMIP5 global climate models. Climate, 3, 391-415.

Lauwaet D., Maiheu B., De Ridder K., Boënne W., Hooyberghs H., Demuzere M., Verdonck M.-L., 2020. A New Method to Assess Fine-Scale Outdoor Thermal Comfort for Urban Agglomerations. Climate, 8, 6; doi:10.3390/cli8010006.

Lazecky, M., Bakon, M., Sousa, J. J., Perissin, D., Hlavacova, I., Patricio, G., Papco, J.,Rapant, P., Real, N. (2015) Potential of Multi-Temporal InSAR Techniques for Structural Health Monitoring, Proceedings of [FP1] FRINGE'15, http://proceedings.esa.int/files/324.pdf

Lazecky, M., Jirankova, E., Bohmova, D. (2010). Usage of insar techniques to detect and monitor terrain subsidence due to mining activities. https://www.researchgate.net/publication/277748130_Usage_of_insar_techniques_to_detect_and_monitor_terrain_subsidence_due_to_mining_activities

Lefebvre, W., Degraeuwe, B., Beckx, C., Vanhulsel, M., Kochan, B., Bellemans, T., Janssens, D., Wets, G., Janssen, S., De Vlieger, I., Int Panis, L., Dhondt, S., 2013b. Presentation and evaluation of an integrated model chain to respond to traffic- and health-related policy questions. Environ. Model. Softw. 40, 160–170.

Lefebvre, W., Van Poppel, M., Maiheu, B., Janssen, S., Dons, E., 2013a. Evaluation of the RIO-IFDM-street canyon model chain. Atmos. Environ. 77, 325–337. https://doi.org/10.1016/j.atmosenv.2013.05.026

Lefebvre, W., Vercauteren, J., Schrooten, L., Janssen, S., Degraeuwe, B., Maenhaut, W., de Vlieger, I., Vankerkom, J., Cosemans, G., Mensink, C., Veldeman, N., Deutsch, F., Van Looy, S., Peelaerts, W., Lefebre, F., 2011. Validation of the MIMOSA-AURORA-IFDM model chain for policy support: Modeling concentrations of elemental carbon in Flanders. Atmos. Environ. 45, 6705–6713. https://doi.org/10.1016/j.atmosenv.2011.08.033

Lemke B., Kjellstrom T. (2012) Calculating Workplace WBGT from Meteorological Data: A Tool for Climate Change Assessment. Industria Health 50, 267–278.

Leuning R, Kelliher FM, De Pury DGG, Schulze ED, *Plant. Cell Environ.* 18, 1183–1200 (1995).

Li, H., Zhou, Y., Li, X., Meng, L., Wang, X., Wu, S., Sodoudi, S. (2018). A new method to quantify surface urban heat island intensity. Science of The Total Environment 624, 262–272.

Liljegren J.C., Carhart R.A., Lawday P., Tschopp S., Sharp R. (2008) Modeling the Wet Bulb Globe Temperature Using Standard Meteorological Measurements. Journal of Occupational and Environmental Hygiene 5(10), 645-655. DOI:10.1080/15459620802310770.

Lindberg, F., Grimmond, C.S.B., Gabey, A., Huang, B., Kent, C.W., Sun, T., Theeuwes, N.E., Järvi, L., Ward, H.C., Capel-Timms, I., Chang, Y., Jonsson, P., Krave, N., Liu, D., Meyer, D., Olofson, K.F.G., Tan, J., Wästberg, D., Xue, L., Zhang, Z., 2018. Urban Multi-scale Environmental Predictor (UMEP): An integrated tool for city-based climate services. *Environ. Model. Softw.* 99, 70–87. https://doi.org/10.1016/j.envsoft.2017.09.020

Marconcini, M., Gorelick, N., Metz-Marconcini, A., Esch, T. (2018). Mapping the Global Settlement Growth from 1985 to 2015 - the World Settlement Footprint Evolution Dataset. 2018 AGU Fall Meeting Conference Paper

Marconcini, M., Metz-Marconcini, A., Üreyen, S. et al. Outlining where humans live, the World Settlement Footprint 2015. Sci Data 7, 242 (2020).

Minderhoud, P. S. J., Hlavacova, I., Kolomaznik, J., and Neussner, O.: Towards unraveling total subsidence of a mega-delta – the potential of new PS InSAR data for the Mekong delta, Proc. IAHS, 382, 327–332, https://doi.org/10.5194/piahs-382-327-2020, 2020

Mitraka, Z., Chrysoulakis, N., Doxani, G., Del Frate, F., Berger, M., 2015. Urban Surface Temperature Time Series Estimation at the Local Scale by Spatial-Spectral Unmixing of Satellite Observations. Remote Sens. 7, 4139–4156. https://doi.org/10.3390/rs70404139

Mitraka, Z., Chrysoulakis, N., Kamarianakis, Y., Partsinevelos, P., Tsouchlaraki, A., 2012. Improving the estimation of urban surface emissivity based on sub-pixel classification of

high resolution satellite imagery. Remote Sens. Environ. 117, 125–134. https://doi.org/10.1016/j.rse.2011.06.025

NASA/METI/AIST/Japan Spacesystems, and U.S./Japan ASTER Science Team. ASTER Level 2 Surface Temperature Product. 2001, distributed by NASA EOSDIS Land Processes DAAC, https://doi.org/10.5067/ASTER/AST_08.003. Accessed 2020-12-10.

Offerle, B., Grimmond, C.S.B.B., Fortuniak, K., 2005. Heat storage and anthropogenic heat flux in relation to the energy balance of a central European city centre. Int. J. Climatol. 25, 1405–1419. https://doi.org/10.1002/joc.1198

Oke, T.R., Mills, G., Christen, A., Voogt, J.A., 2017. Urban Climates. Cambridge University Press, Cambridge. https://doi.org/10.1017/9781139016476

Parastatidis, D., Mitraka, Z., Chrysoulakis, N., Abrams, M., 2017. Online Global Land Surface Temperature Estimation from Landsat. Remote Sens. 9, 1208. https://doi.org/10.3390/rs9121208

Pepe, A., Calò, F. (2017) A review of interferometric synthetic aperture RADAR (InSAR) multi-track approaches for the retrieval of Earth's surface displacements Appl. Sci., 7 (12), 1264: https://www.mdpi.com/2076-3417/7/12/1264/htm

Pope CA, Burnett RT, Thun MJ, Calle EE, Krewski D, Ito K, Thurston GD. Lung cancer, cardiopulmonary mortality and long-term exposure to fine particulate air pollution. JAMA-J Am Med Assoc. 2002;287:1132–1141.

Poursanidis, D., Mitraka, Z., Somarakis, G., Dohr, M., Chrysoulakis, N., 2020. CURE Project Deliverable D7.4 Data Management Plan.

Stagakis, S., Chrysoulakis , N., Spyridakis , N., Feigenwinter, C., Vogt, R., 2019. Eddy Covariance measurements and source partitioning of CO_2 emissions in an urban environment: Application for Heraklion, Greece . *Atm. Environ*., 201, 278-292. https://doi.org/10.1016/j.atmosenv.2019.01.009

U.S. Army (2003) Technical Bulletin Medical 507 and Air Force Pamphlet 48-152(I). Heat stress control and heat casualty management.

Voogt, J.A., Grimmond, C.S.B., 2000. Modeling Surface Sensible Heat Flux Using Surface Radiative Temperatures in a Simple Urban Area. *J. Appl. Meteorol.* 39, 1679–1699. https://doi.org/10.1175/1520-0450-39.10.1679

WHO, 2016. Ambient air pollution: A global assessment of exposure and burden of disease. URL: https://www.who.int/publications/i/item/9789241511353

WHO. Health risks of air pollution in Europe – HRAPIE: Recommendations of concentration-response functions for cost-benefit analysis of particulate matter, ozone and nitrogen dioxide. World Health Organization; [last access: 25 April 2018]. 2013. available at: http://www.euro.who.int/__data/assets/pdf_file/0006/238956/Health_risks_air_pollution_HRAPIE_project.pdf?ua=1.

Willett, K. M. & Sherwood, S. (2012) Exceedance of heat index thresholds for 15 regions under a warming climate using the wet-bulb globe temperature. Int. J. Climatol., 32, 161–177.

Zhou B., Lauwaet D., Hooyberghs H., De Ridder K., Kropp J. P., Rybski D., 2016. Assessing seasonality in the surface urban heat island of London. Journal of Applied Meteorology and Climatology, 55, 493-505.